Cosmic Acceleration as Quantum Gravity Phenomenology

by

Chanda Rosalyn Sojourner Prescod-Weinstein

A thesis
presented to the University of Waterloo
in fulfillment of the
thesis requirement for the degree of
Doctor of Philosophy
in
Physics

Waterloo, Ontario, Canada, 2010

© Chanda Rosalyn Sojourner Prescod-Weinstein 2010

Author's Declaration

I hereby declare that I am the sole author of this thesis. This is a true copy of the thesis, including any required final revisions, as accepted by my examiners.

I understand that my thesis may be made electronically available to the public.

Authorship Statement

This dissertation is partially the product of collaborative research and co-authored publications. The following publications form the basis of three chapters in this dissertation.

- **C. Prescod-Weinstein**, N. Afshordi, & M. Balogh, "Stellar Black Holes and the Origin of Cosmic Acceleration," Phys. Rev. D 80: 043513 (2009), Copyright (2009) by the American Physical Society
- **C. Prescod-Weinstein** & L. Smolin, "Disordered Locality as an Explanation for the Dark Energy," Phys. Rev. D 80: 063505 (2009), Copyright (2009) by the American Physical Society
- **C. Prescod-Weinstein** & N. Afshordi, tentatively titled "A Universal Time for the Cluster Mass Function," submission to the arXiv and Phys. Rev. D planned

The article with Afshordi and Balogh relies on prior work by Afshordi. It was Afshordi who first proposed we consider black holes in the presence of gravitational aether. Most of the fundamental calculations were done by me, and through this work, I made an unexpected discovery. This lead Afshordi and I to propose the Trans-Planckian ansatz. Balogh was asked to contribute an astrophysical perspective to the project. The written product was largely edited by Afshordi and myself and is based on a manuscript that I wrote during the research process. Revisions after the referee's remarks were handled primarily by me, with input from Afshordi.

The article with Smolin relies on prior work by Smolin with Markopoulou-Kalamara. The idea proposed was arrived at individually by myself, separately from Smolin and Markopoulou-Kalamara. Initial calculations were done by both myself and Smolin, and the final version is a combination of those efforts. It was Smolin's idea to introduce concepts from condensed matter physics. Responsibility for the manuscript itself was shared between myself and Smolin, and I was the sole editor of both the version that was resubmitted after receiving comments and corrections from the journal referee and the final version that was submitted for copy editing and publication. The version that appears here has been updated by me to include more detailed discussion.

The third article is based on an idea proposed by Afshordi. The majority of the analytic calculations not attributed to the work of others were done by me alone. The C++ code used for the numerical work, which appears here as an appendix, is entirely my own. The majority of the written product is my work.

Abstract

The discovery of cosmic acceleration has prompted the need for a new understanding of cosmology. The presence of this acceleration is often described as the dark energy problem or the Λ problem.The simplest explanation is that the acceleration is due to addition of a cosmological constant to Einstein's equation, but this resolution is unsatisfactory as it leaves several unanswered questions. Although General Relativity has been tested in the strong-field limit, the apparent dark energy may be urging us to consider experimental cosmology as such a test for large scales. In this vein, I have pursued a study of modifications to Einstein's gravity as well as possible related quantum gravity phenomenology.

Not only must the details of modified gravities be worked out, but their impact on other astrophysics must be checked. For example, structure formation provides a strong test of any cosmic acceleration model because a successful dark energy model must not inhibit the development of observed large-scale structures. Traditional approaches to studies of structure formation in the presence of dark energy or a modified gravity implement the Press & Schechter formalism. I explore the potential for universality in the Press & Schechter formalism and what dark matter haloes may be able to tell us about cosmology.

Acknowledgements

The Igbo saying *Ora na-azu nwa* means that the community raises the child. In my case, it has been many communities. An extraordinary number of extraordinary people helped get me to where I am now, and it is an incredible pleasure to thank them all. I will not apologize for the length: everyone mentioned here deserved more words than they got.[1]

Unfortunately, thank you sounds ridiculous when directed at my mother. There are no words that properly describe and elevate what she has done for me. Without my mother, all of this, all of me, would be, simply put, an impossibility.

My father first encouraged my interest in mathematics and literature, which I think turned out pretty well. The phone calls, instant messages and chess games during this dissertation process meant more than he will likely ever fully understand.

My sister Maya Trinidad Maldonado-Weinstein grew up to be pretty cool, which is awesome and was very useful when I needed company during the long days of writing.

My step-mother Maria is fiercely intelligent, and I hope some of it has rubbed off on me. She provided much love and encouragement along the way, including during a harried weekend of postdoc app writing. Mijn stiefvader Maarten: Hartelijk gefeliciteerd met de PhD van jouw stiefdochter! And also on being the best step-father that anyone could ask for.

My Grandma Elsa, Grandpa Stanley, Uncle Peter, Auntie Rosaline, and mother survived a difficult passage, leaving Barbados to come and make way for me and my cousins, and Uncle Peter gave me my first copy of *A Brief History of Time* when I was 11 basically because he's awesome. My Grandmother Selma provided me with challenges that helped me grow into a person of conscience who practices science, and I appreciate the chance to become that woman.

My cousin Khari and the Lang-McNabb family have always encouraged me, and I am grateful for their support. Thanks to Uncle George and my lovely Preudhomme cousins for the love and support over the years. I also very much appreciate the support from my extended Oostendorp and Maldonado families. To the younger Prescods, Preudhommes, Blackmans, McNabbs, Maldonados, Oostendorps & Gordons: onward and upward!

Many people have gifted me that extraordinary thing we call friendship. Luke, Derek, and Scott: we need to get on The Daily Show and bring the wonderfully supportive and hilarious John Jacobs with us. Alexis Shotwell, Sara Smith, James Rowe,

[1]The *LaTeX* template that I used to produce this document was most recently edited by Stephen Carr and is maintained by University of Waterloo's ISC Client Services.

and Chris Dixon were amazing teachers and friends. Jeremy Steffler, Sean Padilla, and Seneca Joyner gave me so much e-love. Bronwyn Addico, Michelle Sabourin, Mina Le, Joseph Norman and Matthew Lincoln provided countless hours of great conversation and support. Andrew & Catherine Unrau Woelk, Louise Burns, and Niti Seth have been fantastic spiritual guides and friends. I'm glad that if Kevin Spacey ever moves out, there will be space for me in Adam Timmerman's closet. Evan Coole and Islai Rathlin provided lots and lots and lots of love and moral support. Easwarlicious is a sweet guy, and Cozphenomenon is really hard core. Thanks bros! Toby, thanks for 11 years of making my brain work overtime. Sharifah's letters, emails and creations help make the world worth exploring.

Nickolaki: I couldn't think of one joke that was appropriate to put here, so I'll just say thanks for letting me be your purse. Lucy Zhao provided extraordinary love and support through important stages of this process. Narinda, thank you for when you were able to be near. Peter Onyisi is like the brother I never had. I am infinitely grateful to the universe for bringing us together. Peter Boyce II is always an inspiration. Sujay, Elenora, Rajiv and Rohan provided a loving home and family far away from home and family. Thank you so much. Similarly, Daena Cressman was the best Aunt away from home ever! Speaking of getting away from home, I must thank Jim and Sharon Morris for allowing me to spend time at their lake home, which provided a much needed, quiet work space.

Over the years, Kendra and Dan did their best to keep me fed and entertained in the incredible Black Hole Bistro, and I'm sure everyone who is in the know agrees: they are awesome people. Much like Matt Leifer, who I am lucky to call friend.

By the way, everyone, there's a Mongoose running amock and he knows who he is. Meanwhile, I would like everyone to welcome talented author John-Edgar Lopez to East LA! Thanks to Paul M. Davis for letting me occasionally be a crazy writer with an audience. I am indebted to International Master of Chess Attila Turzo, who taught me excellent life/chess lessons.

On the science side, I must begin by thanking Lee Smolin, who took a chance on me and gave me both the resources and freedom to blossom as an independent scientist. He welcomed me into his research world as well as his home at various points, supporting me in a way that I think is unique to Lee. Learning from how he does science has been a privilege. For the rest of my life, I will look at Lee as an example of what it means to be an excellent scientist. He is extraordinarily creative in his management of the technical confines of our highly mathematical field, managing to be careful without becoming unnecessarily rigid.

To my other supervisor Niayesh Afshordi I am extraordinarily indebted. I am constantly trying to keep up with Niayesh, who is both one of the most brilliant and

compassionate people I have ever met in my life. Niayesh pushed me to do better science but never asked me to compromise my other passions, supporting my activism as well as my efforts to diversify physics. I would like to echo something he said in his dissertation acknowledgements: *Let us hope and pray for a day that man-made borders are only part of history books.* To which I add: and for a day when every child may reach hir potential, without the fear or reality of bombs, poverty and other forms of violence.

Although Anthony Aguirre is not formally involved in this dissertation, he played a key role as my supervisor at UC Santa Cruz as well as a reference during my postdoctoral application process. Like Lee, Anthony gave me a lot of freedom, and although I did not always use it wisely, I think in the long run I am the better for it. Anthony was always supportive of my desire to do "crazy" things in science while I also helped to cause a lot of trouble for the University of California administration. He never questioned my commitment to science, which I have come to learn is a gift.

Achim Kempf, Brian McNamara, and Fotini Markopoulou-Kalamara have been gracious committee members, always answering questions and providing guidance when I asked or even when they just thought I could use it. Additional thanks to Frank Wilhelm who provided assistance as the graduate officer and to Robert Brandenberger who agreed to be an external reader for this dissertation.

My cohort in the National Society of Black Physicists (NSBP) and National Society of Hispanic Physicists (NSHP) has consisted of a loving, supportive group of people. Haile Kofi Ankoma Owusu, Willie Merrell, Tehani Finch, Lisa Dyson, Jami Valentine, Teri Robinson, Renee Horton, Nate Moore, Cynthia Correa and Ibrahim Cisse have provided endless hours of amusement, thoughtful discussion and emotional and intellectual support at critical moments. Especially Willie, who crossed the dreaded loops-strings barrier to provide me with a regular discussion partner when I was hopelessly stuck. I hope very much that Beth Brown would have been proud of the work presented here. May we ever endeavor to fill your shoes, Beth.

Between NSBP and NSHP, some incredible faculty have broken barriers, lead the way and made time out of their busy schedules to help me along. Arlie Petters, James Lindesay and S. James Gates helped me see that I had the inner strength required to follow my dreams of becoming a theoretical physicist. The lovely and exuberant Paul Guéye has always gone above and beyond in his efforts to help me achieve success. Jarita Holbrook and Jesús Pando have been important political sounding boards. Dara Norman, Kevin Covey, and Marcel Agueros gave essential help during my postdoc application process. Stephon Alexander, David Ernst, Clifford Johnson, Lawrence Norris and Keith Jackson were always willing to answer my questions about pretty much anything. I thank the entire NSBP and NSHP boards for their hard work.

Additionally, certain faculty allies have gone out of their way to promote the

interests of traditionally underrepresented people in physics and astronomy, running programs, attending conferences, joining committees, writing blogs, speaking out and mentoring diverse students. Edmund Bertschinger, Sean Carroll, Melissa Franklin, Henry Frisch, and Vinothan Manoharan all had a significant impact on my progress as an individual and a scientist. I thank them for their commitment to me and to people like (and not like!) me.

I want to particularly thank the women researchers of Perimeter Institute for being brilliant, innovative, fun and supportive scientists and friends.

Many other members of the scientific community have played crucial roles in supporting me over the years: Mohammed Ansari, Latham Boyle, Sarah Croke, Carol Davis, Simon DeDeo, Claudia de Rham, Martin Elvis, Asa Ericsson, Julia Forman, Ghazal Gheshnizjani, Sean Gryb, Jonathan Hackett, Megumi Harada, Mark Ilton, Katherine Lynn, Fotini Markopoulou, Jonathan McDowell, Isabeau Premont-Schwarz, Sayeh Rajabi, Amir Jafari Salim, David Sanders, Sean Stotyn, Andrew Tolley, Neil Turok, Yidun Wan, Eric Weinstein & Steve Weinstein (no relation!).

I must recognize the incredible pre-college teachers without whom I might have ended up lost at sea. My debt to Frank Wilson is so heavy that I can't even pick it up. As my first math and my first science teacher, one could say that a lot of the last 17 years is his fault. Warren Buckner refused to let me fail or quit because he knew I could do better, and the work presented here is partly due to that tough love and amazing commitment to teaching. Randy Rutschman sparked what I believe will be a life-long love affair with history and really gave me the chance to learn how to think and write critically about complex subjects, which is helpful when doing a dissertation in physics. I hope I have shown him that I do have ganas! Jed Laderman did everything he could to keep my interest in physics alive and thriving, even when he had limited resources. Elaine Berman worked extremely hard to help me realize my dreams and then some, and her encouraging words and friendship over the years have made an enormous difference.

Finally, this work was completed thanks to a lot of talking at Bachelor and Master of Applied Mathematics Ryan Morris, who was a very useful whiteboard. Not only did Ryan ensure I had all of the necessities at each stage of the dissertation process (and I mean everything!), but he also taught me almost everything I know about C++, patiently helping me along when I decided that the final months of my PhD were an appropriate time to learn another language. Everyone who isn't friends with Ryan should be insanely jealous of everyone who is. To the neverending well of bad jokes and love: I do bite my thumb at you, sir, with love.

For Grandpa Norman, who was there every step of the way:
Ikh hob dikh azoyfil nokh gebenkt. Ikh hob dikh lib.
(In English – I have missed you so much. I love you.)

Hold fast to dreams
For if dreams die
Life is a broken-winged bird
That cannot fly.

Hold fast to dreams
For when dreams go
Life is a barren field
Frozen with snow.
– Dreams, *Langston Hughes*

CONTENTS

LIST OF FIGURES

CHAPTER 1

Prologue

1.1 The Astrophysical Picture

Observations of Type Ia supernovae [1, 2] and cosmic microwave background anisotropy measurements [3] seem to have converged on a seemingly simple and yet extraordinary point: the universe is not only expanding – it is accelerating. In other words, the matter-energy content of our universe is apparently dominated by a strange component that can be described as a vacuum energy with negative pressure. While we traditionally consider attractive gravity to be the dominant force on large-scales, this "energy" pushes outward, challenging Newtonian gravity's hegemony. Explaining the source of this acceleration is the great cosmological question of our era.

Approaches to the cosmic acceleration question are as varied and strange as the problem itself. The first of these is the introduction of a "simple" vacuum energy whose value is called the cosmological constant, which is often referred to as Λ.

However, as discussed in § 2.3, Λ is in fact a problem itself and one that is independent of the cosmic acceleration issue. This has been known for decades as the *cosmological constant problem*. Because both are questions of the energy content of the physical vacuum, one from the point of view of general relativity (GR) and the other from the point of view of quantum field theory (QFT), it is expected that they are related. Thus, a resolution to the one would ideally address the other.

An alternative explanation of cosmic acceleration is quintessence, which posits a scalar field with negative pressure as an additional stress-energy source. Quintessence is often used interchangeably with the more general term "dark energy." There is also the possibility that while GR is correct, we are not properly applying it to an inhomogeneous universe. Indeed, Kolb et al. [4] suggest that acceleration of the universe is due to backreaction of cosmological-scale perturbations. Neither of these models addresses the cosmological constant problem. Thus, an attractive alternative is that GR is the culprit and must be modified to properly explain the apparent presence of dark energy. Such models are known as modified gravities (MGs).

Discovering which of these models best fits the data is now central to the cosmological research enterprise. Finding tests for these models can be a challenge, since the evidence for cosmic acceleration that relies on geometric techniques (e.g. supernova distance measures) assumes a Robertson-Walker background metric and Friedmann's equations. While the assumption about the metric is tested and well established, Friedmann's equations may not be the correct description [5].

Moreover, depending on one's assumptions, at a technical level, MGs are indistinguishable from quintessence models because MGs can look like an effective dark energy [6]. A natural way to distinguish between the MGs and quintessence is to see

whether the theory looks more "natural" as a modified gravity or a quintessence in the context of structure formation. In fact, the study of structure formation can provide a powerful, independent test of models of cosmic acceleration [5]. The cosmology community has largely exhausted its efforts to study the cosmological constant in this context [7, 8, 9, 10, 11]. The impact of quintessence models on structure formation is also fairly well understood [12, 13, 14].

However, despite a wealth of study, efforts to discover methods that differentiate between models of cosmic acceleration using modeling of large-scale structure continue.

1.2 Fundamental Problem(s)

Even as we worry about the cosmic acceleration problem, we are faced with another challenge: quantum gravity. The two great accomplishments of the 20^{th} century have yet to find a way to work comfortably with one another. Einstein's GR taught us to see space, time, and matter as inseparable, while quantum mechanics and its eventual successors, QFT and the associated Standard Model (SM), gave us a new vision of the fundamental building blocks that compose all visible matter. One might naïvely assume that in some sense this would have exposed the foundation of the Universe and its evolution to us.

But this has not turned out to be the case. Despite nearly a century of effort, the fundamental structure of the universe is still very much a mystery. Although they are independently enormously successful in the regimes they were designed to describe, GR (which provides us with gravity) and QFT with the SM (which describes the mat-

ter but does not include gravitational interactions) continue to be unwilling partners in the theater of physics research. However willing they are in reality, we cannot yet clearly elucidate in mathematical or philosophical terms how that is possible.

1.3 Astrophysics and Fundamental Physics

As we consider the cosmic acceleration problem and what many consider to be the easiest explanation for it, the cosmological constant, we are left to ponder the question of the vacuum. We tend to think that defining the vacuum in GR is trivial, although in reality, GR says nothing about a vacuum, at least not the vacuum that we conceive of in QFT. In GR, the vacuum is an empty premise: space with no matter-energy content is a vacuum by definition. By contrast, in QFT, the vacuum is similarly a space with no matter-energy content, but with the caveat that it must account for quantum behaviors such as rapid fluctuations in matter-energy content. This divergence in definition leads to incredibly different properties.

What we've learned repeatedly is that connecting these two vacuums turns out to be completely non-trivial. Perhaps it's not that we don't have the right tools so much as our efforts have been focused in the wrong direction. An alternative, creative way of thinking about this problem is looking at another scenario where we are attempting to fit GR and QFT into a single framework: the quantum gravity problem. Vacuum observations and phenomenology could actually be quantum gravity phenomenology. Much of the work contained in this dissertation is inspired by the possibility that cosmic acceleration and quantum gravity are intimately tied together.

One possible way to see cosmic acceleration as a quantum gravitational effect on

the large-scale evolution and structure of the cosmos is the following. It has been suggested by Markopoulou [15] and Markopoulou & Smolin [16] that the transition from an early quantum geometric phase of the universe to a low-temperature phase that is characterized by an emergent metric might lead to a partially disordered locality.

We [17] considered the presence of Λ as a consequence of a quantum gravity where discreteness (and thus some amount of non-locality) is an inherent property. As the universe transitions to its low-temperature phase, non-locality might survive to large scales. Assuming this possibility, we find that the energy associated with the presence of so-called non-local links leads to a small measured vacuum energy, similar in nature to the cosmological constant.

Afshordi's *gravitational aether* [18] provides an example of a novel approach to cosmic acceleration modeling via a modified energy-momentum contribution to Einstein's equation. The aether is an example of degravitation, where gravitation is decoupled from the vacuum. This effectively eliminates the weak and new cosmological constant problems by virtue of making the vacuum solely a matter for quantum field theory. The new gravitation equation satisfies traditional constraints, such as the Bianchi identity, and leads to a modified Friedmann equation. It can be shown that in this particular model, Newton's constant is four thirds its current measured value during an era of radiation domination.

To better understand this model, Afshordi and I [17] studied solutions for static black holes in the presence of the gravitational aether. Because of the aether's fluid-like properties, we began by considering a static metric that describes the perfect fluid-like interior of a star. Here the energy-momentum tensor is particularly simple

because of the absence of a matter density.

The study reveals an interesting so-called UV-IR coupling: aether couples the spacetime metric near the horizon to the metric at infinity via an integration constant that appears in both limits. We fix this constant via what we termed the *Trans-Planckian ansatz*. By doing so, we can make a connection between the contribution of the presence of many stellar-mass black holes and the presence of an apparent dark energy. We can then make a prediction for the equation of state of "dark energy," which can be tested by future observational projects such as the Joint Dark Energy Mission.

As we consider the potential relationship between observations and the universe's expansion history, an important parameter whose value we hope to uncover from data is the equation of state parameter, $w \equiv p/\rho$. The value of w will help us distinguish between different models of cosmic acceleration. A simple cosmological constant model will give $w = -1$, while dynamical scalar field and modified gravity theories may give us a more complex, time-dependent relation. The value of w can be constrained directly by supernova distance-redshift and baryon acoustic oscillations, as observed through efforts such as the Sloan Digital Sky Survey and Hubble Space Telescope.

Of course, the interpretation of this data relies on the assumption that GR, as we know it, is correct. The challenges grow when we consider the possibility of modified gravity [5]. For example, Ishak et al. [19] note that we run the risk of misunderstanding our results if we do not disentangle the interpretation of our data through the lens of dark energy when the reality is a modified gravity, or vice versa. With this in mind, structure formation comes to the fore. Indeed, an ideal scenario

is one where we are able to use structure formation data and modeling to distinguish between cosmological pictures.

The relationship between dark energy and structure formation, i.e. the evolution of small-scale inhomogeneities, manifests via the cluster mass function (CMF), also known as the halo abundance mass function. The CMF gives dark matter halo abundance as a function of mass. It has been noted that the CMF can help to constrain the vacuum energy density as well as other cosmological parameters [20, 21]. In other words, understanding the correlation between galaxy cluster density and the dark energy can provide a powerful test of the dark energy as cosmological constant. In turn, this knowledge may offer hints about the structure of quantum gravity.

Afshordi and I pursued a better understanding of the universality of the cluster mass function, which gives us a measure of galaxy cluster mass density. We find that the universal behavior of the cluster mass function allows us to derive the history of linear structure formation, allowing us to refine how structure formation is used to understand cosmological dynamics. As in the case of other endeavors mentioned in this section, the work is extendable and is by no means concluded here.

1.4 Outline

As part of my doctoral research, I have investigated two competing explanations for the cosmic acceleration and then moved into attempting to develop a better mechanism for using observational information about structure formation to test models of cosmic acceleration. To make this work as accessible as possible, I provide introductions to basics in cosmology and quantum gravity so that the original content can be

read in context.

Chapter 2 will introduce Einstein's theory of gravitation. I will describe the general form of cosmology that can be derived from it. I then discuss this cosmology from the perspective of current astrophysical data, most notably the question of cosmic acceleration. This introduces us to the cosmological constant and its famous three problems.

Chapter 3 describes the idea of Quantum Gravity and problems that we might hope to solve by discovering a model of it. I will discuss some general properties of non-string theory models of quantum gravity, focusing on ideas about non-locality and emergence. The chapter also includes a derivation of the Hawking radiation, a key idea in semiclassical gravity.

Chapter 4 is an updated version of a paper that I co-wrote with Smolin, which appeared in Physical Review D. The paper, entitled *Disordered Locality as an Explanation for the Dark Energy*, introduces an alternative approach to resolving the cosmic acceleration problem that is more directly inspired by ideas in quantum gravity than the model in Chapter 5.

Continuing along the same lines, Chapter 5 is primarily a reproduction of a paper that I co-wrote with Afshordi and Balogh and which also appeared in the Physical Review D. The paper, entitled *Stellar Black Holes and the Origin of Cosmic Acceleration*, describes a novel approach to resolving the cosmological constant and cosmic acceleration problems using a novel tie between black holes and semiclassical quantum gravity phenomenology.

In Chapter 6, I provide a draft of a planned submission for publication in Physical

Review D with Afshordi on the question of what dark matter haloes can teach us about cosmic acceleration.

1.5 Conventions

For the purposes of clarity and consistency, I have chosen a few standard conventions for this dissertation. I will use a standard Lorentzian metric with a $\eta = diag(1, -1, -1, -1)$ signature in Chapter 4 and with a $\eta = diag(-1, +1, +1, +1)$ signature in Chapter 5. Unless it is explicitly stated otherwise, I use natural Planck units [1]: $\hbar = c = G = k_B = 1$, where $\hbar$ is Planck's constant mod 2π, c is the measured speed of light in a vacuum, G_N is Newton's constant and k_B is Boltzmann's constant.

[1] Planck units are described in greater detail as part of a larger discussion about quantum gravity in Chapter 3

CHAPTER 2

Relativity and Cosmology

In this Chapter, I provide a review of fundamental elements of the Lambda-Cold-Dark-Matter model (ΛCDM) that is the most generally accepted model in physical cosmology. This concordance model assumes the presence of a vacuum energy accounting for 70% of the matter-energy content in the universe, cold (as opposed to hot) dark matter accounting for 26%, and baryonic (normal) matter accounting for 4%.

The unexpected reality that the majority of the universe's energy content is composed of two components whose properties we mostly do not understand merits some discussion. This work focuses quite a bit on the cosmic acceleration/cosmological constant/dark energy problem, starting with Section 2.3. The name "dark matter" is due to this matter's lack of an electromagnetic interaction. Its existence is inferred from observations of galaxy rotation curves, whose velocities suggest the presence of more gravitationally interacting matter than what is expected due to observations of

radiation. Most of what is understood about the properties of dark matter is due to theoretical work or inference from the behavior of surrounding baryonic matter, and all of it is well-reviewed.[1]

For the purposes of this section, I will assume a basic familiarity with concepts in General Relativity up to and including Einstein's equation. For a more thorough presentation of many of the topics covered here, Wald [23] and Carroll [24] provide thorough discussions of the basics of general relativity and Friedmann-Robertson-Walker theory.

2.1 The Expanding Universe

In 1929, Edwin Hubble made a momentous discovery that would dominate, if not begin, progress in cosmology for the entirety of the 20th century right into the 21st. While studying the movements of galaxies, he noted that the recession velocity of a galaxy was proportional to its distance [25]. The proportionality factor came to be known as the Hubble Constant, H, and the relation as Hubble's law:

$$\vec{v} = H_0 \vec{r} \tag{2.1}$$

In other words, we can describe the expansion of the universe as the increase, in time, of the proper distance between galaxies. This is not to say that gravitationally bound systems such as galaxies are expanding. In fact, the tension between the expansion and these gravitational instabilities leads to interesting effects such as structure formation, which will be discussed more in depth in Chapter 6.

[1] For example, see Liddle & Lyth [22].

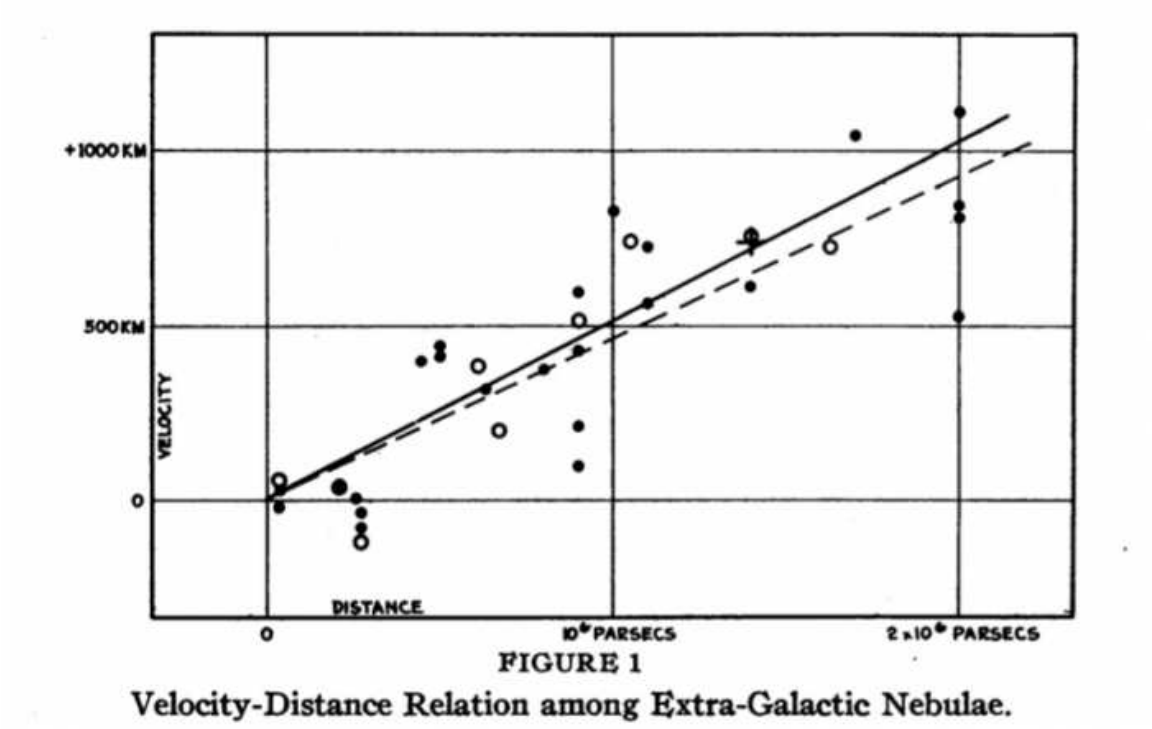

FIGURE 1

Velocity-Distance Relation among Extra-Galactic Nebulae.

Figure 2.1: This diagram, from Hubble's original paper, shows a strong correlation between the distance of galaxies and their recession velocities. Edwin Hubble, Proceedings of the National Academy of Sciences, vol. 15 no. 3, pp.168-173

Although initially rejected by Einstein, Hubble's observations have been confirmed repeatedly during the several decades since and are a cornerstone of experimental evidence for Einstein's General Relativity. Indeed, as discussed in Chapter 1, in 1998 an interesting twist in the narrative was introduced by Supernova Type Ia data which seemed to suggest that the universe is not only expanding but that very expansion is accelerating. The simplest explanation for this acceleration is the presence of a cosmological constant in Einstein's equations, describing a non-zero vacuum energy. But as I describe later, this explanation leaves a lot to be desired.

2.2 Friedmann, Robertson, and Walker

A discussion of the cosmological constant and the problem of the accelerating universe will be richer in the context of underlying theory. Thus, I will take the opportunity to describe the Robertson-Walker metric and Friedmann's equations in order to put the original work of this document in context. The *cosmological principle* (CP) forms the foundation for all models of cosmology. The CP is essentially the statement that on large scales, the universe looks the same to all observers. There are two immediate consequences of this idea:

1. Spatial homogeneity at each time slicing

2. Spatial isotropy at each time slicing

Spatial homogeneity implies that there is no such thing as a privileged observer in the universe, and observables will be the same everywhere. Isotropy implies that this is the case no matter what direction we look in.

It can be shown that the assumption of homogeneity and isotropy is a sufficient constraint to discover a general cosmological metric, commonly known as the Robertson-Walker metric.[2]

$$ds^2 = -dt^2 + a(t)^2 d\Sigma^2, \tag{2.2}$$

where a is a dimensionless scale factor and Σ is a three space of constant curvature. The exact form depends on the internal curvature of the spacetime. It can either be Euclidean, hyperbolic or spherical in nature. These correspond to flat, open and closed universes, respectively. We can see this by writing:

$$d\Sigma^2 = \frac{dr^2}{1 - kr^2} + r^2 d\Omega^2, \tag{2.3}$$

where r has dimensions of distance and k is the curvature parameter with dimensions $[length]^{-2}$. $k = 0$ corresponds to the flat case, $k > 0$ the closed and $k < 0$ the open.

The Robertson-Walker metric, when paired with the assumption that matter can be modeled as a perfect homogeneous fluid as well as with the application of Einstein's equation, forms the Friedmann-Roberston-Walker universe. To see what one means by this, we summarize a portion of Carroll's discussion. Beginning in a frame where a perfect fluid's velocity, U, is at rest with respect to comoving coordinates, $U^\mu = (1, 0, 0, 0)$, we define the energy-momentum tensor:

$$T_{\mu\nu} = (\rho + p) U_\mu U_\nu + p g_{\mu\nu}, \tag{2.4}$$

[2]For example, see Chapter 8 of Carroll [24].

where ρ and p are the density and pressure, respectively, and $g_{\mu\nu}$ is the metric.

When we plug this energy-momentum tensor into Einstein's equation, given by

$$R_{\mu\nu} - \frac{1}{2}Rg_{\mu\nu} = 8\pi G T_{\mu\nu}, \tag{2.5}$$

along with the Robertson-Walker metric, the $\mu\nu = 00$ equation gives us what is known as the second-order Friedmann equation:

$$\frac{\ddot{a}}{a} = -\frac{4\pi G}{3}(\rho + 3p). \tag{2.6}$$

The $\mu\nu = ij$ equation gives us another equation:

$$\frac{\ddot{a}}{a} + 2\left(\frac{\dot{a}}{a}\right)^2 + 2\frac{k}{a^2} = 4\pi G(\rho - p), \tag{2.7}$$

which, when combined with Eqn. 2.6 gives us the well-known first order Friedmann equation:

$$\left(\frac{\dot{a}}{a}\right)^2 = \frac{8\pi G}{3}\overline{\rho} + \frac{k}{a^2} = H^2. \tag{2.8}$$

$H = \frac{\dot{a}}{a}$ defines the Hubble parameter, which in the present epoch, $a(t = today) = 1$, is equivalent to Hubble's "constant."

Extending our assumption about the fluid nature of energy content, we assume that the equation of state for all fluids will be given by $p = w\rho$, where w is a time-independent constant that is often referred to as the equation of state parameter. w will take on different values for different forms of matter-energy content. Indeed, when talking about the problem of cosmic acceleration, the value of w is key. For a simple cosmological constant, which fits many cosmological observations, $w = -1$.

Quintessence and modified gravity models potentially have dynamical equation of state parameters, which present certain theoretical challenges that are discussed in Chapter 6. By contrast, for a dusty universe, $w = 0$, and we use this to approximate gravitating (baryonic and dark) matter.

In keeping with the fundamental premise of GR, that matter shapes geometry while geometry tells matter how to behave, the matter-energy content of the universe, along with intrinsic curvature, determines the geometry of the universe. This geometry is defined as open, closed or flat (as discussed above) relative to the critical density, which is found assuming a zero vacuum energy:

$$\rho_c = \frac{3H^2}{8\pi G}. \tag{2.9}$$

For convenience, matter-energy densities of different components such as baryonic/-dark matter, dark energy/vacuum, radiation and intrinsic curvature are often expressed as fractions of this critical density:

$$\Omega_i = \frac{\rho_i}{\rho_c}, \tag{2.10}$$

where Ω is sometimes called the density parameter. The sum of the density parameters for each component is equal to unity:

$$1 = \Omega_m + \Omega_\Lambda + \Omega_r + \Omega_k. \tag{2.11}$$

If the universe is not flat ($k = 0$), the total energy density will be a function of time, i.e. $\Omega_{total} = \Omega_{total}(t)$ where $\Omega_{total} = 1 - \Omega_k$.

Taking into account an equation of state parameter $w = 0$ for matter, $w = \frac{1}{3}$ for radiation, $w = -1$ for vacuum energy, and $w = -\frac{1}{3}$ for spatial curvature, we can rewrite the Friedmann equation:

$$\left(\frac{H}{H_0}\right)^2 = \Omega_m a^{-3} + \Omega_r a^{-4} + \Omega_k a^{-2} + \Omega_\Lambda, \tag{2.12}$$

where H_0 is the value of the Hubble factor today. It is this form that is used for the codes described in Chapter 6 and found in Appendix A.

2.3 Cosmological Constant

We are most interested in studying the mathematical structures of cosmology because of the insight they may provide into the cosmic acceleration problem. In the context of the foundation of Section 2.2, we can naïvely assume that Einstein's equations continue to satisfactorily describe the universe's cosmology if we merely recall his famed blunder[3] the *cosmological constant* or Λ. Physically, this means we assume the presence of a vacuum energy whose value is set by experimental evidence, for example the value necessary to cause observed cosmic acceleration. Relativity cannot tell us how to deduce this value from theoretical considerations.

This Λ manifests with a fluid equation of state $\rho = -p$, counterintuitively embodying a negative pressure. Furthermore, it appears in Einstein's equation as a mere addition that is not motivated by any theoretical considerations. In the presence of

[3]This characterization is attributed to Einstein by George Gamow in his memoir. [26]

a non-zero cosmological constant, Einstein's equation takes the form:

$$R_{\mu\nu} - \frac{1}{2}Rg_{\mu\nu} + \Lambda g_{\mu\nu} = 8\pi G T_{\mu\nu}. \tag{2.13}$$

In addition, the cosmological constant can be added into the FRW framework with minimal disruption. Friedmann's equations will take a slightly different form, but are largely unchanged. For example, the first order equation will have an additional density contribution[4]:

$$\left(\frac{\dot{a}}{a}\right)^2 = \frac{8\pi G_N}{3}(\overline{\rho} + \rho_\Lambda) = H^2. \tag{2.14}$$

However, the cosmological constant is unsatisfactory because it leaves several questions unanswered. As outlined by Weinberg [27, 28] and many others, the cosmological constant comes with its own set of problems that are independent of cosmological issues. Three major questions arise when talking about Λ, with or without the presence of cosmic acceleration:

1. *The Old Cosmological Constant Problem*: There is a severe mismatch between the measured Λ and the expected value due to quantum field theory (QFT). QFT naïvely predicts an energy density that, in units where $\hbar = c = G = 1$, will be of order unity.

2. *The Weak Cosmological Constant Problem*: Just as we do not understand why the value of Λ is so small, we also do not understand why it is so close to zero but not exactly zero. Current cosmological observations, paired with relativity theory, indicate that there may be a vacuum energy density of order 10^{-120}.

[4]Here, we assume that the curvature constant, k, is zero.

3. *The New Cosmological Constant Problem*: Curiously, the current value of the energy density associated with Λ is comparable to the present mass density. This is also known as the *coincidence problem*.

The old cosmological constant problem is so named because its existence predates observations that indicate the existence of a vacuum energy. In fact, before the discovery of cosmic acceleration, it was a problem that had worried quantum field theorists for decades. The missing energy could not be accounted for in experiment, and it was not clear why. The 1998 discovery of cosmic acceleration added an additional constraint and mystery in the form of the weak cosmological constant problem. The old problem, instead of being eliminated, was compounded by the discovery of an apparent vacuum energy that is incredibly close to zero but just large enough to be noticeably non-zero. It also introduced astrophysical concerns more directly into the phenomenological discussion about vacuum energy. Reconsidering the old cosmological constant problem in the context of the weak problem could be taken to imply that these questions are tied to the larger discussion of how quantum field theory is related to general relativity. In other words, it could be seen as one edge of the multifacted quantum gravity problem.

From a phenomenological perspective, a particularly attractive model of cosmic acceleration that could better address the aforementioned three issues would supplant Λ in cosmological models. While quintessence could potentially explain the cosmic acceleration, addressing the weak cosmological constant problem and the new cosmological constant problem requires fine-tuning of the quintessence field. This is nearly as unsatisfactory as the cosmological constant itself. Chapter 4 and Chapter 5 describe approaches that seek alternative approaches.

CHAPTER 3

Quantum Gravity

3.1 What is Quantum Gravity?

Quantum gravity is a theorized self-consistent union of quantum mechanics with general relativity. It is widely believed that a theory of quantum gravity exists, and research into models of quantum gravity such as string theory, loop quantum gravity, spin foams, causal sets and causal dynamical triangulations is part of an active effort to understand physics at its most fundamental level. Indeed, each model of quantum gravity inspires passionate advocates who all disagree with one another about the proposed properties of the unified theory, and it would be impossible to properly survey all of the ideas here. In view of the broadness and depth of quantum gravity models and their contents, I will only attempt to provide a brief overview of a few topics in the field that are relevant to problems presented later in this thesis.

3.2 Scales and Units in Quantum Gravity

Because general relativity and the standard model have been so successful in the regimes of study where they naturally arose, gravity and particle physics, respectively, a natural question arises in the discussion of their merger. These two theories are dominant at scales that are orders of magnitude apart from each other.[1] It is reasonable to therefore wonder about the scale at which must we be concerned with the need for a quantum gravity. Knowing very little about how the theory is manifest makes this a unique challenge.

Dimensional analysis has given rise to the expectation that quantum gravity becomes not only relevant but necessary at the Planck scale. This is a scale defined solely by the five universal constants:

1. Newton's gravitational constant, G
2. The speed of light, c
3. The Planck constant, h, which is often modulated by 2π and denoted as $\hbar$.

By combining these constants to achieve the appropriate dimensions, a Planck mass, Planck length, Planck time, Planck charge, and Planck temperature can be defined, and from these, other units such as the Planck energy can be extrapolated.

A sense of scale can be gotten by considering the Planck length, $l_p = \sqrt{\frac{\hbar G}{c^3}} = 1.6$ x 10^{-35} m, and the Planck energy, $E_p = 1.22$ x 10^{19} GeV. From the point of view of position space, quantum gravity is relevant at extremely small scales that are far

[1] This is understood as differences in order of magnitude between the coupling constants associated with the models, such as Newton's constant G or Λ, the quantum chromodynamics scale.

removed from every day human life, while from the point of view of momentum space we are concerned with extremely large scales.

As we shall see below, dimensional considerations can be further useful in trying to predict quantum gravity phenomenology. For example, in the case of Hawking radiation, we consider quantum effects when the curvature of a black hole spacetime is not comparable to the Planck length. In other words, we expect our approximation to be effective up to the Planck scale.

3.3 Emergence and Background Independence in Quantum Gravity

Quantum gravity models, at least in the minds of many of their exponents, tend to fall into two categories: background dependent and background independent. Background independence, in physical terms, means independence of the background space-time's geometry. More formally, this is known as diffeomorphism invariance and General Relativity is an example of a background independent/diffeomorphism invariant theory. On the other hand, the Standard Model of particle physics is an example of a background dependent theory. It requires a fixed, flat background and at the moment does not contain gravitational interactions.

String theory takes its cue from the Standard Model and can be construed as background dependent, whereas models like loop quantum gravity are much more concerned with respecting background independence from the start.[2] I mention these

[2]It is hoped by theorists, both strings and non- alike, that the background dependence of String Theory is a temporary concern that can be worked out in the long run.

ideas with the caveat that it is generally agreed that ideally, a complete model will be background independent. The disagreement lies more in the question of when background (in)dependence becomes relevant as a tool in the process of discovering a complete model for quantum gravity. Rovelli [29] provides a much more thorough discussion of this topic than I can provide here. Smolin [30] also provides an overview of background independent approaches to quantum gravity.

It is likely safe to say that those working on background independent formulations have typically been more immediately interested in the question of "emergence" in quantum gravity. Whereas String Theory's approach begins with a background populated by the Standard Model, background independent approaches seek to begin with an abstract concept of quantum gravity that in the appropriate limits reproduces General Relativity and the Standard Model/relativistic quantum mechanics. Hu [31] provides an overview of different approaches to the emergence of quantum gravity itself.

3.4 Quantum Gravity Phenomenology

Indeed, background independence does not easily lend itself to low-energy limits. An example of an effort to resolve this includes that of doubly/deformed special relativity (DSR).[3] A short note by DeDeo & Prescod-Weinstein [32] summarizes some potential pitfalls, and Hossenfelder [33] pursues this line of thinking in greater detail.

When considering ways to approach the problem of quantum gravity, this can be done from the point of view of fundamental questions, and String Theory, Causal

[3]See Smolin [30] for an overview of the current state of DSR.

Dynamical Triangulations, and Spin Foams are all examples of approaches that seek to resolve the question by constructing a model from the ground up. Another approach is from the opposite direction: we consider potential phenomenological behavior of quantum gravity and guided by those results attempt to trace our way upwards to a more complete picture.

While the question of emergence in background-independent approaches to quantum gravity raises challenges, it also opens doors to creative speculation and possible resolution of standing problems in related fields. The work in Chapter 4, which also appeared as a journal paper [34] is an example of the application of ansatzes motivated by quantum gravity to the cosmic expansion problem of cosmology.

A major structural test of that particular model will be feasible once the question of coarse graining from an abstract quantum gravity to classical general relativity is better understood and/or addressed. In saying so, I do not mean to minimize the challenge associated with coarse graining. Understanding how to go from microscopic, as in Planck-level, scales to the relatively macroscopic scale of particle physics and truly macroscopic scale of general relativity could be said to be one way of framing the genuine phenomenological challenge of producing a complete model of quantum gravity. From our elegant stringy and loopy ideas, we must somehow be able to reproduce the limits that dominate the scales that are readily observable in astrophysics as well as in day to day life. The work of Chapter 4 is in part a response to this consideration.

3.5 Some Comments on Semiclassical Gravity & Hawking Radiation

Semiclassical gravity could be said to be slightly more general than quantum gravity phenomenology typically is. It seeks to study quantum gravity via approximation and unlike quantum gravity phenomenology, it is grounded in well understood mathematical and physical constructs. Matter is treated as quantum mechanical fields while gravity is described classically using GR.

The study of semiclassical gravity generally falls within the purview of quantum field theory in curved spaces (QFTCS). The study of QFTCS provides an indication of what results from a more complete theory of quantum gravity might look like. An immediate result, for example, turns out to be that measuring the number of particles in the vacuum depends on the path of the vacuum's observer in spacetime. This is known as the Unruh effect [35, 36, 37].

The semiclassical result most relevant to the present work is the discovery of a phenomenon related to the Unruh effect: Bekenstein-Hawking radiation [38, 39, 40, 41] and the associated Hawking temperature. As texts such as Birrell and Davies [42] describe the Unruh effect and Hawking radiation in great technical detail, I will only mention a few qualitative facts about the topic.

We assume matter fields obey wave equations with the flat space Minkowski metric replaced by a more general (curved) metric, $g_{\mu\nu}$. The source of Einstein's equation is the expectation value of $T_{\mu\nu}$ for these matter fields. Immediately there is trouble trying to do quantum field theory in such a scenario. We start by considering the Unruh effect in Rindler space, which is how flat Minkowski space appears to an accel-

erating observer, where an accelerating observer, as opposed to an inertial observer, is defined as one who is moving with constant acceleration in Minkowski space.[4]

Typically, we define a quantum field theory in terms of annihilation and creation operators. These operators are so named because they reduce or increase the number of particles, respectively, in whatever state they are applied to. In Rindler space one tries to decompose them into positive and negative frequencies, curved spacetime does not allow for invariant definitions of these frequencies. The creation and annihilation operators for the mass field are therefore not uniquely determined, leading inertial observer and a Rindler observer to take vacuum measurements that may not agree. Some mathematical study shows that this leads to the fascinating result that an accelerating observer will observe a thermal spectrum of particles:

$$T = \frac{a}{2\pi}, \tag{3.1}$$

where T is the temperature, and a determines the acceleration of the observer (and completely unrelated to any cosmological parameters mentioned elsewhere in this work).

Generalizing to the curved space of a Schwarzschild black hole, the Hawking Temperature will take a slightly more general form:

$$T = \frac{\kappa}{2\pi}, \tag{3.2}$$

[4]It's worth mentioning that the structure of Rindler space for radii greater than the Schwarzschild radius, is very similar to that of a Schwarzschild black hole.

where κ is the surface gravity. There is an associated entropy given by:

$$S = \frac{A}{4G}, \tag{3.3}$$

where A is the surface area of a black hole horizon.

Smolin [43] and Ansari's [44] work connect the study of Planck-scale phenomenology with issues relating to black hole radiation. An example of a different nature is provided in Chapter 5, where the cosmic expansion problem is resolved via what we termed the *Trans-Planckian ansatz* that could lead to the entire model being characterized as semiclassical.[5] The ansatz relies on relating the Hawking temperature, as scaled by the Planck temperature, to the maximum redshift at the horizon of a Schwarzschild-like black hole in the gravitational aether.

[5]The term "Trans-Planckian ansatz" is inspired by what is known as the *trans-planckian problem*, where depending on frame of reference a particle may have energy that is larger than the Planck energy, which is considered a natural limit.

CHAPTER 4

Non-Locality, Quantum Gravity and Cosmic Acceleration

4.1 Introduction

In this chapter, we discuss a new cosmological scenario in which the consequences of the quantum mechanical nature of spacetime contributes to observable phenomena throughout the lifetime of the universe[45].[1] The movitation is, as proposed in [15, 16], a generic consequence of spacetime having a quantum microscopic structure: that *locality is disordered*. In this scenario, there are small departures from the locality that is typically described by the classical metric occurring on every scale. As we shall show here, this can happen in such a way that it allows a scenario where these departures from locality will be very difficult to see in terrestrial experiments, all the while playing a significant role in the history of the universe on the largest scales.

[1] The majority of this chapter appeared as a publication with L. Smolin in Physical Review D [34]. I have made changes to the contents involving direct discussion of cosmology as well as minor changes elsewhere. The fundamental results remain the same.

As was argued in [15, 16, 46, 47, 48], disordered locality is a natural consequence of the hypothesis that the classical spacetime geometry described by general relativity is an emergent, macroscopic description that captures some but not all of the properties of an underlying microscopic quantum spacetime geometry. This is analogous to the sense in which the continuous description of matter in terms of smooth, thermodynamic quantities approximates some, but not all, of the properties of the underlying atomic physics. In that case, we find proof of the existence of the underlying atomic physics in fluctuations around the continuum description as well as in dis-orderings of classical quantities. If macroscopic locality, as defined by the classical metric, is an approximate and emergent quantity, we may also expect that small departures from macrolocality[2] will be natural indicators of an underlying quantum geometry [16, 46, 47, 48].

Our considerations are rather general and apply to many of the models of quantum gravity that are presently under study. What we assume is only the following schema, which is common to several background-independent approaches to quantum gravity:

- A microscopic model of spacetime, described in terms of states labeled by discrete combinatorial structures, can be represented by graphs. These graphs may be labeled or not, and they may or may not be imbedded up to topology in a background topological manifold.

- The dynamics of the theory leads the graph representing the quantum geometry to evolve by local moves. If there are labels on the nodes or edges of the graph these also evolve by local moves. Local moves are defined as moves between nearest neighbors as typically defined on graphs.

[2]Other possible cosmological consequences of this scenario are discussed in [46, 47, 48, 49].

- The nodes are associated with regions of Planck scale volume. When the state is semiclassical then one can define an emergent classical metric q_{ab}, slowly varying on the Planck scale, such that there is an appropriate correspondence between volumes measured by the classical metric q_{ab} and volumes as determined by counting nodes in the graph that defines the quantum geometry.

- There is some effective description of the dynamics of the labels on the graphs that gives rise to an effective quantum field theory for matter fields on the semiclassical spacetime that is given by a metric q_{ab}.

We emphasize that in all these models the classical metric is an emergent degree of freedom. In other words, the classical metric is not specified by the fundamental kinematics or dynamics of the theory.

In different models of quantum gravity, the microscopic states and their correspondence with an emergent classical geometry are defined differently, but all that we need for this paper are fundamental states that can be described in terms of graphs with a correspondence to an emergent classical geometry.

For example, in loop quantum gravity, the state Ψ has support on a basis of graphs Γ embedded in a bare three manifold Σ with no metric or classical fields. If the state Ψ is semiclassical, or corresponds to a low temperature phase, it will have a course graining that defines a metric q_{ab} on Σ.

In causal dynamical triangulation models the graph is dual to a triangulation of a manifold. This is the case also in Regge calculus models. In the recently proposed quantum graphity models, the graph is an arbitrary subgraph of the complete graph

on N nodes. In matrix models, the matrices can be thought of as defining graphs, whose edges are labeled by the values of the corresponding off-diagonal elements.

In this chapter we want to focus on a common feature of how locality is described in all these models, which is that there are actually two notions of locality. The first is a *microscopic notion of locality*, which is defined by the connectivity of the graph, Γ. This is fundamental because it defines which degrees of freedom are coupled by the fundamental dynamics and are therefore always present.[3]

There is a second, *macroscopic notion of locality* which is present only when the state is semiclassical so that an emergent classical metric can be defined. We say in such cases that the emergent metric gives rise to a second notion of locality.

It has been pointed out in [45, 16] that these two notions of locality may not completely coincide, even in the case when the quantum state defines an emergent classical metric, q_{ab}.

More precisely, we say that *locality is ordered* when macro-locality is defined and it coincides with micro-locality. This means that each edge in Γ connect two nodes whose coarse grained descriptions map to Planck size regions in Σ, that are of the order of l_{Pl} apart, as defined by the classical metric, q_{ab}.

On the other hand, we say that *locality is disordered* when there are links in Γ that connect nodes which are far apart in Σ, compared to the Planck scale, as measured by q_{ab}. This means that the links in Γ can be divided into a set of *local links* which connect nodes of order l_{Planck} apart in the semiclassical metric q_{ab} and the rest, which are non-local links.

[3]If the state is composed of a superposition of micro-local states labeled by graphs then micro-locality is defined seperately for each state in the superposition.

Sometimes it is helpful to describe a state of disordered locality directly in terms of the classical geometry. We can do this by considering the two points in the manifold corresponding to the two ends of a non-local link as being identified in the classical geometry. From a classical point of view, we may thus regard the topology of the spatial slice as Σ with many pairs of points identified.

In this chapter we want to consider the possibility that there may be observable consequences of disordered locality. We find that there are such consequences and that one consequence gives a possible explanation for the apparent presence of a dark energy which is causing the recently discovered cosmic acceleration.

We note that given that in such models there may be 10^{180} nodes to the graph within the present comoving volume[4], there is plenty of room for disordering of locality to be rare in the sense that a very small subset of these nodes will be ends of non-local connections. At the same time, the numbers of such non-local connections can still be very large. Consider for example, the possibility that within the present comoving volume there are 10^{100} non-local links. This is still extremely small compared to the roughly 10^{180} local links, and even smaller compared to the 10^{360} possible non-local links. In this kind of range there can be many non-local links within a comoving volume and still be an essentially zero probability that there be one both of whose ends are contained within a terrestrial laboratory. In this case they can be both common cosmologically and very difficult to detect locally.

We note that any good model of quantum gravity in which the classical metric is emergent will have to explain why disordered locality is rare enough not to dis-

[4]We define the comoving volume in the typical fashion, as determined by the length scale associated with comoving coordinates and scale factor a.

rupt local physics. We do not address how this suppression is accomplished in this chapter and simply assume we are working with a theory in which it is. At the same time we note that there is plenty of room for disordered locality to be sufficiently suppressed that we could not yet have detected it, while still leaving very many non-local connections within a comoving volume. We are interested then in the possible new phenomena that may come from disordered locality in this range.

Because our concern is for the observational consequences of disordered locality there are several questions we do not address, because we assume that a successful model of quantum geometry will provide answers for them. These are:

1. We assume that we are discussing a semiclassical state with an emergent classical metric which, together with some emergent matter fields, defines a solution to Einstein's equations and can be described by classical general relativity.

2. We assume that there is a small amount of disordered locality, small enough that it does not disrupt the experiments by which local quantum field theory is confirmed.

Given these assumptions we describe in the next section a simple modification of the Friedmann-Robertson-Walker (FRW) cosmology in which a small amount of disordered locality has been applied. In the section following we see that this can, under two further assumptions, lead to a model of dark energy.

4.2 A Cosmological Model With Disordered Locality

Based on the ideas just described we propose a simple model of disordered locality in cosmology. We start with the standard local model of the universe in general relativity, the FRW model. The classical metric is as usual

$$ds^2 = -\mathcal{N}^2 dt^2 + a^2(t) q^0_{ij} dx^i dx^j, \tag{4.1}$$

where q^0_{ij} is a flat dimensionless metric on R^3. This 3+1 splitting is made necessary by the nature of this particular model.

At each time t, we fix a region of volume $a^3(t)$. We pick $N_{NL}(t)$ pairs of points (x_I, y_I), for $I = 1, ..., N_{NL}$, and we identify the members of each pair as being connected by a non-local link.

The selection of pairs of points related by non-local links defines a distribution $P(x, y, t)$, given by

$$P(x, y, t) = \frac{1}{2} \left(\sum_I \delta^3(x, x_I)\delta^3(y, y_I) + \delta^3(y, x_I)\delta^3(x, y_I) \right). \tag{4.2}$$

This is a density in the points x and y. It follows that

$$N_{R_1 R_2}(t) = \int_{R_1} d^3x \int_{R_2} d^3y \; P(x, y, t) \tag{4.3}$$

is the number of non-local connections between the regions R_1 and R_2 at time t.

When we integrate over the comoving volume we have

$$N^{NL}(t) = \int_a d^3x \int_a d^3y \; P(x, y, t), \tag{4.4}$$

which are the number of non-local links both of whose ends lie within the comoving volume at time t.

Below, we study a simple model defined by four assumptions[45].

1. The distribution of non-local connections is scale invariant and can depend only on the present $a(t)$ and the Planck scale.

2. For simplicity, all the non-local links will be considered to have both ends within the present comoving volume.

3. The distribution is otherwise random. There is no correlation between the two ends of a non-local link except that both are within a comoving volume, and no correlations between non-local links.

4. The time dependence of the distribution is given by

$$N_{NL}(a) = N_0 \left(\frac{a}{a_0} \right)^p \tag{4.5}$$

for some p.

Below we shall discover that $p = 3$ is necessary to arrive at a model of dark energy with equation of state parameter, $w = -1$. When the equation of state parameter has this value, the dark energy model "simplifies" to a cosmological constant.[5] This

[5]see Chapter 2 for more in depth discussion of the so-called "simplicity" of the cosmological constant model.

means that the number of non-local links within the comoving volume increases in time proportionately to the comoving volume.

This model follows from the basic assumptions of the scenario. Any dependence on the initial scale a_0 would by now either have scaled away, if it was fixed, or grown with the comoving flow and so be represented by the present scale factor.[6] Any dependence on any other scale would be unnatural.

4.3 The energetics of non-locality

We now consider the effects of the matter and gravitational degrees of freedom interacting across the non-local links. A simple model of degrees of freedom on the fundamental graph defining the quantum gravity model is to assume that there are dimensionless spin variables σ_n on each node of the graph. These can stand for gravitational degrees of freedom such as the labelings on a spin network in loop quantum gravity, or the orientation of a simplex in causal dynamical triangulations. They may also stand for matter degrees of freedom.

For the model we are building we do not need to know the nature of these degrees of freedom. It may not even be possible to distinguish between matter and gravitational degrees of freedom at this level, as in the quantum graphity models. We only need to assume that there is a local contribution to the hamiltonian coming from nearest

[6]While a_0 is usually defined to mean the value of the scale factor in the present day, for this work, we define it to mean the initial scale where the classical metric, and thus a concept of the scale factor, is emergent.

neighbor couplings, which are of the simplest possible form:

$$H^{matter} = -\epsilon \frac{1}{l_{Pl}} \sum_{<mn>} \sigma_m \cdot \sigma_n. \tag{4.6}$$

There is one coupling for each nearest neighbor pair $< mn >$ on the graph, and ϵ is a sign which is $+$ for ferromagnetic coupling and $-$ for antiferromagnetic coupling. The $l_{Pl}^2 = \hbar G$ is the gravitational coupling constant of matter to gravity. It is the only dimensional parameter that appears in the fundamental hamiltonian. There may be several σ_n, which we have allowed for by writing the interaction in terms of a product $(\cdot)$ in an internal space.

Given a graph Γ with non-local links, the sum in eq. (4.6) splits into two sums, the first over local links in the graph Γ, the second over non-local links.

$$H^{matter} = H^{local} + H^{NL}, \tag{4.7}$$

where the former is the sum over pairs of nodes connected by local links in the graph and H^{NL} is the sum over non-local links:

$$H^{NL} = -\epsilon \frac{1}{l_{Pl}} \sum_{<mn>}^{\text{non-local}} \sigma_m \cdot \sigma_n. \tag{4.8}$$

It is straightforward to show that the local piece H^{local} can be approximated in terms of a matter field. We can make the identification of a scalar field

$$\phi(x_n) = \frac{1}{l_{Pl}} \sigma_n, \tag{4.9}$$

where x_n is the position in the manifold of the node v_n. In the case that the local links of the graph form a regular lattice with lattice spacing l_{Pl} we can identify

$$\partial_a \phi(x_n) = \frac{1}{l_{Pl}^2} \left(\sigma_{n+\hat{a}} - \sigma_n\right). \tag{4.10}$$

If we recall also that we can make the replacement

$$\sum_n l_{Pl}^3 \to \int d^3x \sqrt{q}. \tag{4.11}$$

The local part of the Hamiltonian becomes

$$H^{local} = \frac{\epsilon}{2} \int d^3x \sqrt{q(x)} \left[q^{ab} \partial_a \phi \partial_b \phi - \mu^2 \phi^2\right], \tag{4.12}$$

where the mass is $\mu^2 = \frac{\sqrt{2}}{l_{Pl}}$.

This is all due to well understood theory, and we have gone through it to ensure that the normalization of the microscopic Hamiltonian is correct. We must now consider what becomes of the non-local piece (4.8) in this scenario.

To write the non-local piece, we keep the field dimensionless and write

$$\sigma(x_n) = \sigma_n. \tag{4.13}$$

The non-local part of the Hamiltonian is then

$$H^{NL} = -\frac{\epsilon}{l_{Pl}} \sum_I^{\text{non-local}} \sigma(x_I) \cdot \sigma(y_I). \tag{4.14}$$

The exact positions of the ends of the non-local links cannot, by definition, be important because we have assumed they are chosen randomly within the comoving volume. Because of that we would like to perform an average of (4.14) over an ensemble of possible positions of the end of the non-local links. We will denote this with an overbar $\bar{H}^{NL}$.

$$\bar{H}^{NL} = \left\langle -\frac{\epsilon}{l_{Pl}} \sum_{I}^{\text{non-local}} \sigma(x_I) \cdot \sigma(y_I) \right\rangle_{\text{non-local edge placement}} . \tag{4.15}$$

To aid the computation of this average we want to define the average value of σ over a region $\mathcal{R}$

$$\langle \sigma \rangle_{\mathcal{R}} = \frac{\int_{\mathcal{R}} \sqrt{q}\sigma}{\int_{\mathcal{R}} \sqrt{q}}. \tag{4.16}$$

The average energy between two regions $\mathcal{R}_1$ and $\mathcal{R}_2$ connected by N_{12} non-local links is then given by

$$\bar{H}_{12} = -\frac{\epsilon}{l_{Pl}} N_{12} \langle \sigma \rangle_{\mathcal{R}_1} \cdot \langle \sigma \rangle_{\mathcal{R}_2}. \tag{4.17}$$

This step is similar to the annealing approximation used in treatments of small world networks [50, 51, 52].

We can take the two regions to be the same, and to be the comoving volume. In that case we have

$$\bar{H}^{NL} = -\frac{\epsilon}{l_{Pl}} N^{NL}(t) \langle \sigma \rangle_a \cdot \langle \sigma \rangle_a, \tag{4.18}$$

where $\langle \sigma \rangle_a$ is the average field over the comoving volume.

To complete the computation of the contribution of the non-local links to the energy let us recall the assumption made above about the evolution of $N^{NL}(t)$ in

time, eq (4.5),

$$H^{NL} = -\frac{\epsilon}{l_{Pl}} \frac{N_0}{a_0^p} \left(\int_a d^3x \sqrt{q} \right)^{\frac{p}{3}} \langle \sigma \rangle_a \cdot \langle \sigma \rangle_a, \tag{4.19}$$

where the $\int_a$ denotes an integral over the comoving volume. We now choose $p = 3$ so that

$$H^{NL} = -\frac{\epsilon}{l_{Pl}} \frac{N_0}{a_0^3} \left(\int_a d^3x \sqrt{q} \right) \langle \sigma \rangle_a \cdot \langle \sigma \rangle_a. \tag{4.20}$$

We next write the corresponding contribution to the effective action, which is then

$$S^{NL} = \int dt \mathcal{N} H^{NL} = -\frac{\epsilon}{l_{Pl}} \frac{N_0}{a_0^3} \int_a d^4x \sqrt{-g} \ \langle \sigma \rangle_a^2. \tag{4.21}$$

This gives rise to a contribution to the effective energy-momentum tensor, which is given by

$$T^{ab} = \frac{1}{\sqrt{-g}} \frac{\delta S^{NL}}{\delta g_{ab}} = -g^{ab} m^4 \langle \sigma \rangle_a^2, \tag{4.22}$$

where the effective mass is given by

$$m^4 = -\frac{\epsilon}{2 l_{Pl}} \frac{N_0}{a_0^3}. \tag{4.23}$$

We see why $p = 3$ was necessary to get a contribution to the energy-momentum tensor with $w = -1$. Otherwise we would not get an energy momentum tensor proportional to the spacetime metric, g^{ab}.

4.4 A possible contribution to dark energy

We have derived a contribution to the energy momentum tensor from the presence of non-local links and the assumption that there are microscopic degrees of freedom that can be identified with spin like variables on the nodes of the graph representing the microscopic quantum geometry. Note that we reached (4.23) by assuming that the spin variable is slowly varying on the comoving scale, hence we can only consider this as a contribution to the homogeneous approximation of the Einstein equations. Other approximations will be needed to draw out consequences for smaller scales.

Nonetheless, we would like to see if we get a reasonable contribution to the dark energy. Before continuing, it is worth taking a moment to say what we mean by "dark energy." Fundamentally we are interested in providing an explanation for the presence of cosmic acceleration. Since the discovery of this phenomenon, there has been renewed interest in Einstein's cosmological constant, which for decades remained a concern of those interested in the details of quantum field theory. Alternatives to the cosmological constant as an explanation for the acceleration were proposed, including quintessence [53].

Because the cosmological constant is a special case of all such models, the phrase "dark energy" is often used to describe proposals to explain the acceleration that go beyond the constant. In essence, it refers to the percentage of the universe's critical density that is composed of the vacuum energy that is pushing our universe outward. Here, we refer to the dark energy, but will primarily focus on the case where the equation of state parameter for this mysterious fluid is set as $w = -1$, i.e. the cosmological constant case. Future efforts to study models like this one might

incorporate attempts to reproduce more complex models, such as dynamical equation of state parameters.

Note first that the observed dark energy is positive. This suggests that $\epsilon = -1$ which implies that the microscopic couplings are anti-ferromagnetic. Next, since the $\sigma(x)$ are dimensionless, we can assume that they are order unity at the present time. Thus, we want to write (4.22) as

$$T^{ab} = -g^{ab} V(\langle\sigma\rangle_a) \tag{4.24}$$

with

$$V(\langle\sigma\rangle_a) = -m^4 \langle\sigma(x_I)\rangle_a^2. \tag{4.25}$$

We want this to be of order $\frac{\Lambda}{G} \approx \frac{10^{-120}}{l_{Pl}^4}$. Since the $\langle\sigma\rangle$ are assumed to be of order unity this tells us that

$$m^4 = \frac{N_0}{2 l_{Pl} a_0^3} = \frac{10^{-120}}{l_{Pl}^4}. \tag{4.26}$$

Let us evaluate this at present. This implies that

$$N^{NL}(\text{now}) = 10^{-120} \left(\frac{a_{now}}{l_{Pl}}\right)^3 \approx 10^{60}. \tag{4.27}$$

That is, to get the present value of dark energy from this model one needs to assume that there are 10^{60} non-local links within the present comoving volume of $\approx 10^{180}$ Planck volumes. This means that the non-local links are very sparce, i.e. only one in 10^{120} nodes is an end of a non-local links. There is only one non-local link end for every region of radius $100km$ on a side.

This number is not surprising, because each end of a non-local link contributes

roughly a Planck energy per this volume and it is easy to confirm that this adds up to a dark energy with a present value that is comparable to the one that is observed. However, we should check that this density of non-local links does not easily lead to contradictions with experiment. One might expect that the effect of an interaction between an elementary particle and a non-local link end carrying a Planck energy would be visible – it might cause a proton to decay or mimic the strike of a cosmic ray carrying a Planck energy of kinetic energy. Initial back of the envelope calculations indicate that the frequency of decay would be very low and within present bounds due to the *AUGER* detector. However, future work is required to better understand this issue.

4.5 Conclusions

We have proposed a new cosmological scenario in which the consequences of spacetime being quantum mechanical contribute to observable phenomena throughout the lifetime of the universe. We explore the possibility that disordered microscopic locality could lead to observable disordered locality at a macroscopic scale, namely cosmological scales. The model we presented here is fairly general and some version of it could be applied to any theory of quantum gravity based on a concept of emergent gravity.

We find that, assuming non-nearest neighbor connections survive coarse graining, the existence of such objects at a macroscopic scale could lead to a contribution to the energy-momentum tensor that looks very much like a cosmological constant. In order to get the present value of the cosmological constant, we need to assume that there are 10^{60} non-local links within the present comoving volume of $\approx 10^{180}$ Planck

volumes.

Notable challenges are faced by such a model. No candidate for quantum gravity successfully describes coarse graining from quantum to classical gravity, making it impossible to evaluate the assumption that micro-non-locality would lead to macro-non-locality. Further investigation would also necessitate a more complete description of the microscopic nature of the non-local links. For example, one question to be answered is the rate at which these non-local link ends change nodes. Additionally, there is currently no unique observational signature that would distinguish this model from other dark energy pictures.

One way to "test" this model in comparison to others is to see how it measures up in addressing the old, weak and new cosmological constant questions as formulated in Section 2.3. The weak cosmological constant problem could be addressed by this model if we are able to discover a motivation for the number of non-local links. This could come from further work on background independent quantum gravity models, such as quantum graphity or spin foams. The old cosmological constant problem may be similarly addressed. Even as gravity is emergent in these kinds of quantum gravity models, there may be an emergence of quantum field theory that is distinct. This could explain a mismatch between vacuum measurements from the perspectives of each model. Future work may attempt to better understand how the presence of such non-local links could impact structure formation, thus attempting to address the new cosmological constant problem.

CHAPTER 5

Stellar-Mass Black Holes and Cosmic Acceleration

5.1 Introduction

This chapter addresses a novel approach to the challenge presented to us by the discovery of recent acceleration of cosmic expansion, which was one of the most surprising findings in modern cosmology [1, 2].[1] The standard cosmological model (also known as the concordance model) drives this expansion with a cosmological constant (CC). While the CC is consistent with (nearly) all current cosmological observations,[2] it requires an extreme fine-tuning of more than 60 orders of magnitude, known as *the cosmological constant problem* [27].

In the context of the concordance cosmological model, there are (at least) three different aspects of the CC problem. For decades, physicists worried about why the

[1] This chapter originally appeared as a publication with N. Afshordi and M. Balogh in Physical Review D [17]. It appears here with very minor changes.

[2] See [54] for an account of observational anomalies in the standard cosmological model.

value of the cosmological constant/vacuum energy seemed to be nearly zero by particle physics standards (known as the *old CC problem*)[55], and the conventional wisdom was that it should vanish exactly, as a result of a yet unknown symmetry of nature. The accelerated cosmic expansion has thus challenged us to address this question on two new fronts. First is the *new CC problem*: why is the vacuum energy density so close to zero, but non-vanishing? Second is the *coincidence problem*: Why did the dark energy dominance and structure formation happen at approximately coincident times?

The race is on to simultaneously address these three questions. A popular alternative approach to the cosmological constant is a model that modifies Einstein's theory of gravity. Traditionally, this involves adding higher order curvature terms to the geometric side of Einstein's equation. However, in [18], one of us proposed a novel approach to modified gravity. This model introduces *gravitational aether*, as a sufficient ingredient to decouple the quantum field theory vacuum from gravity while simultaneously satisfying other tests of gravity. Unlike many models of modified gravity, the gravitational aether model modifies the energy-momentum content of the spacetime, instead of adding higher order curvature terms.

In this model, the right hand side of the Einstein field equation is modified as:

$$(8\pi G')^{-1}G_{\mu\nu} = T_{\mu\nu} - \frac{1}{4}T^{\alpha}_{\alpha}g_{\mu\nu} + p'(u'_{\mu}u'_{\nu} + g_{\mu\nu}), \tag{5.1}$$

where G' is 4/3 times the Newton's constant, and p' and u'_{μ} are aether pressure and four-velocity that are fixed by requiring the conservation of the energy-momentum tensor, $T_{\mu\nu}$, and the Bianchi identity. As argued in [18], while consistent with precision

tests of gravity, this theory is preferred to the standard model by the combination of cosmological observations (with the notable exception of ^{4}He primordial abundance).

In this chapter, we pursue a detailed understanding of static spherical black hole solutions in the gravitational aether theory. The solution we find is, at first glance, a perturbed Schwarzschild metric. However, upon closer inspection we find that this perturbation is divergent both near to and far away from the horizon (where we refer to an infinite redshift surface as a horizon). Thus the static solution in the presence of gravitational aether is fundamentally different from Schwarzschild, which can be characterized as a UV-IR connection: the metric near and far from the horizon is set by the same integration constant. Here, we will explore possible meanings of this property, and whether the cosmological behavior is set by a *Trans-Planckian* ansatz close to the black hole horizon.

We note that the static black hole solution found here also applies to the cuscuton models [56, 57] which have the same energy-momentum tensor as the gravitational aether in the limit of vanishing cuscuton potential.

In Sec. 5.2, we introduce our gravitational aether black hole solution. We describe the properties of the solution, including a preferred coordinate system and the location of the event horizon. We also establish asymptotic properties of the black hole, which are characterized by the same integration constant both close in and far away from the horizon of the black hole.

Sec. 5.3 explores the Trans-Planckian ansatz, as a way to fix the aforementioned integration constant, through quantum gravity effects close to the horizon. We suggest a way to connect the presence of black holes to the existence of a pervasive pressure that behaves like dark energy on cosmological scales.

In Sec. 5.4, we present a study of the contribution that many such black holes would make to the global/cosmological structure of space-time, while Sec. 5.5 provides a census of average black hole mass through cosmic history, which translates into a prediction for the history of cosmic acceleration.

Finally, we will discuss open questions and future prospects in Sec. 5.6.

Throughout the paper, we use the natural Planck units: $\hbar = c = G_N = k_B = 1$. Moreover, we will replace pressure p' by $3p/4$ in Eq. (5.1), so that the vacuum field equations for the aether theory resembles general relativity sourced by a perfect fluid with pressure p and zero density.

5.2 Black Hole in Gravitational Aether

We find a solution for the static black hole in the Gravitational Aether model using assumptions similar to those that lead to the Schwarzschild solution. Namely, we assume a spacetime with no matter content, and we assume spherical symmetry. Given that the aether takes fluid form, the metric in this model is the same as the general static, spherically symmetric metric that describes the interior of a star, as modeled by a perfect fluid. The only notable divergence from the star model is the absence of a energy density (which typically takes form as matter and radiation in the star), leaving an energy-momentum tensor of the following form:

$$T_{\mu\nu} = p(u_\mu u_\nu + g_{\mu\nu}). \tag{5.2}$$

We find the following metric

$$ds^2 = -e^{2\phi}dt^2 + \left(1 - \frac{2m}{r}\right)^{-1} dr^2 + r^2 d\Omega^2, \tag{5.3}$$

where m is a constant mass parameter that is defined similarly to the Schwarzschild mass. The components obey the following differential equation, known as the Tolman-Oppenheimer-Volkoff equations [24]:

$$\frac{d\phi}{dr} = \frac{m + 4\pi r^3 p}{r(r - 2m)}, \tag{5.4}$$

$$\frac{dp}{dr} = \frac{-p(m + 4\pi r^3 p)}{r(r - 2m)}. \tag{5.5}$$

We see immediately that $\exp(\phi)$ and p are inversely related:

$$p = p_0 e^{-\phi}, \tag{5.6}$$

where p_0 is an integration constant. Notice that Eq. (5.6) is equivalent to the condition of hydrostatic equilibrium for aether, and is valid independent of the assumption of spherical symmetry, for any static spacetime. [3] Now, we may rewrite Eqn. 5.4:

$$\frac{d\phi}{dr} = \frac{m + 4\pi r^3 p_0 e^{-\phi}}{r(r - 2m)}. \tag{5.7}$$

We can solve this equation by noting that it is a first-order inhomogeneous linear

[3] This follows from the relativistic Euler equation:$(\rho + p)\mathbf{u} \cdot \nabla \mathbf{u} = -\nabla_\perp p$, assuming a static spacetime and zero density, $\rho = 0$.

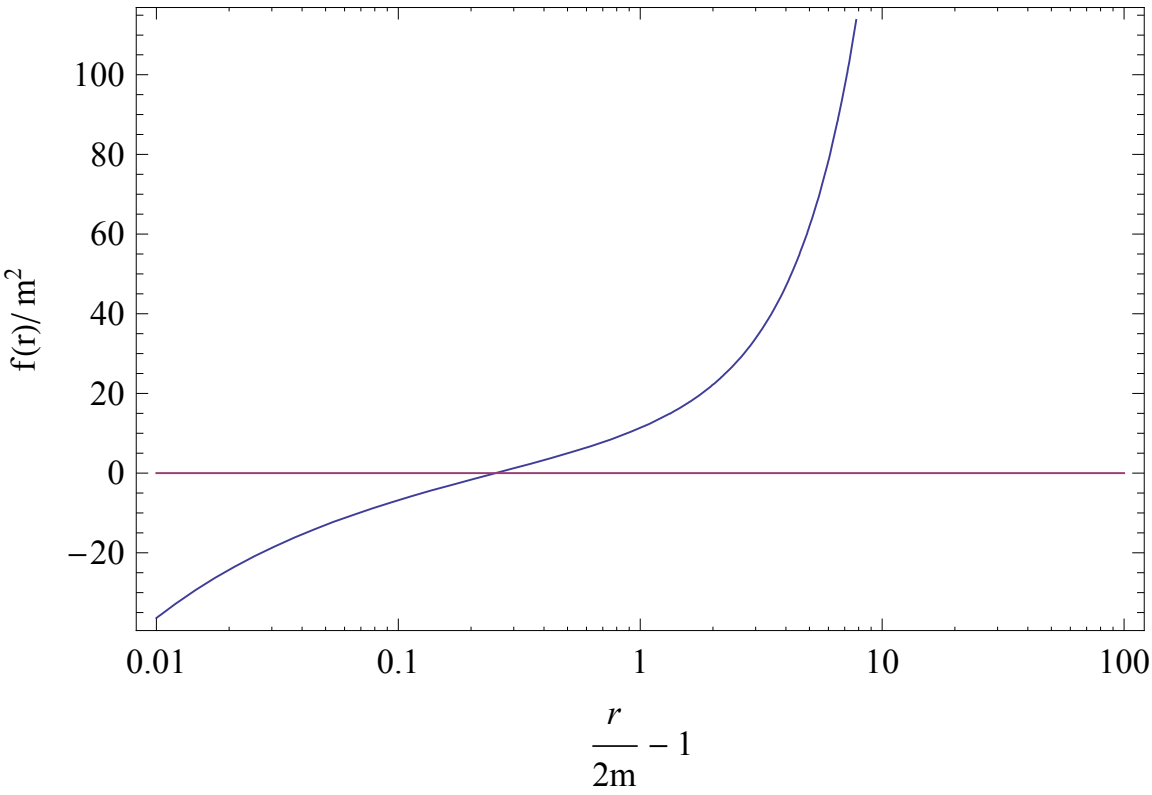

Figure 5.1: Function $f(r)$ [Eq. (5.10)] as a function of the distance from the Schwarzschild radius ($= 2m$). The deviation from the Schwarzschild metric is proportional to $p_0 f(r)$, where p_0 is the integration constant. If p_0 is small, as we argue in Section 5.3, the corrections only become important at the horizon, and on cosmological scales.

differential equation in e^{ϕ}, with the standard solution:

$$e^{\phi(r)} = 4\pi p_0 \left(1 - \frac{2m}{r}\right)^{\frac{1}{2}} \left[\int \frac{(1-\frac{2m}{r'})^{-1/2} r'^2}{r' - 2m} dr' + \text{const.}\right]. \tag{5.8}$$

To put this into more familiar terms, we can set the constant, so that we recover

the Schwarzschild solution as $p_0 \to 0$:

$$e^{\phi(r)} = \left(1 - \frac{2m}{r}\right)^{\frac{1}{2}} \left[4\pi p_0 f(r) + 1\right], \tag{5.9}$$

where $f(r)$ is given by:

$$\begin{aligned} f(r) = \frac{1}{2}\left(1 - \frac{2m}{r}\right)^{-1/2} & \left(-30m^2 + 5mr + r^2\right) \\ & + \frac{15}{2}m^2 \ln\left[\frac{r}{m} - 1 + \frac{r}{m}\left(1 - \frac{2m}{r}\right)^{1/2}\right], \end{aligned} \tag{5.10}$$

and is shown in Fig. (5.1). In the limit where r is large ($r \gg m$):

$$f(r) = \frac{r^2}{2} + 3mr + \mathcal{O}[m^2]. \tag{5.11}$$

while close to the "Schwarzschild horizon" we find:

$$f(r) = -8\frac{\sqrt{2}m^{5/2}}{\sqrt{-2m + r}} + \mathcal{O}[m^{3/2}(r - 2m)^{1/2}]. \tag{5.12}$$

Thus the correction to the Schwarzschild metric dominates in both UV and IR regimes (corresponding to close to and far from the BH horizon). This a nice tie, even for arbitrarily small values of the integration constant p_0. Therefore, a very suggestive conclusion is that, unlike in general relativity, the gravitational aether ties the formation of black hole horizons to cosmological dynamics.

But then, is there really an event horizon for this spacetime? Looking at the trace of the Einstein's equation, we find that the Ricci scalar is proportional to the pressure

of aether, p:

$$-R = 8\pi G'(T - T + \frac{9}{4}p) = 8\pi G'\frac{9}{4}p \tag{5.13}$$

This is, in turn, inversely proportional to the 00 component of the metric, e^{ϕ}. We define the surface where $e^{\phi} \to 0$ as the black hole horizon. Therefore the pressure at the horizon, and thus the Ricci scalar, goes to infinity ($p \propto \mathcal{R} \to \infty$) implying that this surface coincides with a real metric singularity (as opposed to a coordinate singularity).

It appears that that any static, spherically symmetric event horizon in a theory of gravitational aether (like the one we have modeled) coincides with a real metric singularity. In a traditional formulation of general relativity, such a scenario may be given to ambiguous physical interpretation. However, this may not be too surprising in few of the fact that a modified relativity will display properties divergent from traditional relativity. We expect that such a picture is best contextualized by a more comprehensive theory of quantum gravity.

Indeed, we conjecture that any process (for example, quantum gravity) that alleviates/regulates metric singularities will inevitably remove event horizons from the theory of gravitational aether. In other words, it is possible that static event horizons cannot exist in a UV completion of gravitational aether. This is independent of the assumption of spherical symmetry, and only relies on the aether hydrostatic equilibrium condition (5.6), which directly relates pressure to the Ricci curvature of the spacetime. However, we note that, as the singularity is a null surface, the spacetime does not violate the *weak cosmic censorship principle*.

Back to the spherical aether black hole spacetime (5.9), we now notice that the

static metric solution is only well-defined for $r \geq 2m$, as the solution becomes complex inside the Schwarzschild radius, $r < 2m$. More surprisingly, for negative values of p_0, unlike a Schwarzschild black hole, a free-falling observer can reach this boundary within a finite *coordinate* time. The reason is that the redshift of a static source at the Schwarzschild radius is now finite as seen by distant observers:[4]

$$\begin{aligned} 1+z &= e^{-\phi} \simeq \left[\left(1-\frac{2m}{r}\right)^{1/2} - 32\pi p_0 m^2\right]^{-1} \\ &< 1+z_{\max} = -\frac{1}{32\pi p_0 m^2}. \end{aligned} \tag{5.14}$$

As to what happens inside $r = 2m$, it is clear that our current choice of coordinates do not give us a physical metric for $r < 2m$, and if the conjectures above are correct, we may not need such coordinates. However, is it possible that with an appropriate choice of coordinate, we can analytically continue the static solution beyond the Schwarzschild radius? Indeed, we can define a new radial coordinate:

$$\begin{aligned} \lambda &\equiv \int_{2m}^{r} dr' \sqrt{g_{rr}} = \int_{2m}^{r} dr' \left(1-\frac{2m}{r'}\right)^{-1/2} \\ &= 2\left[2m(r-2m)\right]^{1/2} + \mathcal{O}\left[(r-2m)^{3/2} m^{-1/2}\right], \end{aligned} \tag{5.15}$$

which is equivalent to the constant-time proper radial distance. In terms of λ, the metric takes the form:

$$ds^2 = -e^{2\phi} dt^2 + d\lambda^2 + r(\lambda)^2 d\Omega^2, \tag{5.16}$$

[4]Here, distant observers are located at $2m \ll r \ll (-p_0)^{-1/2}$.

where

$$e^{\phi} = -32\pi p_0 m^2 + \frac{\lambda}{4m} + \mathcal{O}[p_0\lambda^2, \lambda^3 m^{-3/2}], \tag{5.17}$$

$$r(\lambda) = 2m + \frac{\lambda^2}{8m} + \mathcal{O}[\lambda^4/m^2]. \tag{5.18}$$

In other words, the metric is analytic and real in terms of the new radial coordinate, λ, at and beyond the Schwarzschild radius, which now corresponds to $\lambda = 0$. Moreover, a static event horizon, which as we argued corresponds to a real curvature singularity, now exists for all (small) values of p_0, as $e^{\phi} = 0$ at:

$$\lambda_H \simeq 128\pi p_0 m^3. \tag{5.19}$$

In the next section, we study the implications of this solution for cosmology. However, we shall postpone a full investigation of the causal structure of this spacetime, as well as its possible analytic continuations, to future studies.

5.3 Trans-Planckian Ansatz and Cosmic Acceleration

In the last section, we saw that within spherically symmetric spacetimes in the gravitational aether theory, the integration constant p_0 ties the geometry close to the horizon to the geometry at infinity. While, in the classical theory, p_0 is an arbitrary integration constant, here we speculate that its value is fixed by quantum gravity effects, especially since the horizon is now a curvature singularity, where quantum

gravity effects should become important.

We first note that the temperature of sources that fall through the Schwarzschild horizon, as seen by distant observers, approaches the Hawking temperature [58]:

$$T_H = \frac{1}{8\pi m}, \tag{5.20}$$

Furthermore, we assume that the maximum rest-frame temperature of sources is comparable to the Planck temperature (or one in Planck units):

$$T_{\max} = \theta_P = \mathcal{O}[1]. \tag{5.21}$$

Here, θ_P is a dimensionless constant that measures $T_{\max}$ in units of Planck temperature, which we shall call the Trans-Planckian parameter. We then adopt the *Trans-Planckian ansatz*, which is the idea that the maximum redshift at Schwarzschild radius (Eq. 5.14) is roughly set by the ratio of the Planck to Hawking temperatures:

$$1 + z_{\max} = -\frac{1}{32\pi p_0 m^2} = \frac{T_{\max}}{T_H} = 8\pi\theta_P m, \tag{5.22}$$

or

$$p_0 = -\frac{1}{256\pi^2\theta_P m^3}. \tag{5.23}$$

With this ansatz, we further see that:

$$\lambda_H = -\frac{1}{2\pi\theta_P} = \mathcal{O}[1], \tag{5.24}$$

i.e. the event horizon is roughly a Planck length away from the Schwarzschild radius.

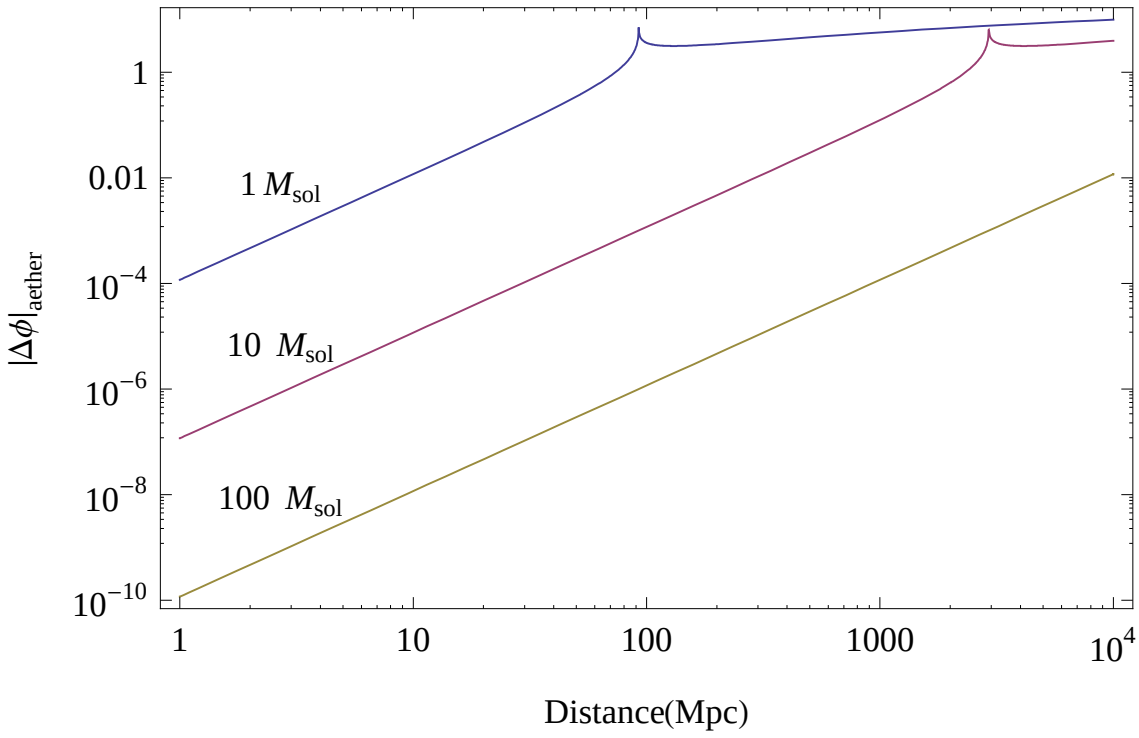

Figure 5.2: Predicted large distance deviation from the vacuum Schwarzschild solution for 1, 10, and 100 $M_\odot$ black holes, based on the Trans-Planckian ansatz. Here, we assumed $\theta_P = 100$ in Eq. (5.23) for non-rotating black holes to find p_0, which is then plugged into Eq. (5.9) to find the metric. As pointed out in the text, the corrections become important on today's cosmological horizon scale for solar/stellar-mass black holes.

Equivalently, the short-distance aether corrections to the Schwarzschild metric only become important at about a planck distance from the horizon/singularity, which is a reasonable expectation from a possible quantum gravitational mechanism.

While this may imply that tests of strong gravity close to the horizon of a black hole may have a hard time testing the influence of aether on the spacetime metric, the Trans-Planckian ansatz has a curious prediction for the numerical value of p_0, i.e. aether pressure far from the black hole. Comparing the scale of p_0 with the density ($\simeq -$ pressure) of the cosmological dark energy, ρ_Λ:

$$\frac{p_0}{\rho_\Lambda} = -\frac{2}{3}\theta_P^{-1}\left(\frac{m}{85\ M_\odot}\right)^{-3}, \tag{5.25}$$

where we assumed $\Omega_\Lambda = 0.7$ and $H_0 = 70$ km/s/Mpc. The resulting deviation from the Schwarzschild metric is shown in Fig. (5.2) for stellar mass black holes.

This leads us to a very interesting possibility, which was first conjectured in [18]: that the formation of stellar-mass black holes could trigger the onset of cosmic acceleration, especially since aether and dark energy have similar pressures, assuming that the aether pressure is set by the Trans-Planckian ansatz for stellar mass black holes. To see this, we can explicitly compare the black hole spacetime (Eqs. 5.3 and 5.11) far from the black hole ($r \gg m$):

$$ds^2 = -(1 + 2\pi p_0 r^2)^2 dt^2 + dr^2 + r^2 d\Omega^2, \tag{5.26}$$

with the de-Sitter spacetime:

$$ds^2 = -(1 - 8\pi\rho_\Lambda r^2/3)dt^2 + (1 - 8\pi\rho_\Lambda r^2/3)^{-1} dr^2 + r^2 d\Omega^2. \tag{5.27}$$

We thus notice that non-relativistic particles close to the origin, but far from the black hole horizon ($2m \ll r \ll |p_0|^{-1/2}$) see the same Newtonian potential (or g_{tt}) in both spacetimes, if $p_0 = -2\rho_\Lambda/3$. In other words, close-by non-relativistic test particles (such as galaxies, stars, or other black holes) accelerate away from the origin/black hole, similar to a de-Sitter space. Moreover, this acceleration will correspond to the current cosmological observations, if the mass of the black holes is roughly:

$$m \simeq 85\ \theta_P^{-1/3}\ M_\odot. \tag{5.28}$$

So far, our solution has neglected the effects of black hole spin. Indeed, spin is expected in realistic black holes, which are fed by astrophysical accretion disks. For example, the dimensionless spin parameter, $a_* = a/m$ was recently measured for two stellar-mass black holes, to be within the range $0.65 - 0.85$ [59]. In order to include this effect, we conjecture that p_0 scales as T_H^3 (as suggested in [18]), for general black hole spins. This is justified, as the Trans-Planckian ansatz is controlled by the Hawking temperature, T_H, while $f(r)$ also depends on the surface gravity close to the black hole horizon, which is also proportional to T_H. With this assumption, the scale-dependence should go as:

$$\frac{p_0(m, a_*)}{p_0(m, 0)} = 8\left[1 + \left(1 - a_*^2\right)^{-1/2}\right]^{-3}, \tag{5.29}$$

which is in the range $0.2 - 0.6$ for $a_* = 0.65 - 0.85$.

While this paper only deals with static vacuum solutions, it was shown in [18] that for non-relativistic fluids (e.g. stars, planets): $p' \approx -T^\alpha_\alpha/4$+const., i.e. the local matter density sets the aether pressure up to a constant. One expects that the

constant term would be set by the boundary conditions at infinity, or by cosmology. Alternatively, what we suggest in this section is that the boundary condition can be set at the horizons of the black holes. The fact that this can naturally explain the onset of cosmic acceleration is certainly very suggestive, but the best way to test this hypothesis is to see how/if this boundary condition can emerge from the process of (classical or quantum) gravitational collapse into a black hole. We leave this question to future studies.

A further implication of this hypothesis is that solar/stellar mass is the minimum mass of black holes allowed in the model. A discovery of significantly sub-solar mass black holes (e.g. primordial black holes with $M \ll M_{\odot}$) could potentially rule out the Trans-Planckian ansatz, as it would imply much larger than observed cosmic acceleration rates for $\theta_P \sim 1$.

Of course, we also need to patch together and coarse-grain individual black hole spacetimes into a de-Sitter space, in order to rigorously prove this correspondence. However, the above argument is already very suggestive, as long as there are many black holes within the cosmological/de-Sitter horizon, so that one can trust the above Newtonian argument. In the next section, we provide an approximation to the cosmological spacetime of multiple black holes.

5.4 Global Contribution of Multiple Black Holes

In this section, we will seek an approach to approximately find the spacetime of multiple black holes with gravitational aether, which can be used to describe an approximate FRW cosmology. Here, for simplicity, we focus on the quasi-static Newtonian

regime, where we could assume hydrostatic equilibrium for aether in the vacuum (5.6). For simplicity, we ignore the matter in-between black holes,[5] and assume that black holes are much farther apart than their horizon sizes, but are much closer than the cosmological horizon. In this limit, using Eq. (5.6) we have:

$$\nabla^2 \ln p = -\nabla^2 \phi = 0, \tag{5.30}$$

where the assumption of $\nabla^2\phi = 0$ is the equivalent of the Poisson equation in Newtonian gravity, for zero matter density (which also applies to aether). We thus see that fixing the aether pressure in the vicinity of black holes, through the Trans-Planckian ansatz (5.23), is equivalent to solving the Laplace equation (5.30) with Dirichlet boundary conditions at (or close) to the horizon of the black holes.[6]

This problem is analogous to finding the electrostatic potential between multiple conducting spheres, which can be solved using the Green's function for the appropriate geometry. For a single sphere of radius at the origin (and in a flat space), there is an exact expression for the Green's function, which can be found using the *method of images* (e.g. [60]):

$$G_D(\mathbf{x}, \mathbf{x}') = \frac{1}{|\mathbf{x} - \mathbf{x}'|} - \frac{a}{x'|\mathbf{x} - \frac{a^2}{x'^2}\mathbf{x}'|}. \tag{5.31}$$

For n spheres (black holes) at positions $\mathbf{x}_i$ and with radii a_i $(= 2m_i)$, we may expand

[5] This is not a bad approximation since, as we argued in the last section, the effect of matter on the aether pressure is localized and does not extend into vacuum in the non-relativistic regime.

[6] Since pressure approaches p_0 at several BH horizon radii for individual black holes, as long as the distance in-between black holes is much larger than their horizon radii, the exact radius at which the boundary condition is set is not important.

this Green's function, up to first image, as

$$\begin{aligned} G_D(\mathbf{x},\mathbf{x}') &= \frac{1}{|\mathbf{x}-\mathbf{x}'|} \\ - \sum_{i=1}^{n} &\frac{a_i}{|\mathbf{x}'-\mathbf{x}_i||\mathbf{x}-\mathbf{x}_i-\frac{a_i^2}{|\mathbf{x}'-\mathbf{x}_i|^2}(\mathbf{x}'-\mathbf{x}_i)|} + \mathcal{O}\left[\frac{a^2}{|\boldsymbol{\Delta}\mathbf{x}|^3}\right], \end{aligned} \tag{5.32}$$

which is a good approximation, as long as the distance between the spheres/black holes is much larger than their sizes. Now, using Green's theorem, we can find aether pressure in-between the black holes, in terms of the pressure on the surfaces of the spheres, p_i's:

$$\ln p(\mathbf{x}) - \ln \bar{p} = -\frac{1}{4\pi}\sum_{i=1}^{n}\oint_{S_i} \mathbf{ds}' \cdot \frac{\partial G_D}{\partial \mathbf{x}'}[\ln p_i(\mathbf{x}') - \ln \bar{p}], \tag{5.33}$$

where $\ln \bar{p}$ is the log of pressure at infinity, and $\oint_{S_i} \mathbf{ds}'$ are surface integrals over the horizons of the black holes (assuming a flat geometry), while $p_i \propto m_i^{-3}$ are fixed by the masses of the blacks holes, using the Trans-Planckian ansatz (5.23). Since the Green's function (5.32) is analogous to superposition of electrostatic potentials of point charges, we can use Gauss's theorem to evaluate the surface integrals:

$$\ln p(\mathbf{x}) - \ln \bar{p} = \sum_{i=1}^{n} \frac{a_i[\ln p_i(\mathbf{x}') - \ln \bar{p}]}{|\mathbf{x}-\mathbf{x}_i|}. \tag{5.34}$$

Now, using the assumption of statistical homogeneity, we expect the spatial/ensemble average of $\ln p$ to be the same as $\ln \bar{p}$. If we take ensemble averages of both sides of

Eq. (5.34), this yields:

$$\ln \bar{p} = \frac{\langle a_i \ln p_i \rangle}{\langle a_i \rangle}, \tag{5.35}$$

or alternatively:

$$\bar{p} = -\frac{2}{3}\rho_{\rm DE,eff} = -\frac{1}{256\pi^2\theta_P m_*^3}, \;\; \ln m_* \equiv \frac{\langle m_i \ln m_i \rangle}{\langle m_i \rangle}, \tag{5.36}$$

where we used $p_i \propto m_i^{-3}$ and $a_i = 2m_i$, as well as Eq. (5.23). In other words, in the presence of multiple black holes, the mean aether pressure, and thus FRW cosmology, is set by m_*, which is the mass-weighted geometric mean of black hole masses. Subsequently, the correspondence of this mean aether pressure with an effective *Dark Energy* or cosmological constant density was demonstrated in the last section.

Furthermore, taking the Laplacian of Eq.(5.34), we can find an equation for the perturbation of effective Dark Energy, for sub-horizon perturbations (but on scales larger than the size of the blacks holes):

$$\nabla^2 \delta_{\rm DE,eff} = -8\pi \rho_{\rm BH} \ln(p_i/\bar{p}), \tag{5.37}$$

where $\delta_{\rm DE,eff}$ is the overdensity of the effective dark energy, while $\rho_{\rm BH}$ is the black hole density. Eq. (5.37) can be, in principle, used to track cosmological structure formation and the impact on CMB anisotropies (through the Integrated Sachs-Wolfe effect), but we postpone a study of these effects to future work.

In the next section, we will provide a quantitative picture of how the cosmic history of accretion into stellar and super-massive black holes (or active galactic nuclei) leads to an estimate of m_* as a function of redshift, and its implications for the effective

dark energy scenarios.

5.5 Cosmic History of Black Holes and Cosmic Acceleration

An up-to-date inventory of cosmic energy at the present day, including the contribution from stellar-mass and supermassive black holes, is provided by [61]. In order to measure $m_*(z)$ we need to take this a step farther and understand the mass distribution of such black holes, and their redshift evolution.

The mass distribution of stellar–mass black holes is not well-determined observationally, but estimates are that it is fairly broad, with a mean of around $\sim 7M_\odot$ [62, 63]. We base our calculations on the theoretical predictions of [64], which show that the distribution can be approximately represented by a power-law such that the number density of black holes decreases by a factor 5 between $M = 3M_\odot$ and $M = 15M_\odot$. Assuming this distribution, the average black hole mass is $8.2M_\odot$. We will treat the uncertainty in this distribution by varying the slope sufficiently to alter this mean mass by $\pm 1M_\odot$.

To determine the redshift evolution in black hole abundance, we use observations of the cosmic star formation history, from [65]. There is significant uncertainty in the shape of this history. However, it must obey the integral constraint that the total stellar mass density today be $\rho_* = 0.0027\rho_{\rm crit} = 3.67 \times 10^8 M_\odot {\rm Mpc}^{-3}$, which is known to a precision of ~ 30 per cent [61]. We will therefore normalize the black hole number density at $z = 0$ to1.46×10^6 Mpc^{-3} [61]. The effect of this normalization is to ensure

that the integral constraint is satisfied while maintaining the shape of the history. This is necessary because the conversion of observables into the star formation rate has several uncertainties that do not necessarily give the correct stellar mass today.

We assume that changes to the initial mass function do not significantly alter the shape of the star formation rate density evolution, but primarily affect the number of black holes formed. By default we assume a Kroupa IMF [66], which is the "second model" considered in [61]. For this choice, 1.9 per cent of stars formed end up as black holes;[7] a more useful number is that for every solar mass of stars formed 0.0025 black holes are created. These numbers change by less than 5 per cent if we assume a Chabrier IMF [67]; we expect therefore the uncertainty on the normalization of the black hole mass function to be dominated by the 30 per cent uncertainty in the present day stellar mass function. Note, however, that a pure Salpeter IMF [68] would produce significantly fewer black holes, only 0.0013 for every solar mass formed.

In general, there is little observational constraint on the evolution of the IMF. It may be constant out to $z = 2$ but at higher z, there are some observations and theoretical ideas that suggest the IMF may change shape. If this is true it could change both the shape of the star formation rate-time curve assumed in this model, since this is derived from observables assuming a constant IMF, as well as the fraction of mass formed into black holes.

We base our estimate of the supermassive black hole mass distribution on observations of the quasar luminosity function. This requires assumptions about the lifetime and obscuring column density of quasars; for this we adopt the model of [69] who

[7] This is due to [61] and assumes that neutron stars result from stars with initial masses $8-25M_{\odot}$. It also assumes the average mass of a neutron star is $1.35M_{\odot}$.

describe a merger-driven scenario of black hole growth. Using this model, the $z = 0$ mass density of supermassive black holes is $2.9^{+2.3}_{-1.2} \times 10^5 M_\odot \mathrm{Mpc}^{-3}$. This is somewhat smaller than the value of $5.4 \times 10^5 M_\odot \mathrm{Mpc}^{-3}$ determined from the correlation between black hole mass and bulge luminosity [70, 71], as computed by [61]. However, the uncertainty on the latter is a factor of two, and a lower value of $3.4 \times 10^5 M_\odot \mathrm{Mpc}^{-3}$ is obtained [61] if one uses the correlation with velocity dispersion for early type galaxies [72, 73] rather than luminosity.

With this in hand we are able to compute the expected $m_*(z)$, and this is shown in the bottom panel of Figure 5.3. Our best estimate of the local, mass-weighted geometric mean of black hole masses is $m_*(0) = 12.7 M_\odot$. The dashed lines represent the range of uncertainty on this $z = 0$ normalization. A larger value of m_* is obtained by reducing the contribution of stellar-mass black holes (assuming the local density is 30% lower than our fiducial model, and assuming the mass distribution is more steeply weighted to lower masses, so the average mass is $7.2 M_\odot$), and increasing the contribution of supermassive black holes (by increasing the $z = 0$ space density within the 1σ uncertainty, to $5.2 \times 10^5 M_\odot \mathrm{Mpc}^{-3}$). This yields $m_*(0) = 24.7 M_\odot$. Pushing the numbers in the opposite direction, we obtain $m_*(0) = 10.5 M_\odot$. Using Eq. (5.28) for the current effective density of dark energy, and ignoring the spin of black holes, this range in $m_*(0)$ translates to a range for the Trans-Planckian parameter θ_P:

$$\theta_P = (0.4 - 5) \times 10^2. \tag{5.38}$$

We can consider spinning black holes, using our scaling argument from Section 5.3 and taking a nominal value of $a_* = 0.75$. This implies a lower range for the Trans-

Planckian parameter, $\theta_P = 20 - 300$, in order to match the current rate of cosmic acceleration. The fact that $\theta_P \sim 1$, further justifies a Trans-Planckian, or quantum gravitational origin for the observed "dark energy phenomenon".

The evolution of the stellar-mass black hole mass density is dependent upon the shape of the star-formation-rate density plot from [65]. To consider the effect of this, we construct two star formation histories that are consistent with those data within the 1σ error bars, but which produce as many stars as possible at either high redshift ($z > 1$) or at low redshift ($z < 0$). We still renormalize this to match the local stellar mass density. These extremes are shown in Figure 5.3 as dashed lines. The evolution of the supermassive black hole distribution is very model dependent, and not well constrained. We note that the two different predictions shown by [69], which make different assumptions about the quasar space density evolution at $z > 2$, have a subdominant effect on the predictions shown here, relative to the other uncertainties considered.

Within an effective dark energy description of FRW cosmology, a fixed dark energy equation of state, w, implies that dark energy density evolves as $(1+z)^{3(1+w)}$, as a function of redshift, z. The effective equation of state (which is simply a way to parameterize cosmic expansion history) is observationally constrained to

$$w(z) = -1.06 \pm 0.14 + (0.36 \pm 0.62)\frac{z}{1+z}, \tag{5.39}$$

at 68% confidence level, based on cosmic microwave background, baryonic acoustic oscillations, and supernovae Ia observations, assuming a spatially flat cosmology [74], and a linear dependence of $w(z)$ on the cosmological scale factor $= (1+z)^{-1}$.

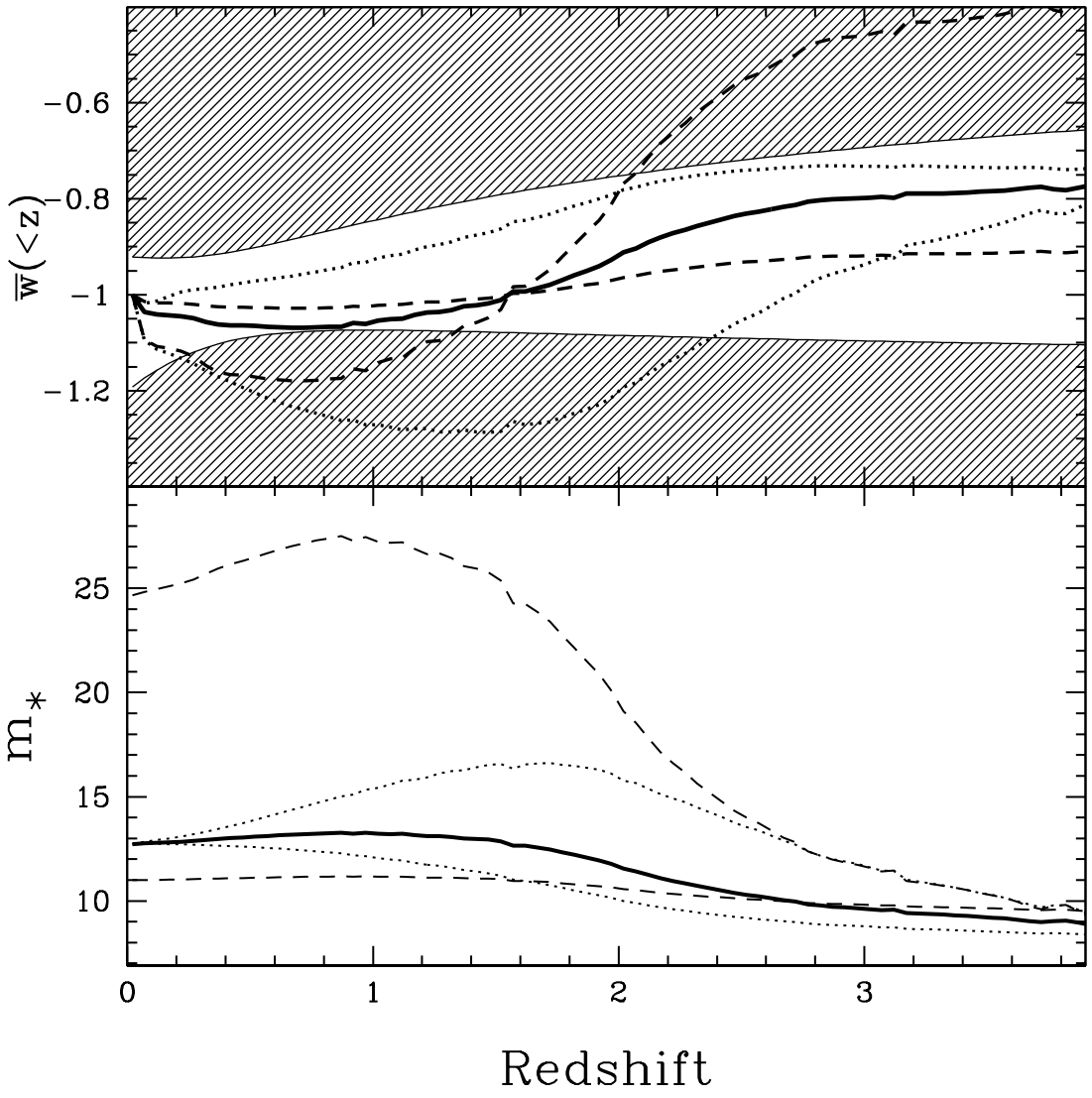

Figure 5.3: **Bottom panel:** The mass-weighted geometric mean of black hole masses, m_*, in units of $M_\odot$ as a function of redshift. Our fiducial model (solid, black line) assumes our best estimates of the mass distribution evolution of the black hole mass distribution. Dashed lines indicate the range of uncertainty expected due to the unknown relative contribution of supermassive and stellar-mass black holes at $z = 0$, while the dotted lines represent the uncertainty in the shape of the star formation density evolution from [65]. **Top panel:** The prediction of the equation of state parameter $\bar{w}(< z)$ from Equation 5.40, for the same models. The dashed area shows the region excluded at 68% confidence level for this parameter, as measured from independent observations [74].

We can define a mean equation of state as:

$$1 + \bar{w}(< z) \equiv \frac{1}{3}\frac{\ln[\rho_{\rm DE,eff}(z)/\rho_{\rm DE,eff}(0)]}{\ln(1+z)} = -\frac{\ln[m_*(z)/m_*(0)]}{\ln(1+z)}, \tag{5.40}$$

since, $\rho_{\rm DE,eff}(z) \propto m_*^{-3}(z)$, as we saw in the last section. We show this estimate of w for the models described above, in the top panel of Figure 5.3. Our fiducial model predicts a value of w that deviates from -1 by less than 5 per cent out to $z \sim 2$, but predicts it should reach $w = -0.8$ by $z = 3$. There is considerable uncertainty on this, however, due both the unknown distribution of black hole masses at $z = 0$ (dashed lines) and the unknown shape of the star formation rate density evolution (dotted lines).

While most these models are consistent with the current bounds on the effective dark energy equation of state (using Eq. 5.39):

$$\bar{w}(< z) = -1.06 \pm 0.14 + (0.36 \pm 0.62)\left[1 - \frac{z}{(1+z)\ln(1+z)}\right], \tag{5.41}$$

stage IV dark energy missions, as quantified by the dark energy task force report [75], are expected to have percent level sensitivity to $\bar{w}(< 1-3)$, and thus should be able to distinguish the aether model with these $m_*(z)$ histories from a cosmological constant.

5.6 Conclusions and Future Prospects

We have shown that static black hole solutions exist in the gravitational aether model of [18]. The model is an attractive alternative to the cosmological constant, which does not suffer from the tremendous fine-tuning problem of vacuum energy in standard model. We find that in the presence of a gravitational aether, the Schwarzschild black hole is sufficiently perturbed so as to result in a Trans-Planckian connection between physics near the black hole horizon and cosmology. This could be a phenomenological product of quantum gravity, and it naturally explains the present-day acceleration of cosmic expansion as a result of formation of stellar/solar-mass black holes.

Indeed, the recent discovery of cosmic acceleration, or dark energy [1, 2] might be the first concrete evidence for quantum gravity and/or Trans-Planckian physics. Future work may include an exploration of quantum properties of this black hole solution. In particular, a natural next step would be to understand how quantum gravity can resolve the null singularity at the event horizon.

As discussed in Sec. 5.3, another important question yet to be addressed is whether dynamical evolution could lead to the static solutions found in this work. While prior to formation of black holes, the integration constant p_0 is set by large-scale conditions, as black hole horizons form, we speculate that the constant is instead set by conditions at the event horizon. In order to understand the causal transition between these two boundaries, and how fast the effect will propagate away from the black hole, a more complete dynamical picture is necessary.

Furthermore, in the presence of multiple black holes with relative motion, the aether is expected to be locally dragged by different black hole horizons. However, for

black holes at large separations compared to their horizon sizes and non-relativistic velocities (as expected in astrophysical situations), the perturbations to the static solution is expected to be small.

To conclude, we would like to entertain the exciting possibility that the gravitational aether [18] might provide a complete solution to the three aspects of the cosmological constant (CC) problem, as discussed in the Introduction:

1. *Old CC problem*: Gravitational aether theory decouples quantum vacuum from geometry, which allows a nearly flat spacetime even in the presence of large vacuum energy densities expected from the standard model of particle physics. The model makes specific predictions for physics at big bang nucleosynthesis and radiation-matter transition era, which will be tested with precision cosmological probes over the next decade [18].

2. *New CC problem*: Formation of black holes leads to a UV-IR coupling, which connects near-horizon Planck-scale physics to cosmology, and can naturally lead to cosmic acceleration, even in the absence of a real dark energy component.

3. *Coincidence problem*: As we showed in Sec. (5.5), the stellar mass black holes expected in standard star formation, can naturally lead to the observed present-day acceleration of the Universe. The competition between the contribution of stellar mass black holes, and super-massive black holes leads to an evolution of the effective dark energy density, which can be tested with NASA's future *Joint Dark Energy Mission (JDEM)*[8] or its European counterpart *Euclid*[9].

[8]http://jdem.gsfc.nasa.gov/
[9]http://sci.esa.int/science-e/www/object/index.cfm?fobjectid=42266

CHAPTER 6

What do dark matter haloes teach us about cosmic acceleration?

6.1 Introduction

The two previous chapters focus primarily on unique and arguably speculative approaches to explaining cosmic acceleration and solving the cosmological constant problem. An important part of the effort to resolve these issues is testing proposed models in the context of what are, at this stage, better-established physical pictures. Structure formation could prove to be an incredibly useful phenomenological method for distinguishing models of cosmic acceleration.

It is currently believed that large-scale structure formation has its seeds in small quantum fluctuations in the early universe (e.g. [76]). The current model for structure formation is elegant in its fundamental simplicity. Random inhomogeneities, artifacts

of cosmic inflation, create a runaway effect in which overdense regions attract more matter, thus becoming more dense and leading to galaxies, stars, and planets.

Better understanding this process is independently an intriguing enterprise in the field of cosmology. In this work we focus on the relationship between the cosmic acceleration and structure formation. More specifically, different cosmological pictures (cosmologies with differing causes of acceleration, such as a cosmological constant, dark energy, or modifications of Einstein gravity) might have expansion histories that are similar to one another but leave different imprints on large-scale structures, and in particular on galaxy clusters. Therefore, structure formation provides a unique testing ground for models of cosmic acceleration (*e.g.*, [19, 77, 78]). Here we critically examine some of the assumptions in this program, and develop a framework to enhance the accuracy of this kind of work.

The first step in this direction is to revisit how the Press-Schechter formalism [79] (PSF) is used to predict the cluster mass function. Press and Schechter [79] have argued that the number density of dark matter haloes (or galaxy clusters) of mass M is given by:

$$\frac{dn(M,z)}{dM} = f[\sigma(M,z)]\frac{\bar{\rho}_m(z)}{M}\frac{\partial \ln \sigma^{-1}(M,z)}{\partial M}, \tag{6.1}$$

where $\sigma^2(M,z)$ is the variance of *linear* overdensity in spherical regions of mass M at redshift z, while $\bar{\rho}_m(z)$ is the mean matter density of the universe. For random gaussian initial conditions, $f[\sigma]$ is given by:

$$f_{PS}[\sigma] = \sqrt{\frac{2}{\pi}}\frac{\delta_{sc}}{\sigma}\exp\left[-\frac{\delta_{sc}^2}{2\sigma^2}\right], \tag{6.2}$$

where δ_{sc} ($\simeq 1.68$ for most ΛCDM cosmologies) is the spherical collapse threshold for

linear overdensities [80].

While the PSF successfully predicts the broad features of the simulated cluster mass functions, it proves too simplistic for detailed model comparisons required for precision cosmology. Consequently, several authors including Sheth & Tormen [81], Jenkins et al. [82], Evrard et al. [83], Warren et al. [84], and Tinker et al. [85] have refined the function $f(\sigma)$ to better match the simulated mass functions in N-body simulations. For example, [84] and [85] propose a fitting formula of the form:

$$f(\sigma) = A\left[\left(\frac{\sigma}{b}\right)^{-a} + 1\right] e^{-c/\sigma^2}, \tag{6.3}$$

where $(A, a, b, c) = (0.186, 1.47, 2.57, 1.19)$ give a good fit to simulated haloes of overdensity $\Delta = 200$, in a concordance ΛCDM cosmology at $z = 0$ [85] (see Fig. 6.1). While most of this work is based on fitting formulae to simulated mass functions, Sheth & Tormen [86] argue that an approximate implementation of ellipsoidal collapse can account for most of the deviations from the PSF.

However, a more pressing question for cosmological applications is whether the function $f(\sigma)$ is *universal*, or rather can vary for different cosmologies or cosmic acceleration models. In other words, could the same modified PSF be used to accurately predict halo abundance in cosmologies with different cosmological parameters? While earlier studies failed to find such dependence, Tinker et al. [85] first noticed a systematic evolution of $f(\sigma)$ with redshift, implying a breakdown of universality at the $10-30\%$ level (also see [87]). Courtin et al. [88] note that universality is limited by the nonlinearity of structure formation, and the cluster mass function shows some redshift dependence at higher redshifts that can be (partially) understood in the context of

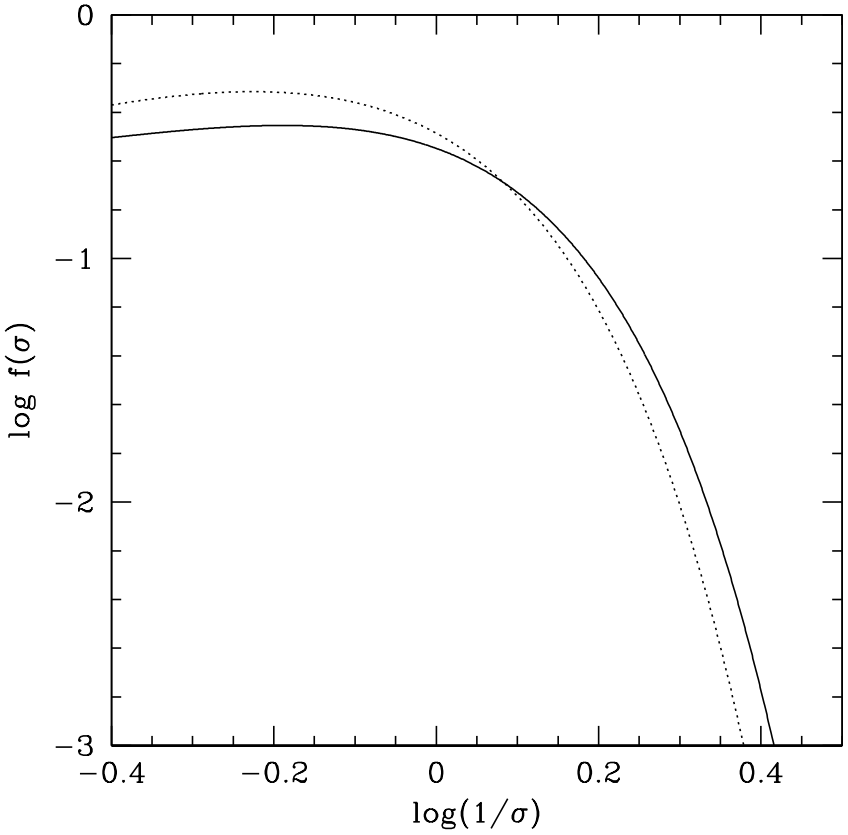

Figure 6.1: A comparison of Press-Schechter prediction for the function $f(\sigma)$ (dotted line; Eq. 6.2), with a parameterized fit to the numerical simulations (solid line; Eq. 6.3).

spherical collapse. However, the spherical collapse model falls short of explaining the $10-30\%$ deviations from universality in all but the most massive clusters (see Fig. 6.6).

In this work, we contribute to the effort to better understand the role and limits of universality in the cluster mass function by introducing a new parameter that appears to be universal across cosmological models.[1] In particular, the PSF relies on $\sigma(M)$, the root-mean-square of *linear* density fluctuations at the time of observation, when in reality, observed clusters are very non-linear objects with overdensities exceeding 200. We thus seek to calculate a universal time in the past when we could make a connection between the nonlinear structures that we observe in the present and the linear structures that existed in the past, since all structures go through a linear phase. Our basic strategy is to find the time in the past at which the linear density of the structures that collapse today show minimum dispersion, as we vary cosmologies.

In § 6.2, we introduce linear perturbation theory for modeling structure formation which leads to a linear differential equation.

In § 6.3, we present the complete nonlinear differential equation that governs the growth of matter perturbations in spherical overdense regions in the presence of a cosmological constant.

In § 6.4, we describe a numerical code that appears in Appendix A which we developed in order to solve both the nonlinear and linear structure formation equations in the presence of a cosmological constant. In § 6.5, we discuss the implications of

[1]Here we define cosmological models to mean different values of the cosmological constant density Ω_Λ or different values of the dark energy equation of state parameter, w. For now, we do not consider quintessence models where w is dynamical in nature. Future work will extend our study to this possibility.

our study for analyses of structure formation in the presence of a physical factor that produces cosmic acceleration.

We then seek to generalize from a cosmological constant to models of dynamical dark energy. § 6.6 presents the results of this study. In § 6.7 we reexamine the idea of universality of mass functions in light of the results of previous sections, including the effect of ellipsoidal collapse on the formalism, and propose a new mass function for general dark energy models.

Finally, in § 6.8, we conclude with an overview of our results and a discussion of future prospects.

6.2 Background: Linear Perturbations

The linear perturbation theory that is used to describe structure formation can be derived via a fluid picture. We use a Newtonian treatment because when density perturbations are small, the gravitational potential will be nonrelativistic [89]. The standard equations of fluid dynamics are reviewed here. First, the continuity equation:

$$\frac{\partial \rho}{\partial t} + \nabla \cdot (\rho \vec{v}) = 0, \tag{6.4}$$

where ρ is the matter density and $\vec{v}$ is the fluid velocity. The Euler equation is:

$$\frac{\partial \vec{v}}{\partial t} + (v \cdot \nabla)\vec{v} = -\frac{\nabla P}{\rho} - \nabla \phi, \tag{6.5}$$

where ϕ is the gravitational potential. Finally, the Poisson equation is:

$$\nabla^2\phi = 4\pi G_N \rho. \tag{6.6}$$

As discussed in Chapter 2, the Universe is in a state of expansion. We recall the Hubble flow equation describing cosmic expansion:

$$\vec{v}(\vec{r},t) = H(t)\vec{r} \tag{6.7}$$

We introduce comoving coordinates $\vec{x} = \frac{\vec{r}}{a(t)}$. We find the velocity in terms of the comoving coordinates and $a(t)$, which is the familiar scale factor from Chapter 2:

$$\vec{v} = \frac{d\vec{r}}{dt} = \dot{a}\vec{x} + \dot{\vec{x}}a = \frac{\dot{a}}{a}\vec{r} + \vec{u}(\frac{\vec{r}}{a},t) \tag{6.8}$$

where $\vec{u} = \dot{\vec{x}}a(t)$ is the peculiar velocity. Note that we want a partial time derivative that respects comoving coordinates, i.e. one that keeps $\vec{x}$ fixed:

$$\left(\frac{\partial\rho(\vec{r},t)}{\partial t}\right)_r = \left(\frac{\partial\rho(\frac{\vec{r}}{a},t)}{\partial t}\right)_r. \tag{6.9}$$

Note that at constant r, $\frac{d\vec{r}}{dt} = 0$ so $\dot{a}\vec{x} + a\dot{\vec{x}} = 0$, giving us $\frac{\dot{a}}{a}\vec{x} = -\frac{\partial\vec{x}}{\partial t}$. This leads us to the following relation:

$$\left(\frac{\partial\rho(\vec{r},t)}{\partial t}\right)_r = \left(\frac{\partial\rho(\vec{r},t)}{\partial t}\right)_x + \frac{\partial\vec{x}}{\partial t}\cdot\frac{\partial\rho}{\partial\vec{x}} = \left(\frac{\partial\rho(\vec{r},t)}{\partial t}\right)_x - \frac{\dot{a}}{a}\vec{x}\cdot\nabla_x\rho(\vec{x},t). \tag{6.10}$$

We now wish to rewrite equation 6.4 in terms of the comoving coordinates, which essentially means replacing the partial differential with the modified one from equa-

tion 6.10. Moreover, what we are really interested in is the development of relative deviations from the mean density, or the density contrast: $\delta = \frac{\rho}{\overline{\rho}} - 1$. Thus, we write $\rho = \overline{\rho}(1+\delta)$ and assuming that $\overline{\rho}$ is regular matter density, we expect $\overline{\rho} \propto a^{-3}$. This gives:

$$0 = \left(\frac{\partial \delta}{\partial t}\right) + \frac{1}{a}\nabla \cdot (1+\delta)\vec{u}. \tag{6.11}$$

We make similar transformations for the Poisson and Euler equations. Next we drop higher order terms (e.g. $O(u^2)$ or $u\delta$). We differentiate the linearized continuity equation and take the divergence of the linearized Euler equation. This gives us a differential equation that depends entirely on δ and not on ρ:

$$\ddot{\delta} + 2\frac{\dot{a}}{a}\dot{\delta} = 4\pi G_N \overline{\rho}\delta. \tag{6.12}$$

The linear growth factor $D(t)$ is defined as the growing solution for δ in this equation.

6.3 Λ & Non-linear Structure Formation

In § 6.2, we derived the differential equation that governs the growth of linear matter perturbations. We used a familiar fluid dynamics picture to do so. Here we derive the full non-linear equation for spherical overdensities using only cosmological considerations. It should be noted that this particular form of the non-linear equation is only strictly valid for ΛCDM cosmologies, where the inside of a spherical top-hat overdensity can be considered as a separate universe. More complex models such as dark energy models with different values of w require additional considerations which will be described later.

We consider a physical picture in which structure formation arises due to a uniformly positive spherical perturbation away from an average matter density, i.e. a top-hat matter overdensity. This scenario is similar to considering two cosmologies with two distinct scale factors: one for the outer universe and another for the overdense region. Of course, we are interested in a scenario where a dark energy component similar to a cosmological constant is at play, so we will assume the presence of one as part of our base model.

For the external universe, we write the Friedmann equation with zero curvature:

$$\left(\frac{\dot{a}_o}{a_o}\right)^2 = \frac{8\pi G_N}{3}(\overline{\rho} + \rho_\Lambda) = H^2. \tag{6.13}$$

As we did in § 6.2, we can assume $\overline{\rho} \propto a^{-3}$ for ordinary matter, while $\rho_\Lambda = \text{const.}$ denotes the cosmological constant density. We also note that the value of the cosmological constant will be the same inside the overdense region and the background.

In a general scenario with dynamical dark energy models we cannot assume that curvature, often denoted by k, will be a constant inside the overdense region due to the presence of pressure gradients. Therefore, Wang & Steinhardt [12] point out that we are compelled to use the time-time component of Einstein's equations, as these do not explicitly involve the curvature term. However, in the presence of a cosmological constant, or $w = -1$, we can ignore these considerations and begin with the first order Friedmann equation. We then calculate k, which can be seen as an integration constant that arises in going from second to first order Friedmann formulations, using initial conditions.

The scale factor in the overdense region is governed by:

$$\left(\frac{\dot{a}_i}{a_i}\right)^2 + \frac{k}{a_i^2} = \frac{8\pi G_N}{3}(\rho_i + \rho_\Lambda). \tag{6.14}$$

Again, we define $\rho_i = \overline{\rho}(1+\delta)$. A little bit of algebra yields the following full differential equation for δ:

$$[\overline{\rho}(1+\delta)]^{-\frac{2}{3}}\left[-\frac{8\pi G_N}{3}\delta\overline{\rho} - \frac{2}{3}\frac{H\dot{\delta}}{1+\delta} + \frac{1}{9}\frac{\dot{\delta}^2}{(1+\delta)^2}\right] + k = 0 \tag{6.15}$$

It is important to reiterate the importance of having access to both linear and nonlinear solutions. As noted by Pace et al. [90] amongst others, although initially both the complete solution and its linear approximation will track, eventually the nonlinear solution will grow much faster relative to the scale factor.

Following Lyth and Liddle [91], we can show that knowing nonlinear theory is necessary. A critical point in the evolution of a structure's collapse is the turnaround event in which universal expansion's dominance over the perturbation is eclipsed by gravitational collapse. In other words, at the turnaround point, a potential structure has detached from background expansion, but complete gravitationally-bound structure formation has not yet begun. This might be thought as the true birth of a structure within the void. Knowing the nonlinear solution allows us to find out the value of the scale factor and the overdensity at this so-called "turn-around point."

Numerically, at the point of complete collapse the nonlinear solution will "blow up" and approach infinity. The linear density at this point, δ_{sc} is the quantity that enters the original Press-Schechter formalism (see § 6.1) and is used as proxy between linear and non-linear structures. Physically, we do not expect an actual singularity.

This "blow up" point is considered to be the beginning of virialization, a process whereby energy in the bulk infall of matter is redistributed into random motion of dark matter particles, leading to a system in virial equilibrium, where kinetic energy T and the potential energy U are related by the virial theorem:

$$T_{vir} = \frac{1}{2}(R\ \partial U/\partial R)_{vir}, \tag{6.16}$$

(see Maor & Lahav [92]). For the purposes of this study, more details on this process are not necessary.

6.4 Numerical Techniques

Although Gunn & Gott [80] showed that the perturbation equation with the assumption of spherical symmetry (also known as the spherical top-hat problem) can be solved analytically for the case of an Einstein-de Sitter (EdS) universe ($\Lambda = 0$), we are interested in cases where the cosmological constant/dark energy are non-zero. Therefore, a numerical solution is necessary.

We built a code in C++ that utilizes the Runge-Kutta method for numerical solutions of ordinary differential equations. The full code can be found in Appendix A. The code runs an instance of a loop for each value of $\Omega_{\Lambda_{present}}$ in the range of 0 to 0.7 (the currently measured value of dark energy density), which solves the second-order linear differential equation, Equation 6.12, as well as the full non-linear equation, Equation 6.15. In order to solve both equations, the solution to the differential equation for the background scale factor, Equation 6.13, is found. The curvature

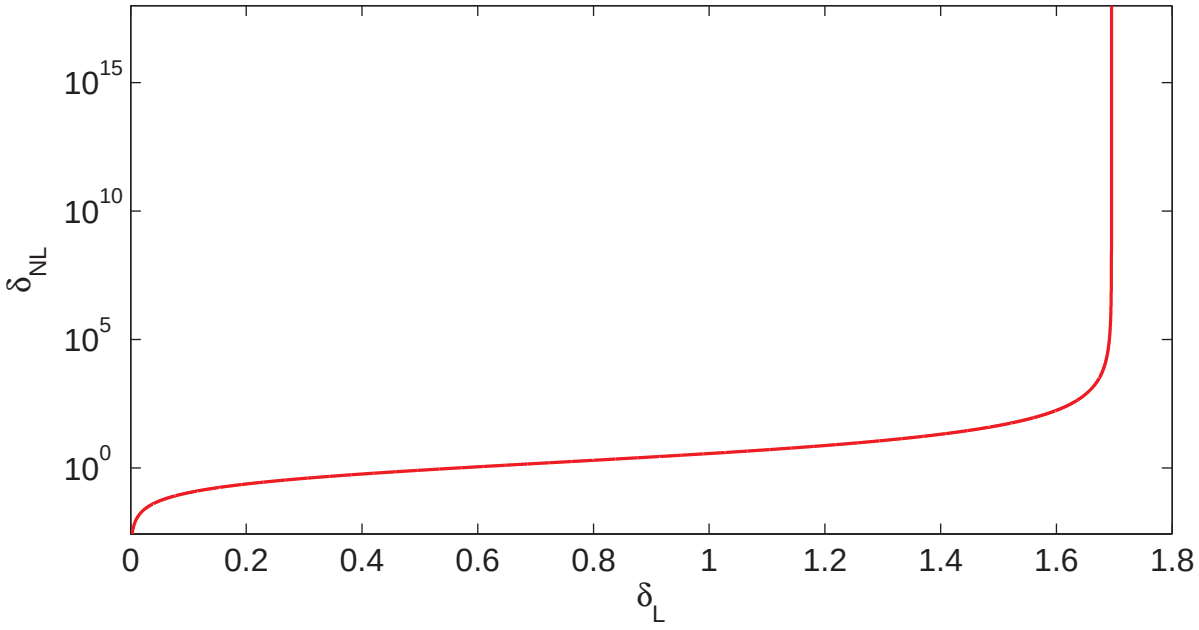

Figure 6.2: This plot shows nonlinear vs. linear overdensities in the Einstein-de Sitter Universe. The code produces, as expected, a δ_{NL} that diverges when $\delta_L \approx 1.68$.

constant is calculated before proceeding to a solution for both the linear and nonlinear differential equations. We set the present Hubble parameter to one. In other words, all time steps are in units of the present value of the Hubble time.

Collapse time is formally defined to be the time at which nonlinear overdensity, δ_{NL} goes to infinity. However, we define collapse numerically by requiring a large ratio of nonlinear to linear overdensities $\delta_{NL} = 200\delta_L$. The initial conditions are calibrated such that they provide the same results as the analytical EdS model, namely that $\delta_L(t_{collapse}) \approx 1.7$. This is essentially done by assuming that at early times δ scales linearly with the scale factor a, as expected for the growing solution to equation (6.12) in the matter era. [2]

[2]It is important to remember that δ is a ratio of two numbers whose units are that of density. Therefore, δ is dimensionless.

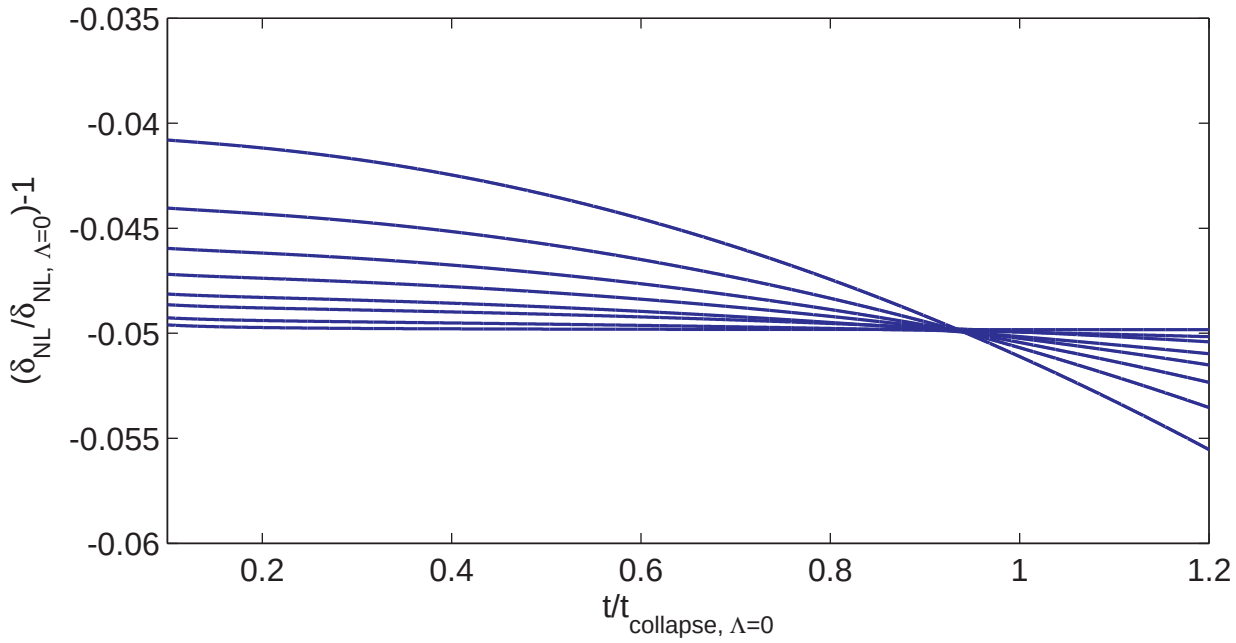

Figure 6.3: Relative change in $\delta_L(t/t_{collapse})$ in ΛCDM cosmologies ($\Omega_\Lambda = 0.1, 0.2, ..., 0.7$), with respect to the Einstein-de Sitter Universe. $t_{collapse}$ is calculated for spherical overdensities. The curves seem to intersect at $t/t_{collapse} \simeq 0.94$, and a calculation of the point of minimum variance between the lines confirms this.

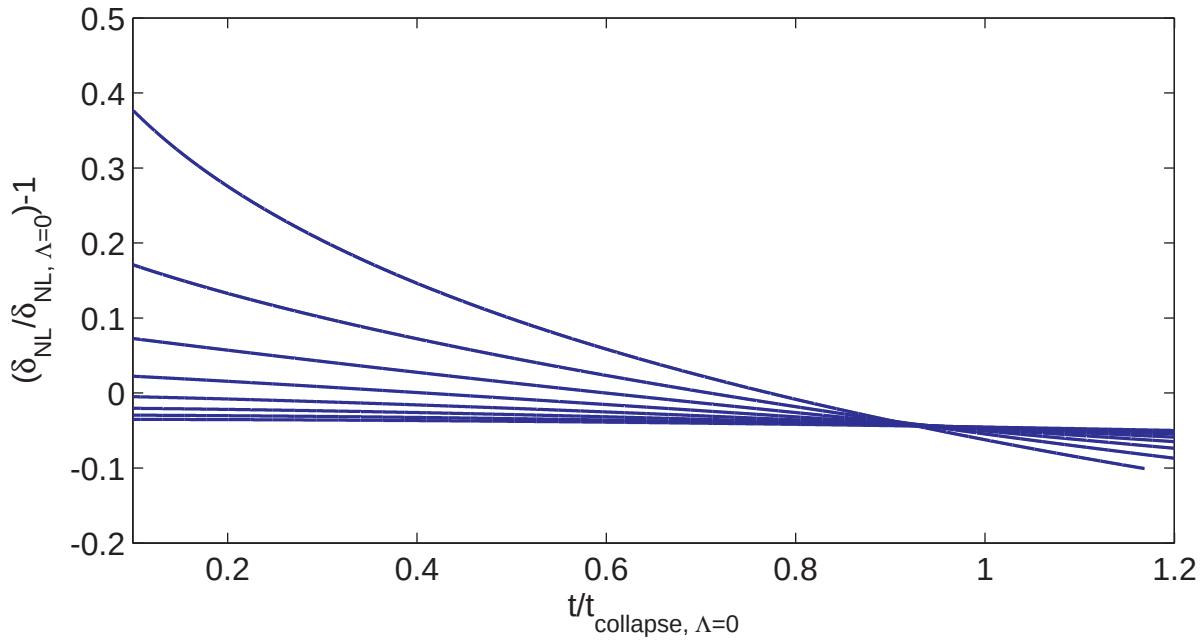

Figure 6.4: Same as Fig. (6.3), but with varying values of dark energy equation of state ($w = -0.3, -0.4, ..., -1$), at $\Omega_\Lambda(today) = 0.7$. Again, curves seem to intersect at $t/t_{collapse} \simeq 0.94$, and, again, a calculation of the point of minimum variance between the lines confirms this. We begin at the value -0.3 because current data constrains the parameter to be smaller than this value.

6.5 Results for Cosmological Constant Models

As stated in the Introduction, we wish to discover the time (as a fraction of the collapse time) such that the variance of $\delta_L(t)$ is at a minimum, as we vary cosmologies. In doing so, we find the time in cosmological history where linear theory is most likely to accurately predict gravitational collapse, independent of cosmology.

For simplicity, we chose to plot the relative difference of $\delta_L(t)$ for different cosmologies with respect to the fraction of time to the collapse time in the Einstein-de Sitter universe. However, it should be noted that the results are independent of this choice, and one could easily calibrate with respect to a universe with a non-zero Λ instead. Having found a common ground, all the data was searched for a single point in time (in units of collapse time) where the variance of $\frac{\delta_L(Q)}{\delta_L(\Lambda=0)} - 1$ was at a minimum, where Q stands for different dark energy models under consideration, whether a general fluid or a cosmological constant.

The interpolations and variance computations were carried out using a script in MatLab, which can be found in Appendix A.3. In the case of the simple cosmological constant models, Fig. 6.3 shows the result that at $\frac{t}{t_{collapse}} \simeq 0.94$, the variance in $\delta_L(t/t_{collapse})$ for different cosmological constant models hits a minimum of 1.8035 x 10^{-9}. Values of δ_L range from 1.602 for Einstein-de Sitter[3] to 1.599 in the $\Lambda = 0.7$ universe.

[3]This is below the predicted analytic value of 1.68 at collapse because while $\delta_L = 1.68$ is expected as $\delta_{NL} \to \infty$, we have set the collapse to occur at $\delta_{NL} = 200$, resulting in a lowered collapse value.

6.6 Dynamical Dark Energy & Structure Formation

Satisfied that our spherical collapse code successfully reproduces cosmologies that include the presence of a cosmological constant as well as the Einstein-de Sitter universe, we may now move on to considering cosmologies with a more complex evolutionary dynamics. Such models are often known as quintessence models, and these are described in reviews [93, 14].

As described in § 6.3, in general, we cannot assume that curvature will be a constant inside the overdense region due to the presence of pressure gradients. Put differently, in a universe where $w = -1$, we can assume that the overdense region and the background universe evolve independently. In a universe where $w = w(a)$, dynamical pressure gradients will force these two "universes" into a dynamical relationship.

These considerations force us to arrive at our non-linear equation differently than before, as the time-time component of Einstein's equations gives us the second-order form of Friedmann's equation. For the external, background universe, we use the Friedmann equation which gives us the background scale factor:

$$\left(\frac{\dot{a}_o}{a_o}\right)^2 = \frac{8\pi G_N}{3}(\overline{\rho} + \rho_Q) = H^2. \tag{6.17}$$

As we did in § 6.2, we say that $\overline{\rho} \propto a^{-3}$. Here Q refers to a general form of dark energy, such as a quintessence.

Referring to the density in the overdense region as $\rho_{cluster}$, we find the time-time

term gives us the second order Friedmann equation:

$$\frac{\ddot{R}}{R} = -4\pi G\left(p_Q + \frac{\rho_Q + \rho_{cluster}}{3}\right) \tag{6.18}$$

$$= -4\pi G\left(\rho_Q(w + \frac{1}{3}) + \frac{1}{3}\rho_{cluster}\right), \tag{6.19}$$

where, treating the system like a fluid, we use the following relation to get the second form of the equation: $p_Q = w\rho_Q$. R can be thought of explicitly as the radius of the overdense cluster.

Abramo et al. [94] provides a comprehensive derivation of the full non-linear equation, which we refer the interested reader to for complete details. For our purposes, it will suffice to show the final result, which is Equation 7 in [94]:

$$\ddot{\delta}_j + \left(2H - \frac{\dot{w}_j}{1+w_j}\right)\dot{\delta}_j - \frac{4+3w_j}{3(1+w_j)}\frac{\dot{\delta}_j^{\,2}}{1+\delta_j} - 4\pi G\sum_k \overline{\rho}_k(1+w_k)(1+3w_k)\delta_k(1+\delta_k) = 0 \tag{6.20}$$

The subscripts j and k refer to different fluids in the system, e.g. matter and dark energy. In a scenario where the dark energy can clump, this becomes a system of equations. As we discuss below, we do not allow this possibility. Therefore, noting that $w = 0$ for matter, we get the following non-linear equation governing the behavior of matter perturbations:

$$\ddot{\delta}_m + 2H\dot{\delta}_m - \frac{4}{3}\frac{\dot{\delta}_m^2}{1+\delta_m} - 4\pi G\overline{\rho}_m\delta_m(1+\delta_m) = 0. \tag{6.21}$$

But, why exactly are we allowed to ignore the clumping in dark energy?

The discussion about dark energy perturbations is often cast in terms of the

effective speed of sound for dark energy (*e.g.*, [95]). Typically one may expect that for an adiabatic fluid with a constant equation state parameter w, the speed of sound is given by $c^2 = \delta P/\delta\rho = w$. However, when $w_{de} < 0$, clearly this becomes imaginary, suggesting a catastrophic instability (*e.g.*, see [96]), and thus we must use a more general definition of the c. In other words, dark energy with constant w cannot be an adiabatic fluid, implying $w = \frac{\delta p}{\delta\rho} \neq \frac{P}{\rho}$. While the equation of state parameter can still give us information about the background evolution, the full action of the fluid is necessary to compute its effective speed of sound: $c^2_{eff} \equiv \frac{\delta p}{\delta\rho}$. It turns out that for the simplest quintessence models $c_{eff} = 1$, although for more general actions c_{eff} could essentially take any value (*e.g.*, [97]).

As to the question of dark energy clumping, we know that pressure fluctuations propagate with the speed of sound c_{eff}. Therefore, dark energy should be smooth on scales smaller than its sound horizon $\sim c_{eff}/H$. As long as $c_{eff} \sim 1$, all the collapsed structures at late times are much smaller than the sound horizon, implying that dark energy perturbations δ_{DE} should be negligible for their formation.

Computing the solution to equation (6.21) requires some modifications to the code. The altered code can be found in § A.2. Instead of scanning over different cosmological constant values, this version of the code varies between constant values of w. Moreover, as current observations (*e.g.*, [98]) set a (very conservative) upper limit of $-1/3$ for the value of w , we studied cases where w was smaller than $-1/3$.

Because the cosmological constant is a special case of this scenario with $w = -1$, we are able to check the self-consistency of our methods (Eq. 6.15 vs. Eq. 6.21) finding that both versions of the code produce the same results for a universe with $\Omega_\Lambda = 0.7$ (approximately the universe that we live in).

Fig. (6.4) shows a similar comparison to that of Fig. (6.3), but with different values of equation of state, w, with $\Omega_{DE} = 0.7$. Interestingly, we can again clearly see a point of minimum variance at $t/t_{collapse} \simeq 0.94$, suggesting that this result might be quite independent of the dark energy model (at least within the spherical collapse approximation). The variance at this minimum is 7.5376 x 10^{-7}. In the next section, we discuss the physical significance of this result.

6.7 What does the Cluster Mass Function teach us about cosmology?

At first, one might be puzzled by the fact that δ_L happens to have almost the same value at 94% of the collapse time, independent of w or Λ, even though the linear approximation breaks down long before this point. In other words, why should non-linear collapse show such strong correlation with the linear evolution? This can be understood as the near cancelation of two different effects with opposite signs:

1. With the exact same initial conditions, the presence of dark energy weakens the gravitational attraction near the turn around point, which in turn stretches the collapse time.

2. The linear growth factor $D(t)$, which is the growing solution to equation (6.12), slows down as dark energy starts to dominate, since the Hubble friction $2H\delta$ stops decaying ($H \rightarrow$ const.), while matter density decays exponentially $\bar{\rho} \propto a^{-3} \propto \exp(-3Ht)$.

It turns out that for near ΛCDM cosmologies, these two effects nearly cancel each other, i.e. the linear growth is slowed down, but $t_{collapse}$ is also longer, resulting in nearly the same value of δ_L close to (i.e. at 94% of) the collapse time.

However, we should note that this result is specific to the spherical collapse scenario. On the other hand, real collapsing regions are far from spherical. Even though very rare peaks of a random gaussian field can be approximated as spheres, more abundant haloes could significantly deviate from sphericity (*e.g.*, [99]). For Einstein-de Sitter universe, Sheth & Tormen [86] give a simple numerical fit for the impact of ellipticity on the linear collapse threshold, δ_{ec}:

$$\delta_{ec} \simeq \delta_{sc} \left[1 + \sigma(M)^{1.23}\right], \tag{6.22}$$

where $\delta_{sc} \simeq 1.686$ is the spherical collapse threshold. Since $\delta_L \propto t^{2/3}$ in an Einstein-de Sitter universe, this implies that, for the same initial overdensity, the collapse time of an elliptical region is longer than that of a spherical region by a factor of:

$$\frac{t_{collapse,elliptical}}{t_{collapse,spherical}} \simeq \left[1 + \sigma(M)^{1.23}\right]^{3/2}. \tag{6.23}$$

In other words, we need to extrapolate the linear theory predictions in Figs. (6.3-6.4) farther beyond the point of intersection to actually hit gravitational collapse. Therefore, combining equation (6.23) with the results of previous sections implies that the point of minimum variance in δ_L is shifted to small values of $t/t_{collapse}$, i.e.:

$$\frac{t_*}{t_{collapse}} = \frac{0.94}{\left[1 + \sigma(M)^{1.23}\right]^{3/2}}, \tag{6.24}$$

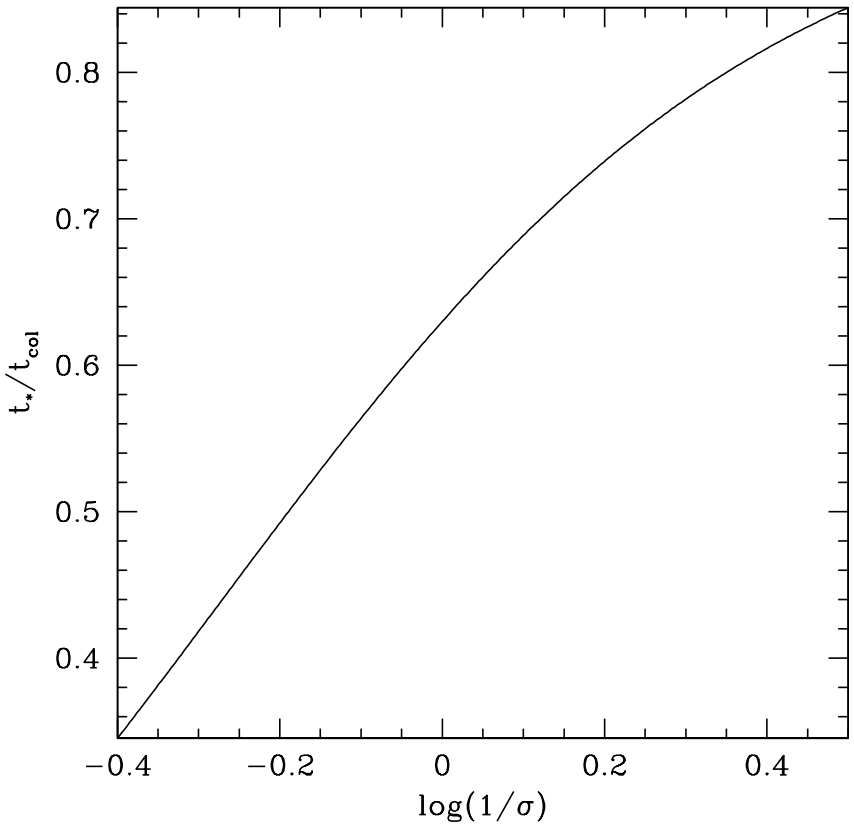

Figure 6.5: The expected time of minimum variance in linear overdensity, in units of ellipsoidal collapse time. Observing the cluster number counts at t_{col} should tell us the linear overdensity of the collapsing region at t_*, independent of the dark energy model.

if we include the impact of ellipsoidal collapse. This result is shown in Fig. (6.5), and demonstrates how measuring the mass function of clusters at a given era may tell us about the entire history of linear growth, and not just a snapshot at the time of observation (as is in the traditional universal mass function hypothesis).

Inspired by the fitting formula Eq. (6.3), Equation (6.24) leads us to propose a new universal cluster mass function:

$$f(\sigma;Q) \simeq g(\sigma)e^{-h(\sigma)/\sigma_*^2}, \sigma_* = \sigma D\left[\frac{0.94\times t}{(1+\sigma^{1.23})^{3/2}}\right], \tag{6.25}$$

where the actual mass function is related to $f(\sigma;Q)$ through equation (6.1), and t is the time of observation at which $D(t)$ is normalized to unity. In other words, equation (6.25) suggests that the exponential cut-off in the cluster number counts at any time t is set by the linear density fluctuations σ_* at an earlier time t_*, which is set by equation (6.24). As suggested by several recent numerical studies (see Introduction) $f(\sigma;Q)$ depends on cosmology (denoted by Q), but we propose the functions g and h to be universal, while the dependence on cosmology (or dark energy models) only enters through $D(t_*)$. The explicit dependence of g and h on σ at the time of observation is justified, as the value of σ acts as a proxy for the asphericity of the collapsing region [86].

Comparing to Eq. (6.3), we fix g and h as:

$$g(\sigma) = A\left[\left(\frac{\sigma}{b}\right)^{-a}+1\right], h(\sigma) = cD^2\left[\frac{0.94\times t}{(1+\sigma^{1.23})^{3/2}}\right]_{\Omega_\Lambda=0.7}, \tag{6.26}$$

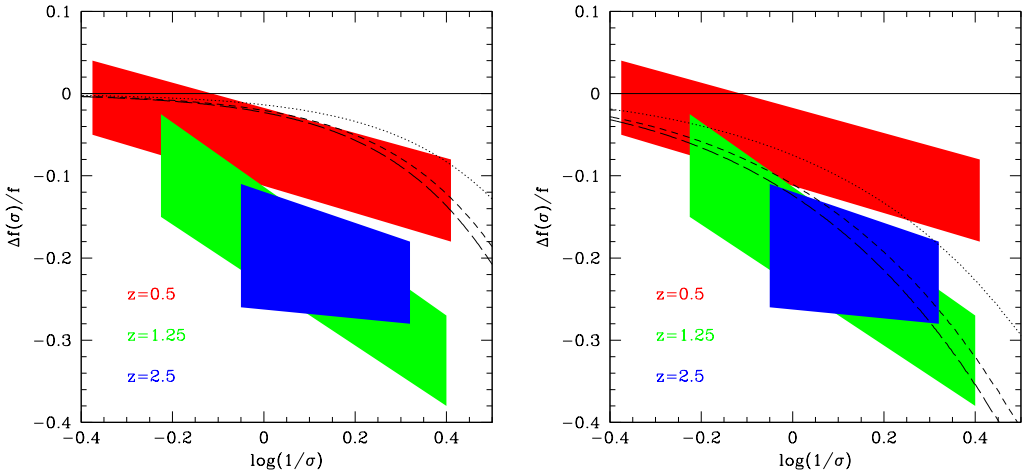

Figure 6.6: The relative change in $f(\sigma)$ at high redshifts, compared to $z = 0$. The colored regions show the simulated results from [85]. Curves in left panel show our analytic prediction without ellipticity corrections, while curves in the right panel include the ellipticity corrections (Eq. 6.25). The solid, dotted, short-dashed, and long-dashed curves refer to z=0, 0.5, 1.25, and 2.5 respectively.

where $(A, a, b, c) = (0.186, 1.47, 2.57, 1.19)$ [4].

Fig. (6.6) compares the evolution in the function $f(\sigma; Q)$ in N-body simulations, with our prediction from Eqs. (6.25-6.26). We see that while the result from spherical collapse, $t_* = 0.94 \times t_{collpase}$, underpredicts the evolution (left panel), Eq. (6.25), which includes the ellipsoidal correction to the collapse time (Eq. 6.24), can successfully reproduce the evolution in $f(\sigma; Q)$.

[4] We recognize that these choices for g and h are not unique, but as Fig. (6.6) demonstrates, these are sufficient to fit current simulations

6.8 Conclusions and Future Prospects

In this chapter, we have presented a study of non-linear gravitational collapse in different models of dark energy/cosmic acceleration. In particular, we critically examined the correlation between the linear growth of fluctuations and the emergence and statistics of collapsed objects (such as dark matter haloes or galaxy clusters). First, we focused on the collapse of spherical overdensities, and discovered that they all have the same linear ovderdensity ($\simeq 1.50$), at $\simeq 94\%$ of the time of collapse/virialization, independent of the density or equation of state of dark energy. We then used a simple prescription to include the impact of ellipsoidal collapse in our finding, and then used this result to propose a new universal mass function for galaxy clusters/dark matter haloes. Our semi-analytic predictions are consistent with the observed evolution in mass function of haloes in N-body simulations.

Future work will include the adaptation of this prescription to study models with dynamical equations of state, such as quintessence or modified gravity models. A particularly challenging application would be to the gravitational aether/black hole model that is described in Chapter 5. Because of the way dark energy is sourced in the gravitational aether model, there are unique numerical challenges associated with properly describing structure formation in its presence.

Finally, we recognize that a more systematic approach to the question of universal mass functions should be possible, and given the level of theoretical and observational activities in this field, it is unlikely that the present work provides the last word on this subject. However, the novel (albeit trivial) observation of this work is that measuring the cluster mass function will teach us about the entire history of linear

growth. This is in contrast to many previous cosmological applications of cluster mass functions, which assume a one-to-one correspondence with the linear $\sigma(M)$ at the time of observation. Similar to a multi-level archeological excavation, dark matter haloes can be thought of as artifacts of linear growth. As Fig. (6.5) and Eq. (6.25) suggest, the number of smaller haloes (with larger $\sigma(M)$) can teach us about the early evolution of linear growth, while the bigger haloes (with smaller $\sigma(M)$) tell us about its more recent history.

We thus speculate that this perspective can eventually lead to yet untapped information about the nature and history of cosmic acceleration, especially as the releases of several large scale cluster surveys such as Atacama Cosmology Telescope (ACT) [100], South Pole Telescope (SPT) [101], Planck [102], and Red Sequence Cluster Sequence 2 (RCS2) [103] are now looming on the horizon.

CHAPTER 7

Accelerating Forward: Conclusions

The American National Academy of Sciences has completed its decadal survey, and the cosmic acceleration problem is at the top of the list of enduring questions that we wish to explore during the next decade. Indeed, the data has become undeniably intriguing, and multiple efforts such as the *Joint Dark Energy Mission* and *Dark Energy Survey* are part of an endeavor to better understand the tip initially given to us by Type Ia supernovae.

Many open questions, of course, remain. It is clear that a better understanding of the cosmological constant problem as a distinct problem that arises in quantum field theory, as well as its potential connection to the question of cosmic acceleration, will be necessary for a complete theory of quantum gravity. In recognition of this, we can investigate the cosmic acceleration problem either directly as quantum gravity phenomenology or at least as motivation for considering a connection between questions in fundamental physics and those in astrophysics.

Its worth reconsidering our ideas about the vacuum itself. We often think that defining the vacuum in general relativity is trivial, although in reality, it says nothing about a vacuum, at least not the vacuum that we conceive of in QFT, which is, relatively speaking, trivial to define. What we have repeatedly learned is that connecting these two vacuums is non-trivial. While it's possible that part of the problem is that we do not look at spacetime the way we should, maybe we are trying to do the wrong thing, simply connecting two vacuums from two different models.

It is potentially useful to reconsider this problem in the context of another scenario where GR and QFT seem unable to share a narrative: the quantum gravity problem. Perhaps questions of vacuum observations and phenomenology are actually quantum gravity phenomenology. With this in mind, I have presented original research that attempts to explain cosmic acceleration by connecting this astrophysical problem with questions in fundamental physics. I have also offered a new consideration in the effort to use structure formation to constrain potential explanations for cosmic acceleration.

The results presented in Chapter 5 present one potential cause of cosmic acceleration. It is also an example of the unexpected turns exploratory research can take. Initially part of an attempt to better understand black holes in a modified gravity theory, this work with Afshordi revealed a unique potential connection between physics at small scales and physics at large scales. We formulated a picture where the pressureful presence of a dark energy-like component is sourced on the event horizon of black holes. This particular approach to the cosmic acceleration problem divorces the vacuum from gravity, reconfiguring the questions and answers related to the *cosmological constant problem*.

Work with Smolin in Chapter 4 shows one way that the cosmic acceleration and

cosmological constant problems can be approached from the other direction: beginning with quantum gravity considerations. This novel idea involves positing that a certain level of non-locality survives coarse graining from a quantum gravitational scale in a model such as spin foams. The distribution of these so-called non-local links through the universe sources an energy density that is indistinguishable from a cosmological constant. This work simultaneously answers the question of what phenomenology may result from certain assumptions about the properties of quantum gravity as well as the question of how cosmic acceleration might arise under such a quantum gravity.

Having considered possible approaches to the problem, we are also interested in understanding how to connect these ideas with the data. In the hunt for effective and independent ways to study the impact of different models on the cosmology we observe, structure formation presents us with a fruitful arena. Although different cosmic acceleration models can present indistinguishable background evolution, structure formation may be altered. Essentially, the impact on structure formation is independent of the impact on the background evolution, making structure formation a useful test of cosmological models.

In Chapter 6, I present an analysis of spherical top-hat model collapse in different cosmological models, allowing us to better understand universality of the cluster mass function (CMF) in the Press-Schechter formalism. It is shown that the CMF's universal behavior may allow us to learn about the history of linear structure formation. We expect this knowledge will be helpful when studying the impact of cosmic acceleration models on structure formation, thus allowing us to refine our understanding of the universe's accelerating expansion and its causes. In a scenario where cosmic accelera-

tion is quantum gravity phenomenology, a better understanding of the mechanism(s) behind the acceleration will help us formulate a true theory of quantum gravity.

APPENDIX A

C++ Code for Solving Spherical Collapse Problem

These codes are relevant to the work described in Chapter 6.

A.1 Varying Cosmological Constant

```
1  //structure_formation will solve the linear and non-linear
       differential equations for spherical collapse.
2
3  #include <iostream>
4  #include <cmath>
5  #include <fstream>
6  #include <string>
7  #include <sstream>
8  #include <vector>
9  #include <windows.h>
10
11 using namespace std;
12
13 static double one_sixth = (1/6.0f);
14
15 // Calculation of Adot when A = a. (and lambda = L)
16 double evaluate_Adot( double a, double L) {
17   return sqrt((1-L)*pow((double)a,(double)-1.0f)+L*pow((double)a,(
         double)2.0f));
18 }
19
20 // calculate the 4 k values for runge-kutta on 'a', return them in
       the passed in pointers.
```

```
21 void get_runge_kutte_k_vals_for_a( double a, double L, double dt,
22                   double* k1, double *k2, double *k3, double *k4) {
23   *k1 = evaluate_Adot( a, L );
24   *k2 = evaluate_Adot( a + 0.5 * dt * (*k1), L );
25   *k3 = evaluate_Adot( a + 0.5 * dt * (*k2), L );
26   *k4 = evaluate_Adot( a + dt * (*k3), L );
27 }
28
29 // calculate the next value of a in a runge_kutta integration
30 double runge_kutta_a(  double a, double L, double dt ) {
31
32   double k1, k2, k3, k4;
33
34   get_runge_kutte_k_vals_for_a( a, L, dt,
35                   &k1, &k2, &k3, &k4);
36
37   return a + one_sixth * dt * ( k1 + 2 * k2 + 2 * k3 + k4 );
38 }
39
40 // evaluate the determinant in the calucation of ndeltadot
41 double evaluate_determinant_in_ndeltadot(fstream & filestra, double
       ndelta, double a, double L, double k ) {
42
43   double adot = evaluate_Adot( a, L );
44
45   double d = (1+ndelta) * (1-L) / (a*a*a);
46   double D = pow( (double)d, (double)-2/3.0f );
47   double c = (D * ndelta * (L-1) / (a*a*a)) + k;
48   double b = D * (-2/3.0f) * (adot/a) / (1+ndelta);
49   double A = D * (1/9.0f) * pow( 1+ndelta, (double)-2.0f);
50
51   return pow( b,2 ) - 4*A*c;
52 }
53
54 // calculation of ndeltadot
55 double evaluate_ndeltadot( fstream & filestra, double ndelta, double
        a, double L, double k, int &m ) {
56
57   double adot = evaluate_Adot( a, L );
58
59   double d = (1+ndelta) * (1-L) / (a*a*a);
60   double D = pow( (double)d, (double)-2/3.0f );
61   double c = (D * ndelta * (L-1) / (a*a*a)) + k;
62   double b = D * (-2/3.0f) * (adot/a) / (1+ndelta);
63   double A = D * (1/9.0f) * pow( 1+ndelta, (double)-2.0f);
64   double in_sq = pow( b,2 ) - 4*A*c;
65
66   if( in_sq < 0 ) {
```

```
67      in_sq = 0;
68      m = 1;
69    }
70
71    return (-b + m * sqrt(in_sq) ) / (2 * A);
72  }
73
74  // calculate the next value of ndelta using runge-kutta.
75  // Since ndelta depends on a, and we don't have an explicit formula
        for a,
76  // we have to treat this as an integration of a system of equations
        using runge-kutta.
77  // We've already integrated a, but we still need the runge-kutta k
        values from the 'a'
78  // integration in order to calculate the k values for the ndelta
        integration.
79  double runge_kutta_ndelta( fstream & filestra, double ndelta, double
        a, double L, double k, int &m, double dt) {
80
81    double k1, k2, k3, k4;
82    double ka1, ka2, ka3, ka4;
83
84    get_runge_kutte_k_vals_for_a( a, L, dt,
85                    &ka1, &ka2, &ka3, &ka4);
86
87    k1 = evaluate_ndeltadot( filestra, ndelta, a, L, k, m );
88    k2 = evaluate_ndeltadot( filestra, ndelta + 0.5 * dt * k1,
89                  a + 0.5 * dt * ka1,
90                  L,
91                  k,
92                  m );
93    k3 = evaluate_ndeltadot( filestra, ndelta + 0.5 * dt * k2,
94                  a + 0.5 * dt * ka2,
95                  L,
96                  k,
97                  m);
98    k4 = evaluate_ndeltadot( filestra, ndelta + dt * k3,
99                  a + dt * ka3,
100                 L,
101                 k,
102                 m);
103
104   return ndelta + one_sixth * dt * (k1 + 2 * k2 + 2 * k3 + k4 );
105 }
106
107 // calculate the second derivative of delta.
108 double evaluate_deltadubdot( double delta, double ddot, double a,
        double L ) {
```

```
109
110   // Stuff for linear equation: second order deriv of lin delta
111   double adot = evaluate_Adot( a, L );
112   return ((3/2.0f)*(1-L)*delta/(a*a*a)) - (2*adot*ddot/a);
113 }
114
115 // returns the next value of delta from runge_kutta integration.
      The integrated value of ddot is returned by pointer
116 // in the last parameter.
117 // Here we are integrating a system of 2 equations (delta and ddot),
      but again 'a' is not a known function,
118 // so we have to treat this as a runge-kutta integration of a system
      of 3 equations, but again we don't need
119 // to explicitly do the integration of 'a' since we've already done
      so.
120 double runge_kutta_delta( fstream & filestra, double delta, double
      ddot, double a, double L, double dt, double * ddot_ret ) {
121
122   double k1, k2, k3, k4;
123   double ka1, ka2, ka3, ka4;
124
125   get_runge_kutte_k_vals_for_a( a, L, dt,
126                   &ka1, &ka2, &ka3, &ka4);
127
128   k1 = evaluate_deltadubdot( delta, ddot, a, L );
129   k2 = evaluate_deltadubdot( delta + 0.5 * dt * ddot,
130                 ddot + 0.5 * dt * k1,
131                 a + 0.5 * dt * ka1,
132                 L );
133   k3 = evaluate_deltadubdot( delta + 0.5 * dt * ddot + 0.25 * dt *
        dt * k2,
134                 ddot + 0.5 * dt* k2,
135                 a + 0.5 * dt * ka2,
136                 L );
137   k4 = evaluate_deltadubdot( delta + dt * ddot + 0.5 * dt * dt * k3,
138                 ddot + dt * k3,
139                 a + dt * ka3,
140                 L );
141
142   *ddot_ret =  ddot + one_sixth * dt * ( k1 + 2 * k2 + 2 * k3 + k4 )
        ;
143
144   return delta + dt * ddot + one_sixth * dt * dt * ( k1 + k2 + k3 );
145 }
146
147 int main()
148 {
149   int m,alpha;
```

```
150   double adot, ddot, ndelta, nddot, dubdot,omega; //a, derivative of
          a, delta(lin), deriv of deltalin, nonlindelta, deriv of nonlin
151   double d, D;//D and the variables below are all used to simplify
          the non-linear delta diff eq
152   double A, b, c, sq;
153   int t,time;
154   double dt=0.000001f,acoll,tcoll; //time step
155   double L, Lin, Lout, Lstep; //this is lambda, initial for range,
          and final for range, step for moving in range
156   double k; //this is the curvature constant, which is set by the
          value of lambda in the background
157   const double Pi = 3.14159265358979323846;
158
159   CreateDirectory ("data",0); //the 0 is a security_attributes value
160
161   Lin=0;
162   Lstep=0.1;
163   Lout=0.7;
164
165   vector<double> eds;//this stores linear delta for the Einstein-de
          Sitter case
166
167   for(L=Lin; L<=Lout; L+=Lstep)
168   {
169     ostringstream streama;
170     streama << "data\\" << L << ".txt";
171
172     fstream filestra;
173     filestra.open (streama.str().c_str(), fstream::out);
174
175     ostringstream streamturn;
176     streamturn << "data\\" << L << ".turn.txt";
177
178     fstream fileturn;
179     fileturn.open (streamturn.str().c_str(), fstream::out);
180
181     //Vector Definitions
182     vector<double> advector;//this vector class stores the
            background scale factor
183     advector.push_back(1); //this initializes the 0th element of the
            vector, advector[0]=1
184
185     vector<double> z;//this vector class will store the redshift, as
            correlated with the values of advector
186     z.push_back(advector[0]-1);//this initializes the redshift at
            zero
187
```

```
188     vector<double> delta;//this vector class stores the value of
            linear delta
189
190     vector<double> in_sq; //this vector indexes the characteristic
            of the non-linear quadratic
191     in_sq.push_back(0);
192
193     vector<double> logdelta; //this vector indexes the logarithm of
            linear delta
194     //vector<double> tcoll;
195     //end of Vector definitions
196
197     //Indices
198     int i=0; //i will index our dynamical array, aka vector
199     int j=1; //j will index the characteristic of the non-linear
            quadratic
200     int q=0; //q will index the values of linear delta
201
202     cout << "advector[0]: " << advector[0] << endl;
203     cout << "redshift: " << z[0] << endl;
204
205
206     //Background integration. we are integrating backwards in time,
            but i is indexing positively
207     //which is why if you look a few lines down, t=-i
208     do
209     {
210       adot = evaluate_Adot( advector[i], L );
211       advector.push_back( runge_kutta_a( advector[i], L, -dt ) ); //
              run a runge-kutta iteration with a negative timestep
212       z.push_back((advector[0]/advector[i])-1.0f);
213       i+=1;
214     } while(0.1*advector[i] > adot*dt); // just looking for when a
            goes below zero 0.01*advector[i] > adot*dt
215
216     i--; // i is now the index of the last advector value greater
            than 0
217     int maxindex=i; //this records the i-value of the stopping point
             of the previous loop
218
219     cout << "advector[i]: " << advector[i] << endl;
220     cout << "adot: " << adot << endl;
221
222     delta.push_back(4.0*advector[i]); //initialize linear delta
223     ndelta = delta[q]; //initialize non-linear delta
224     ddot = delta[q]*adot/advector[i]; //initial value of delta-dot
225     cout << "ddot: " << ddot << endl;
226     cout << "ndelta initial: " << ndelta << endl;
```

```
227     d = (1+ndelta) * (1-L) / (advector[i]*advector[i]*advector[i]);
228     D = pow( (double)d, (double)-2/3.0f );
229     k = -D*(((1/9.0f)*(ddot*ddot)/(pow(1+ndelta,(double)2.0f)))
            -((2/3.0f)*(ddot*adot)/((1+ndelta)*advector[i]))-
             (ndelta*(1-L)/(advector[i]*advector[i]*advector[i])));
230     omega = L/((1-L)*pow(advector[i],(double)-3.0f) + L);
231
232     //This vector is explained somewhere else!
233     if( L==0 ){
234         eds.push_back(delta[q]);
235       }
236
237     //We want the indexing of the background to not be confusing, so
            we are going to switch variables.
238     t=-maxindex;
239     time = t + maxindex + 1; //this is the time variable that goes
            forward in time
240     int timemax = time;
241     double linear[5] = {time,z[i],advector[i],delta[q],omega}; //We
            will store the collapse values in this array.
242
243     cout << "k: " << k << endl;
244
245     //m is an integer that will switch signs when the characteristic
            of the non-linear equation switches signs, thus allowing
246     //us to use the appropriate solution for delta-dot
247     m=-1;
248     alpha=-1;
249
250     //this loop will use the values of a that we found before to
            find the linear and non-linear deltas from the past until the
             present time.
251     for(;i>0;i--)     //(initial: already have i; exit when false:
            when i=0, stop; decrement by -1)
252     {
253       //filestra << "Iteration t: " << t << "\n";
254       adot = sqrt( (1-L) * pow(advector[i],(double)-1.0f) + L * pow(
              advector[i],(double)2.0f) );
255
256       omega = L/((1-L)*pow(advector[i],(double)-3.0f) + L);
257
258       //Determine collapse values
259       if((alpha == -1) && ( ndelta > 200.0f )) {
260         alpha=1;
261         linear[0]=time;
262         linear[1]=z[i];
263         linear[2]=advector[i];
264         linear[3]=delta[q];
265
```

```
266           linear[4]=omega;
267           cout << "linear delta at collapse: " << linear[3] << "\n";
268         }
269
270         //if (j%10==0){
271         //filestra << time << " , " << z[i] << " , " << advector[i] <<
                " , " << delta[q] << " , " << ndelta << " , "
272         //  << omega <<  "\n";
273         //}
274         //" , " << eds[q] <<
275
276         //We want to store the linear delta values for use later
277         if( L==0 ){
278           eds.push_back(runge_kutta_delta( filestra, delta[q], ddot,
                advector[i], L, dt, & ddot ));
279           delta.push_back( eds[q+1] );
280         } else {
281           // push back the next value of delta, and also, ddot will
                get updated too.
282           delta.push_back( runge_kutta_delta( filestra, delta[q], ddot
                , advector[i], L, dt, & ddot ) );
283         }
284
285
286
287         //logdelta.push_back(log10(delta[q]));
288
289         // calculate the next value of ndelta
290         ndelta = runge_kutta_ndelta( filestra, ndelta, advector[i], L,
              k, m, dt);
291
292         if (j%10==0){
293         filestra << time << " , " << z[i] << " , " << advector[i] << "
              , " << delta[q] << " , " << ndelta << " , "
294           << omega <<  "\n";
295         }
296
297         t += 1;
298         time += 1;
299         j++;
300         q++;
301       }
302
303       //This loop transforms t and a to ratios with collapse values
304       j=1;
305       time=timemax;
306       int gamma;
307
```

```
308     //This is simply for the sake of rescaling the linear-delta,
            ensuring that we can do the following calculation.
309     if(delta.size()-1 > eds.size()-1){
310       gamma=eds.size()-1;
311     } else{
312       gamma=delta.size()-1;
313     }
314
315     for(i=maxindex;i>maxindex-gamma;i--){
316         tcoll=time/linear[0];
317         double zcoll=z[i]/linear[1];
318         acoll=advector[i]/linear[2];
319         double delratio=(delta[j]/(1.686*pow(tcoll,(double)2.0/3.0f)
                ))-1;
320         //double delratio=(delta[j]/eds[j])-1;
321         if (j%10==0){
322           fileturn << tcoll << " , " << acoll << " , " << advector[i
                ] << " , " << delratio << "\n";
323         }
324         time += 1;
325         j++;
326       }
327
328       fileturn.close();
329       filestra.close();
330   }
331
332   cout << "Program is done...";
333   cin.get();
334   cin.get();
335
336   return 0;
337 }
```

A.2 Varying w

```
1 #include <iostream>
2 #include <cmath>
3 #include <fstream>
4 #include <string>
5 #include <sstream>
6 #include <vector>
7 #include <windows.h>
8
9 using namespace std;
```

```
10
11 static double one_sixth = (1/6.0f);
12
13 // Calculation of Adot when A = a. (and lambda = L)
14 double evaluate_Adot( double a, double L, double w) {
15   return sqrt((1-L)*pow((double)a,(double)-1.0f)+L*pow((double)a,(
        double)-1.0f-(3.0f*w)));
16 }
17
18 // calculate the 4 k values for runge-kutta on 'a', return them in
       the passed in pointers.
19 void get_runge_kutte_k_vals_for_a( double a, double L, double dt,
       double w,
20                   double* k1, double *k2, double *k3, double *k4) {
21   *k1 = evaluate_Adot( a, L, w );
22   *k2 = evaluate_Adot( a + 0.5 * dt * (*k1), L, w );
23   *k3 = evaluate_Adot( a + 0.5 * dt * (*k2), L, w );
24   *k4 = evaluate_Adot( a + dt * (*k3), L, w );
25 }
26
27 // calculate the next value of a in a runge_kutta integration
28 double runge_kutta_a(  double a, double L, double dt, double w ) {
29
30   double k1, k2, k3, k4;
31
32   get_runge_kutte_k_vals_for_a( a, L, dt, w,
33                   &k1, &k2, &k3, &k4);
34
35   return a + one_sixth * dt * ( k1 + 2 * k2 + 2 * k3 + k4 );
36 }
37
38 // calculation of ndeltadot
39 double evaluate_ndeltadubdot(double ndelta, double nddot, double a,
       double L, double w) {
40
41   double adot = evaluate_Adot( a, L, w );
42   double A, B, C;
43
44   // Stuff for non-linear equation, n2dot = second order non-linear
        delta derivative wrt time
45   A = -2.0f*(adot/a)*nddot;
46   B = (3/2.0f)*(1-L)*(1+ndelta)*ndelta*pow(a,(double)-3.0f);
47   C = (4/3.0f)*(nddot*nddot)/(1+ndelta);
48   return A + B + C;
49 }
50
51 // calculate the next value of ndelta using runge-kutta.
```

```
52 // Since ndelta depends on a, and we don't have an explicit formula
       for a,
53 // we have to treat this as an integration of a system of equations
       using runge-kutta.
54 // We've already integrated a, but we still need the runge-kutta k
       values from the 'a'
55 // integration in order to calculate the k values for the ndelta
       integration.
56 double runge_kutta_ndelta( double ndelta, double nddot, double a,
       double L, double dt, double w, double * nddot_ret) {
57
58   double k1, k2, k3, k4;
59   double ka1, ka2, ka3, ka4;
60
61   get_runge_kutte_k_vals_for_a( a, L, dt, w,
62                  &ka1, &ka2, &ka3, &ka4);
63
64   k1 = evaluate_ndeltadubdot( ndelta, nddot, a, L, w );
65   k2 = evaluate_ndeltadubdot( ndelta + 0.5 * dt * nddot,
66                nddot + 0.5 * dt * k1,
67                a + 0.5 * dt * ka1,
68                L,
69                w);
70   k3 = evaluate_ndeltadubdot( ndelta + 0.5 * dt * nddot + 0.25 * dt
       * dt * k2,
71                nddot + 0.5 * dt* k2,
72                a + 0.5 * dt * ka2,
73                L,
74                w);
75   k4 = evaluate_ndeltadubdot( ndelta + dt * nddot + 0.5 * dt * dt *
       k3,
76                nddot + dt * k3,
77                a + dt * ka3,
78                L,
79                w);
80
81   *nddot_ret =  nddot + one_sixth * dt * ( k1 + 2 * k2 + 2 * k3 + k4
         );
82
83   return ndelta + dt * nddot + one_sixth * dt * dt * ( k1 + k2 + k3
       );
84 }
85
86 // calculate the second derivative of delta.
87 double evaluate_deltadubdot( double delta, double ddot, double a,
       double L, double w ) {
88
89   // Stuff for linear equation: second order deriv of lin delta
```

```
90    double adot = evaluate_Adot( a, L, w );
91    return ((3/2.0f)*(1-L)*delta/(a*a*a)) - (2*adot*ddot/a);
92  }
93
94  // returns the next value of delta from runge_kutta integration.
        The integrated value of ddot is returned by pointer
95  // in the last parameter.
96  // Here we are integrating a system of 2 equations (delta and ddot),
        but again 'a' is not a known function,
97  // so we have to treat this as a runge-kutta integration of a system
        of 3 equations, but again we don't need
98  // to explicitly do the integration of 'a' since we've already done
        so.
99  double runge_kutta_delta( double delta, double ddot, double a,
        double L, double dt, double w, double * ddot_ret ) {
100
101   double k1, k2, k3, k4;
102   double ka1, ka2, ka3, ka4;
103
104   get_runge_kutte_k_vals_for_a( a, L, dt, w,
105                   &ka1, &ka2, &ka3, &ka4);
106
107   k1 = evaluate_deltadubdot( delta, ddot, a, L, w );
108   k2 = evaluate_deltadubdot( delta + 0.5 * dt * ddot,
109                 ddot + 0.5 * dt * k1,
110                 a + 0.5 * dt * ka1,
111                 L,
112                 w);
113   k3 = evaluate_deltadubdot( delta + 0.5 * dt * ddot + 0.25 * dt *
        dt * k2,
114                 ddot + 0.5 * dt* k2,
115                 a + 0.5 * dt * ka2,
116                 L,
117                 w);
118   k4 = evaluate_deltadubdot( delta + dt * ddot + 0.5 * dt * dt * k3,
119                 ddot + dt * k3,
120                 a + dt * ka3,
121                 L,
122                 w);
123
124   *ddot_ret =  ddot + one_sixth * dt * ( k1 + 2 * k2 + 2 * k3 + k4 )
        ;
125
126   return delta + dt * ddot + one_sixth * dt * dt * ( k1 + k2 + k3 );
127 }
128
129 int main()
130 {
```

```
131   double w, omega;//omega is dark energy fraction as function of a
132   int m,alpha;
133   double adot, ddot, ndelta, nddot, dubdot, n2dot;
134   double A, B, C;
135   int t,time;
136   double dt=0.000001f,acoll,tcoll; //time step
137   double L; //this is the value of dark energy today
138   const double Pi = 3.14159265358979323846;
139
140   CreateDirectory ("data",0); //the 0 is a security_attributes value
141
142   double win=-0.3;
143   double wstep=-.1;
144   double wout=-1.0;
145
146   L=0.7;
147
148   vector<double> eds;//this stores the cosmological constant case
149
150   for(w=win; w>=wout; w+=wstep)//w = w + wstep
151   {
152
153     ostringstream streama;
154     streama << "data\\" << w << ".w.txt";
155
156     fstream filestra;
157     filestra.open (streama.str().c_str(), fstream::out);
158
159     ostringstream streamturn;
160     streamturn << "data\\" << w << ".w.turn.txt";
161
162     fstream fileturn;
163     fileturn.open (streamturn.str().c_str(), fstream::out);
164
165     //Vector Definitions
166     vector<double> advector;//this vector class stores the
          background scale factor
167     advector.push_back(1); //this initializes the 0th element of the
          vector, advector[0]=1
168
169     vector<double> z;//this vector class will store the redshift, as
          correlated with the values of advector
170     z.push_back(advector[0]-1);//this initializes the redshift at
          zero
171
172     vector<double> delta;//this vector class stores the value of
          linear delta
173
```

```
174     //Indices
175     int i=0; //i will index our dynamical array, aka vector
176     int j=1; //j will index the characteristic of the non-linear
            quadratic
177     int q=0; //q will index the values of linear delta
178
179     cout << "advector[0]: " << advector[0] << endl;
180     cout << "redshift: " << z[0] << endl;
181
182     //Background integration. we are integrating backwards in time,
            but i is indexing positively
183     //which is why if you look a few lines down, t=-i
184     do
185     {
186       adot = evaluate_Adot( advector[i], L, w );
187       advector.push_back( runge_kutta_a( advector[i], L, -dt, w ) );
              // run a runge-kutta iteration with a negative timestep
188       z.push_back((advector[0]/advector[i])-1.0f);
189       i+=1;
190     } while(0.1*advector[i] > adot*dt); // just looking for when a
            goes below zero 0.01*advector[i] > adot*dt
191
192     i--; // i is now the index of the last advector value greater
            than 0
193     int maxindex=i; //this records the i-value of the stopping point
             of the previous loop
194
195     cout << "advector[i]: " << advector[i] << endl;
196     cout << "adot: " << adot << endl;
197     cout << "w: " << w << endl;
198
199     //Initialize deltas, w's
200     delta.push_back(4.0*advector[i]);
201     ndelta = delta[q];
202     ddot = delta[q]*adot/advector[i];
203     nddot = ddot;
204     omega = L/((1-L)*pow(advector[i],(double)-3.0f) + L*pow(advector
            [i],(double)-3.0f*(1+w)));
205
206     cout << "ddot: " << ddot << endl;
207     cout << "delta initial: " << delta[q] << endl;
208     cout << "ndelta initial: " << ndelta << endl;
209
210     //We want the indexing of the background to not be confusing, so
             we are going to switch variables.
211     t=-maxindex;
212     time = t + maxindex + 1; //this is the time variable that goes
            forward in time
```

```
213     int timemax = time;
214     double linear[5] = {time,z[i],advector[i],delta[q],omega}; //We
            will store the collapse values in this array.
215
216     if( w==-0.3 ){
217         eds.push_back(delta[q]);
218     }
219
220     //m is an integer that will switch signs when the characteristic
            of the non-linear equation switches signs, thus allowing
221     //us to use the appropriate solution for delta-dot
222     m=-1;
223     alpha=-1;
224
225     //this loop will use the values of a that we found before to
            find the linear and non-linear deltas from the past until the
             present time.
226     for(;i>0;i--)     //(initial: already have i; exit when false:
            when i=0, stop; decrement by -1)
227     {
228       //filestra << "Iteration t: " << t << "\n";
229       adot = sqrt((1-L)*pow((double)advector[i],(double)-1.0f)+L*pow
             ((double)advector[i],(double)-1.0f-(3.0f*w)));
230
231       omega = L/((1-L)*pow(advector[i],(double)-3.0f) + L*pow(
             advector[i],(double)-3.0f*(1+w)));
232
233       //Determine collapse values
234       if((alpha == -1) && ( ndelta > 200.0f )) {
235         alpha=1;
236         linear[0]=time;
237         //cout << "collapse time: " << linear[0] << "\n";
238         linear[1]=z[i];
239         linear[2]=advector[i];
240         //cout << "collapse a: " << linear[2] << "\n";
241         linear[3]=delta[q];
242         cout << "linear delta at collapse: " << linear[3] << "\n";
243         linear[4]=omega;
244       }
245
246
247       if (j%10==0){
248       filestra << time << " , " << z[i] << " , " << advector[i] << "
              , " << delta[q] << " , " << ndelta << " , "
249       << omega << "\n";
250       }
251       //" , " << eds[q] <<
252
```

```
253         //get new values of linear and non-linear delta
254
255         //We want to store the linear delta values for use later
256         if( w==-0.3 ){
257           eds.push_back(runge_kutta_delta( delta[q], ddot, advector[i
                ], L, dt, w, &ddot ));
258           delta.push_back( eds[q+1] );
259         } else {
260           // push back the next value of delta, and also, ddot will
                get updated too.
261           delta.push_back( runge_kutta_delta( delta[q], ddot, advector
                [i], L, dt, w, &ddot ) );
262         }
263
264         ndelta = runge_kutta_ndelta( ndelta, nddot, advector[i], L, dt
              , w, &nddot );
265
266         t += 1;
267         time += 1;
268         j++;
269         q++;
270       }
271
272       //This loop transforms t and a to ratios with collapse values
273       j=1;
274       time=timemax;
275
276       int gamma;
277
278       //This is simply for the sake of rescaling the linear-delta,
             ensuring that we can do the following calculation.
279       if(delta.size()-1 > eds.size()-1){
280         gamma=eds.size()-1;
281       } else{
282         gamma=delta.size()-1;
283       }
284
285       for(i=maxindex;i>maxindex-gamma;i--){
286       //for(i=maxindex;i>0;i--){
287           tcoll=time/linear[0];
288           //double zcoll=z[i]/linear[1];
289           acoll=advector[i]/linear[2];
290           double delratio=(delta[j]/(1.676*pow(tcoll,(double)2.0/3.0f)
                ))-1;
291           if (j%10==0){
292             fileturn << tcoll << " , " << acoll << " , " << advector[i
                  ] << " , " << delratio << "\n";
293           }
```

```
294         time += 1;
295         j++;
296     }
297       fileturn.close();
298       filestra.close();
299   }
300   cout << "Program is done...";
301   cin.get();
302   cin.get();
303
304   return 0;
305 }
```

A.3 Interpolation and Variance Computations

This is a simple script for Matlab that calculates the variances discussed in Chapter 6.

```
1  %yi = interp1(x,Y,xi)
2  filename = '0.turn.txt';
3  handle = fopen( filename );
4  A00 = fscanf( handle, '%g , %g , %g , %g', [4, inf] );
5  fclose( handle );
6
7  filename = '0.1.turn.txt';
8  handle = fopen( filename );
9  A11 = fscanf( handle, '%g , %g , %g , %g', [4, inf] );
10 fclose( handle );
11
12 filename = '0.2.turn.txt';
13 handle = fopen( filename );
14 A22 = fscanf( handle, '%g , %g , %g , %g', [4, inf] );
15 fclose( handle );
16
17 filename = '0.3.turn.txt';
18 handle = fopen( filename );
19 A33 = fscanf( handle, '%g , %g , %g , %g', [4, inf] );
20 fclose( handle );
21
22 filename = '0.4.turn.txt';
23 handle = fopen( filename );
24 A44 = fscanf( handle, '%g , %g , %g , %g', [4, inf] );
25 fclose( handle );
26
27 filename = '0.5.turn.txt';
28 handle = fopen( filename );
29 A55 = fscanf( handle, '%g , %g , %g , %g', [4, inf] );
```

```
fclose( handle );

filename = '0.6.turn.txt';
handle = fopen( filename );
A66 = fscanf( handle, '%g , %g , %g , %g', [4, inf] );
fclose( handle );

filename = '0.7.turn.txt';
handle = fopen( filename );
A77 = fscanf( handle, '%g , %g , %g , %g', [4, inf] );
fclose( handle );

%legend for indices: 1st one is the file home of the delratio, the 2nd is
%the file home of the time or scale factor.
ratio10 = interp1(A11(1, :), A11(4,:), A00(1,:));
ratio20 = interp1(A22(1, :), A22(4,:), A00(1,:));
ratio30 = interp1(A33(1, :), A33(4,:), A00(1,:));
ratio40 = interp1(A44(1, :), A44(4,:), A00(1,:));
ratio50 = interp1(A55(1, :), A55(4,:), A00(1,:));
ratio60 = interp1(A66(1, :), A66(4,:), A00(1,:));
ratio70 = interp1(A77(1, :), A77(4,:), A00(1,:));


%plot(A00(1,:),A00(4,:), 'k');
plot(A00(1,:),ratio10);
hold on;
plot(A00(1,:),A00(4,:));
plot(A00(1,:),ratio20);
plot(A00(1,:),ratio30);
plot(A00(1,:),ratio40);
plot(A00(1,:),ratio50);
plot(A00(1,:),ratio60);
plot(A00(1,:),ratio70);
hold off;

xlabel('t/t_{collapse, \Lambda=0}');
ylabel('(\delta_{NL}/\delta_{NL, \Lambda=0})-1');

%int1 = gcf;
%exportfig(int1, 'interpolations.eps', 'format', 'eps', 'Width', 7, 'Height', 3.5, 'Color','cmyk', 'FontMode', 'Fixed', 'FontSize', 12, 'LineMode', 'Fixed', 'LineWidth', 1.2);

%this just copies the data into a new array
variancearray = ratio10;

%this says make a second row and put interp1 in it.  There would be
```

```
    trouble if interp1 was a different size than interp0.
variancearray(2,: ) = ratio20;
variancearray(3,: ) = ratio30;
variancearray(4,: ) = ratio40;
variancearray(5,: ) = ratio50;
variancearray(6,: ) = ratio60;
variancearray(7,: ) = ratio70;
variancearray(8,: ) = A00(4,:);

variances = var( variancearray, 0, 1);

%that will give you a 1-d array of the variances at each of your
   time points.
%If you want the minimum value:
minvariance = min( variances )
maxvariance = max( variances )

%if you want the position(s) where this minimum occurs:
timeofnearness = find ( variances == min(variances) )

meanval = mean ( variancearray );
meanvalatimeofnearness = meanval( timeofnearness )
```

BIBLIOGRAPHY

[1] Adam G. Riess et al. Observational Evidence from Supernovae for an Accelerating Universe and a Cosmological Constant. *Astron. J.*, 116:1009–1038, 1998. arXiv:astro-ph/9805201, doi:10.1086/300499. 1, 45, 69

[2] S. Perlmutter et al. Measurements of Omega and Lambda from 42 High-Redshift Supernovae. *Astrophys. J.*, 517:565–586, 1999. arXiv:astro-ph/9812133, doi:10.1086/307221. 1, 45, 69

[3] D. N. Spergel, R. Bean, O. Doré, M. R. Nolta, C. L. Bennett, J. Dunkley, G. Hinshaw, N. Jarosik, E. Komatsu, L. Page, H. V. Peiris, L. Verde, M. Halpern, R. S. Hill, A. Kogut, M. Limon, S. S. Meyer, N. Odegard, G. S. Tucker, J. L. Weiland, E. Wollack, and E. L. Wright. Three-Year Wilkinson Microwave Anisotropy Probe (WMAP) Observations: Implications for Cosmology. ApJS, 170:377–408, June 2007. arXiv:astro-ph/0603449, doi:10.1086/513700. 1

[4] E. W. Kolb, S. Matarrese, A. Notari, and A. Riotto. Primordial inflation explains why the universe is accelerating today. *ArXiv High Energy Physics - Theory e-prints*, March 2005. arXiv:hep-th/0503117. 2

[5] E. Bertschinger. On the Growth of Perturbations as a Test of Dark Energy and Gravity. ApJ, 648:797–806, September 2006. arXiv:astro-ph/0604485, doi:10.1086/506021. 2, 3, 6

[6] E. Bertschinger and P. Zukin. Distinguishing modified gravity from dark energy. Phys. Rev. D, 78(2):024015–+, July 2008. arXiv:0801.2431, doi:10.1103/PhysRevD.78.024015. 2

[7] O. Lahav, P. B. Lilje, J. R. Primack, and M. J. Rees. Dynamical effects of the cosmological constant. MNRAS, 251:128–136, July 1991. 3

[8] J. S. Bullock, T. S. Kolatt, Y. Sigad, R. S. Somerville, A. V. Kravtsov, A. A. Klypin, J. R. Primack, and A. Dekel. Profiles of dark haloes: evolution, scatter and environment. MNRAS, 321:559–575, March 2001. arXiv:astro-ph/9908159, doi:10.1046/j.1365-8711.2001.04068.x. 3

[9] T. Padmanabhan. Cosmological constant-the weight of the vacuum. Phys. Rep., 380:235–320, July 2003. arXiv:hep-th/0212290, doi:10.1016/S0370-1573(03)00120-0. 3

[10] M. G. Abadi, J. F. Navarro, M. Steinmetz, and V. R. Eke. Simulations of Galaxy Formation in a Λ Cold Dark Matter Universe. I. Dynamical and Photometric Properties of a Simulated Disk Galaxy. ApJ, 591:499–514, July 2003. arXiv:astro-ph/0211331, doi:10.1086/375512. 3

[11] U. Seljak, A. Makarov, P. McDonald, S. F. Anderson, N. A. Bahcall, J. Brinkmann, S. Burles, R. Cen, M. Doi, J. E. Gunn, Ž. Ivezić, S. Kent, J. Loveday, R. H. Lupton, J. A. Munn, R. C. Nichol, J. P. Ostriker, D. J. Schlegel, D. P. Schneider, M. Tegmark, D. E. Berk, D. H. Weinberg, and D. G. York. Cosmological parameter analysis including SDSS Lyα forest and galaxy bias: Constraints on the primordial spectrum of fluctuations, neutrino mass, and dark energy. Phys. Rev. D, 71(10):103515–+, May 2005. arXiv:astro-ph/0407372, doi:10.1103/PhysRevD.71.103515. 3

[12] L. Wang and P. J. Steinhardt. Cluster Abundance Constraints for Cosmological Models with a Time-varying, Spatially Inhomogeneous Energy Component with Negative Pressure. ApJ, 508:483–490, December 1998. arXiv:astro-ph/9804015, doi:10.1086/306436. 3, 79

[13] L. Wang, R. R. Caldwell, J. P. Ostriker, and P. J. Steinhardt. Cosmic Concordance and Quintessence. ApJ, 530:17–35, February 2000. arXiv:astro-ph/9901388, doi:10.1086/308331. 3

[14] E. J. Copeland, M. Sami, and S. Tsujikawa. Dynamics of Dark Energy. *International Journal of Modern Physics D*, 15:1753–1935, 2006. arXiv:arXiv:hep-th/0603057, doi:10.1142/S021827180600942X. 3, 86

[15] F. Markopoulou. New directions in Background Independent Quantum Gravity. *ArXiv General Relativity and Quantum Cosmology e-prints*, March 2007. arXiv:arXiv:gr-qc/0703097. 5, 28, 29

[16] F. Markopoulou and L. Smolin. Disordered locality in loop quantum gravity states. *ArXiv General Relativity and Quantum Cosmology e-prints*, February 2007. arXiv:arXiv:gr-qc/0702044. 5, 28, 29, 31

[17] C. Prescod-Weinstein, N. Afshordi, and M. L. Balogh. Stellar black holes and the origin of cosmic acceleration. Phys. Rev. D, 80(4):043513–+, August 2009. arXiv:0905.3551, doi:10.1103/PhysRevD.80.043513. 5, 45

[18] N. Afshordi. Gravitational Aether and the thermodynamic solution to the cosmological constant problem. *ArXiv e-prints*, July 2008. arXiv:0807.2639. 5, 46, 57, 58, 69, 70

[19] M. Ishak, A. Upadhye, and D. N. Spergel. Probing cosmic acceleration beyond the equation of state: Distinguishing between dark energy and modified gravity models. Phys. Rev. D, 74(4):043513–+, August 2006. arXiv:arXiv:astro-ph/0507184, doi:10.1103/PhysRevD.74.043513. 6, 72

[20] N. A. Bahcall and X. Fan. The Most Massive Distant Clusters: Determining Omega and delta 8. ApJ, 504:1–+, September 1998. arXiv:arXiv:astro-ph/9803277, doi:10.1086/306088. 7

[21] G. Holder, Z. Haiman, and J. J. Mohr. Constraints on Ω_m, Ω_Λ, and σ_8, from Galaxy Cluster Redshift Distributions. ApJ, 560:L111–L114, October 2001. arXiv:arXiv:astro-ph/0105396, doi:10.1086/324309. 7

[22] A. R. Liddle and D. H. Lyth. The cold dark matter density perturbation. Phys. Rep., 231:1–105, August 1993. arXiv:arXiv:astro-ph/9303019, doi:10.1016/0370-1573(93)90114-S. 11

[23] R. M. Wald. *General relativity*. 1984. 11

[24] S. M. Carroll. *Spacetime and geometry. An introduction to general relativity*. 2004. 11, 14, 49

[25] E. Hubble. A Relation between Distance and Radial Velocity among Extra-Galactic Nebulae. *Proceedings of the National Academy of Science*, 15:168–173, March 1929. doi:10.1073/pnas.15.3.168. 11

[26] G. Gamow. *My world line: An informal autobiography*. 1970. 17

[27] S. Weinberg. The cosmological constant problem. *Reviews of Modern Physics*, 61:1–23, January 1989. doi:10.1103/RevModPhys.61.1. 18, 45

[28] S. Weinberg. The Cosmological Constant Problems (Talk given at Dark Matter 2000, February, 2000). *ArXiv Astrophysics e-prints*, May 2000. arXiv:astro-ph/0005265. 18

[29] C. Rovelli. *Quantum Gravity*. November 2004. 23

[30] L. Smolin. The case for background independence. *ArXiv High Energy Physics - Theory e-prints*, July 2005. arXiv:arXiv:hep-th/0507235. 23

[31] B. L. Hu. Emergent/quantum gravity: macro/micro structures of spacetime. *Journal of Physics Conference Series*, 174(1):012015–+, June 2009. arXiv:0903.0878, doi:10.1088/1742-6596/174/1/012015. 23

[32] S. DeDeo and C. Prescod-Weinstein. Macroscopic Objects in Theories with Energy-dependent Speeds of Light. *ArXiv e-prints*, November 2008. arXiv:0811.1999. 23

[33] S. Hossenfelder. Bounds on an Energy-Dependent and Observer-Independent Speed of Light from Violations of Locality. *Physical Review Letters*, 104(14):140402–+, April 2010. arXiv:1004.0418, doi:10.1103/PhysRevLett.104.140402. 23

[34] C. Prescod-Weinstein and L. Smolin. Disordered locality as an explanation for the dark energy. Phys. Rev. D, 80(6):063505–+, September 2009. arXiv:0903.5303, doi:10.1103/PhysRevD.80.063505. 24, 28

[35] S. A. Fulling. Nonuniqueness of Canonical Field Quantization in Riemannian Space-Time. Phys. Rev. D, 7:2850–2862, May 1973. doi:10.1103/PhysRevD.7.2850. 25

[36] P. C. W. Davies. Scalar production in Schwarzschild and Rindler metrics. *Journal of Physics A Mathematical General*, 8:609–616, April 1975. doi:10.1088/0305-4470/8/4/022. 25

[37] W. G. Unruh. Notes on black-hole evaporation. Phys. Rev. D, 14:870–892, August 1976. doi:10.1103/PhysRevD.14.870. 25

[38] S. W. Hawking. Black hole explosions? Nature, 248:30–31, March 1974. doi:10.1038/248030a0. 25

[39] J. D. Bekenstein. Generalized second law of thermodynamics in black-hole physics. Phys. Rev. D, 9:3292–3300, June 1974. doi:10.1103/PhysRevD.9.3292. 25

[40] J. D. Bekenstein. Statistical black-hole thermodynamics. Phys. Rev. D, 12:3077–3085, November 1975. doi:10.1103/PhysRevD.12.3077. 25

[41] S. W. Hawking. Particle creation by black holes. In C. J. Isham, R. Penrose, & D. W. Sciama, editor, *Quantum Gravity*, pages 219–267, 1975. 25

[42] N. D. Birrell and P. C. W. Davies. *Quantum fields in curved space*. 1982. 25

[43] L. Smolin. Loop Quantum Gravity and planck Scale Phenomenology. In J. Kowalski-Glikman & G. Amelino-Camelia, editor, *Lecture Notes in Physics, Berlin Springer Verlag*, volume 669 of *Lecture Notes in Physics, Berlin Springer Verlag*, pages 363–408, 2005. doi:10.1007/11377306_11. 27

[44] M. H. Ansari. Spectroscopy of a canonically quantized horizon. *Nuclear Physics B*, 783:179–212, November 2007. arXiv:arXiv:hep-th/0607081, doi:10.1016/j.nuclphysb.2007.01.009. 27

[45] F. Markopoulou. personal communication, 2006 and. preprint, in preparation. 28, 31, 35

[46] T. Konopka. Statistical mechanics of graphity models. Phys. Rev. D, 78(4):044032–+, August 2008. arXiv:0805.2283, doi:10.1103/PhysRevD.78.044032. 29

[47] T. Konopka, F. Markopoulou, and S. Severini. Quantum graphity: A model of emergent locality. Phys. Rev. D, 77(10):104029–+, May 2008. arXiv:0801.0861, doi:10.1103/PhysRevD.77.104029. 29

[48] T. Konopka, F. Markopoulou, and L. Smolin. Quantum Graphity. *ArXiv High Energy Physics - Theory e-prints*, November 2006. arXiv:arXiv:hep-th/0611197. 29

[49] J. Magueijo, L. Smolin, and C. R. Contaldi. Holography and the scale invariance of density fluctuations. *Classical and Quantum Gravity*, 24:3691–3699, July 2007. arXiv:arXiv:astro-ph/0611695, doi:10.1088/0264-9381/24/14/009. 29

[50] B. Kozma, M. B. Hastings, and G. Korniss. Diffusion Processes on Power-Law Small-World Networks. *Physical Review Letters*, 95(1):018701–+, June 2005. arXiv:arXiv:cond-mat/0501509, doi:10.1103/PhysRevLett.95.018701. 39

[51] B. Kozma, M. B. Hastings, and G. Korniss. Roughness Scaling for Edwards-Wilkinson Relaxation in Small-World Networks. *Physical Review Letters*, 92(10):108701–+, March 2004. arXiv:arXiv:cond-mat/0309196, doi:10.1103/PhysRevLett.92.108701. 39

[52] M. B. Hastings. An ϵ-expansion for small-world networks. *European Physical Journal B*, 42:297–301, November 2004. arXiv:arXiv:cond-mat/0407374, doi:10.1140/epjb/e2004-00383-6. 39

[53] I. Zlatev, L. Wang, and P. J. Steinhardt. Quintessence, Cosmic Coincidence, and the Cosmological Constant. *Physical Review Letters*, 82:896–899, February 1999. arXiv:arXiv:astro-ph/9807002, doi:10.1103/PhysRevLett.82.896. 41

[54] N. Afshordi, G. Geshnizjani, and J. Khoury. Observational Evidence for Cosmological-Scale Extra Dimensions. *ArXiv e-prints*, December 2008. arXiv:0812.2244. 45

[55] Norbert Straumann. The history of the cosmological constant problem. 2002. arXiv:gr-qc/0208027. 46

[56] N. Afshordi, D. J. H. Chung, and G. Geshnizjani. Causal field theory with an infinite speed of sound. Phys. Rev. D, 75(8):083513–+, April 2007. arXiv:arXiv:hep-th/0609150, doi:10.1103/PhysRevD.75.083513. 47

[57] N. Afshordi, D. J. H. Chung, M. Doran, and G. Geshnizjani. Cuscuton cosmology: Dark energy meets modified gravity. Phys. Rev. D, 75(12):123509–+, June 2007. arXiv:arXiv:astro-ph/0702002, doi:10.1103/PhysRevD.75.123509. 47

[58] M. Nouri-Zonoz and T. Padmanabhan. The classical essence of black hole radiation. *ArXiv General Relativity and Quantum Cosmology e-prints*, December 1998. arXiv:arXiv:gr-qc/9812088. 55

[59] R. Shafee, J. E. McClintock, R. Narayan, S. W. Davis, L.-X. Li, and R. A. Remillard. Estimating the Spin of Stellar-Mass Black Holes by Spectral Fitting of the X-Ray Continuum. ApJ, 636:L113–L116, January 2006. arXiv:arXiv:astro-ph/0508302, doi:10.1086/498938. 58

[60] J. D. Jackson. *Classical Electrodynamics*. John Wiley & Sons, New York, 3 edition, 1998. 60

[61] M. Fukugita and P. J. E. Peebles. The Cosmic Energy Inventory. ApJ, 616:643–668, December 2004. arXiv:arXiv:astro-ph/0406095, doi:10.1086/425155. 63, 64, 65

[62] C. D. Bailyn, R. K. Jain, P. Coppi, and J. A. Orosz. The Mass Distribution of Stellar Black Holes. ApJ, 499:367–+, May 1998. arXiv:arXiv:astro-ph/9708032, doi:10.1086/305614. 63

[63] K. A. Postnov and A. M. Cherepashchuk. Masses of Stellar Black Holes and Testing Theories of Gravitation. *Astronomy Reports*, 47:989–999, December 2003. doi:10.1134/1.1633612. 63

[64] C. L. Fryer and V. Kalogera. Theoretical Black Hole Mass Distributions. ApJ, 554:548–560, June 2001. arXiv:arXiv:astro-ph/9911312, doi:10.1086/321359. 63

[65] A. M. Hopkins and J. F. Beacom. On the Normalization of the Cosmic Star Formation History. ApJ, 651:142–154, November 2006. arXiv:arXiv:astro-ph/0601463, doi:10.1086/506610. 63, 66, 67

[66] P. Kroupa. On the variation of the initial mass function. MNRAS, 322:231–246, April 2001. arXiv:arXiv:astro-ph/0009005, doi:10.1046/j.1365-8711.2001.04022.x. 64

[67] G. Chabrier. Galactic Stellar and Substellar Initial Mass Function. PASP, 115:763–795, July 2003. arXiv:arXiv:astro-ph/0304382, doi:10.1086/376392. 64

[68] E. E. Salpeter. The Luminosity Function and Stellar Evolution. ApJ, 121:161–+, January 1955. doi:10.1086/145971. 64

[69] P. F. Hopkins, L. Hernquist, T. J. Cox, T. Di Matteo, B. Robertson, and V. Springel. A Unified, Merger-driven Model of the Origin of Starbursts, Quasars, the Cosmic X-Ray Background, Supermassive Black Holes, and Galaxy Spheroids. ApJS, 163:1–49, March 2006. arXiv:arXiv:astro-ph/0506398, doi:10.1086/499298. 64, 66

[70] L. Ferrarese. Beyond the Bulge: A Fundamental Relation between Supermassive Black Holes and Dark Matter Halos. ApJ, 578:90–97, October 2002. arXiv:arXiv:astro-ph/0203469, doi:10.1086/342308. 65

[71] K. Gebhardt, J. Kormendy, L. C. Ho, R. Bender, G. Bower, A. Dressler, S. M. Faber, A. V. Filippenko, R. Green, C. Grillmair, T. R. Lauer, J. Magorrian, J. Pinkney, D. Richstone, and S. Tremaine. Black Hole Mass Estimates from Reverberation Mapping and from Spatially Resolved Kinematics. ApJ, 543:L5–L8, November 2000. arXiv:arXiv:astro-ph/0007123, doi:10.1086/318174. 65

[72] D. Merritt and L. Ferrarese. The M_{bh}-σ Relation for Supermassive Black Holes. ApJ, 547:140–145, January 2001. arXiv:arXiv:astro-ph/0008310, doi:10.1086/318372. 65

[73] S. Tremaine, K. Gebhardt, R. Bender, G. Bower, A. Dressler, S. M. Faber, A. V. Filippenko, R. Green, C. Grillmair, L. C. Ho, J. Kormendy, T. R. Lauer, J. Magorrian, J. Pinkney, and D. Richstone. The Slope of the Black Hole Mass versus Velocity Dispersion Correlation. ApJ, 574:740–753, August 2002. arXiv:arXiv:astro-ph/0203468, doi:10.1086/341002. 65

[74] E. Komatsu, J. Dunkley, M. R. Nolta, C. L. Bennett, B. Gold, G. Hinshaw, N. Jarosik, D. Larson, M. Limon, L. Page, D. N. Spergel, M. Halpern, R. S. Hill, A. Kogut, S. S. Meyer, G. S. Tucker, J. L. Weiland, E. Wollack, and E. L. Wright. Five-Year Wilkinson Microwave Anisotropy Probe Observations: Cosmological Interpretation. ApJS, 180:330–376, February 2009. arXiv:0803.0547, doi:10.1088/0067-0049/180/2/330. 66, 67

[75] A. Albrecht, G. Bernstein, R. Cahn, W. L. Freedman, J. Hewitt, W. Hu, J. Huth, M. Kamionkowski, E. W. Kolb, L. Knox, J. C. Mather, S. Staggs, and N. B. Suntzeff. Report of the Dark Energy Task Force. *ArXiv Astrophysics e-prints*, September 2006. arXiv:arXiv:astro-ph/0609591. 68

[76] V. F. Mukhanov, H. A. Feldman, and R. H. Brandenberger. Theory of cosmological perturbations. Phys. Rep., 215:203–333, June 1992. doi:10.1016/0370-1573(92)90044-Z. 71

[77] V. Acquaviva, A. Hajian, D. N. Spergel, and S. Das. Next generation redshift surveys and the origin of cosmic acceleration. Phys. Rev. D, 78(4):043514–+, August 2008. arXiv:0803.2236, doi:10.1103/PhysRevD.78.043514. 72

[78] A. Vikhlinin, A. V. Kravtsov, R. A. Burenin, H. Ebeling, W. R. Forman, A. Hornstrup, C. Jones, S. S. Murray, D. Nagai, H. Quintana, and A. Voevodkin. Chandra Cluster Cosmology Project III: Cosmological Parameter Constraints. ApJ, 692:1060–1074, February 2009. arXiv:0812.2720, doi:10.1088/0004-637X/692/2/1060. 72

[79] W. H. Press and P. Schechter. Formation of Galaxies and Clusters of Galaxies by Self-Similar Gravitational Condensation. ApJ, 187:425–438, February 1974. doi:10.1086/152650. 72

[80] J. E. Gunn and J. R. Gott, III. On the Infall of Matter Into Clusters of Galaxies and Some Effects on Their Evolution. ApJ, 176:1–+, August 1972. doi:10.1086/151605. 73, 81

[81] R. K. Sheth and G. Tormen. Large-scale bias and the peak background split. MNRAS, 308:119–126, September 1999. arXiv:arXiv:astro-ph/9901122, doi:10.1046/j.1365-8711.1999.02692.x. 73

[82] A. Jenkins, C. S. Frenk, S. D. M. White, J. M. Colberg, S. Cole, A. E. Evrard, H. M. P. Couchman, and N. Yoshida. The mass function of dark matter haloes. MNRAS, 321:372–384, February 2001. arXiv:arXiv:astro-ph/0005260, doi:10.1046/j.1365-8711.2001.04029.x. 73

[83] A. E. Evrard, T. J. MacFarland, H. M. P. Couchman, J. M. Colberg, N. Yoshida, S. D. M. White, A. Jenkins, C. S. Frenk, F. R. Pearce, J. A. Peacock, and P. A. Thomas. Galaxy Clusters in Hubble Volume Simulations: Cosmological Constraints from Sky Survey Populations. ApJ, 573:7–36, July 2002. arXiv:arXiv:astro-ph/0110246, doi:10.1086/340551. 73

[84] M. S. Warren, K. Abazajian, D. E. Holz, and L. Teodoro. Precision Determination of the Mass Function of Dark Matter Halos. ApJ, 646:881–885, August 2006. arXiv:arXiv:astro-ph/0506395, doi:10.1086/504962. 73

[85] J. Tinker, A. V. Kravtsov, A. Klypin, K. Abazajian, M. Warren, G. Yepes, S. Gottlöber, and D. E. Holz. Toward a Halo Mass Function for Precision Cosmology: The Limits of Universality. ApJ, 688:709–728, December 2008. arXiv:0803.2706, doi:10.1086/591439. 73, 93

[86] R. K. Sheth, H. J. Mo, and G. Tormen. Ellipsoidal collapse and an improved model for the number and spatial distribution of dark matter haloes. MNRAS, 323:1–12, May 2001. arXiv:arXiv:astro-ph/9907024, doi:10.1046/j.1365-8711.2001.04006.x. 73, 90, 92

[87] S. Bhattacharya, K. Heitmann, M. White, Z. Lukić, C. Wagner, and S. Habib. Mass Function Predictions Beyond LCDM. *ArXiv e-prints*, May 2010. arXiv:1005.2239. 73

[88] J. Courtin, Y. Rasera, J. -. Alimi, P. -. Corasaniti, V. Boucher, and A. Fuzfa. Imprints of dark energy on cosmic structure formation: II) Non-Universality of the halo mass function. *ArXiv e-prints*, January 2010. arXiv:1001.3425. 73

[89] P. J. E. Peebles. *Principles of physical cosmology*. 1993. 76

[90] F. Pace, J.-C. Waizmann, and M. Bartelmann. Spherical collapse model in dark-energy cosmologies. MNRAS, pages 1011–+, July 2010. arXiv:1005.0233, doi:10.1111/j.1365-2966.2010.16841.x. 80

[91] A. R. Liddle and D. H. Lyth. *Cosmological Inflation and Large-Scale Structure*. April 2000. 80

[92] I. Maor and O. Lahav. On virialization with dark energy. *Journal of Cosmology and Astro-Particle Physics*, 7:3–+, July 2005. arXiv:arXiv:astro-ph/0505308, doi:10.1088/1475-7516/2005/07/003. 81

[93] P. J. Peebles and B. Ratra. The cosmological constant and dark energy. *Reviews of Modern Physics*, 75:559–606, April 2003. arXiv:arXiv:astro-ph/0207347, doi:10.1103/RevModPhys.75.559. 86

[94] L. R. Abramo, R. C. Batista, L. Liberato, and R. Rosenfeld. Structure formation in the presence of dark energy perturbations. *Journal of Cosmology and Astro-Particle Physics*, 11:12–+, November 2007. arXiv:0707.2882, doi:10.1088/1475-7516/2007/11/012. 87

[95] R. Bean and O. Doré. Probing dark energy perturbations: The dark energy equation of state and speed of sound as measured by WMAP. Phys. Rev. D, 69(8):083503–+, April 2004. arXiv:arXiv:astro-ph/0307100, doi:10.1103/PhysRevD.69.083503. 88

[96] N. Afshordi, M. Zaldarriaga, and K. Kohri. Instability of dark energy with mass-varying neutrinos. Phys. Rev. D, 72(6):065024–+, September 2005. arXiv:arXiv:astro-ph/0506663, doi:10.1103/PhysRevD.72.065024. 88

[97] C. Armendariz-Picon, V. Mukhanov, and P. J. Steinhardt. Essentials of k-essence. Phys. Rev. D, 63(10):103510–+, May 2001. arXiv:arXiv:astro-ph/0006373, doi:10.1103/PhysRevD.63.103510. 88

[98] E. Komatsu, K. M. Smith, J. Dunkley, C. L. Bennett, B. Gold, G. Hinshaw, N. Jarosik, D. Larson, M. R. Nolta, L. Page, D. N. Spergel, M. Halpern, R. S. Hill, A. Kogut, M. Limon, S. S. Meyer, N. Odegard, G. S. Tucker, J. L. Weiland, E. Wollack, and E. L. Wright. Seven-Year Wilkinson Microwave Anisotropy Probe (WMAP) Observations: Cosmological Interpretation. *ArXiv e-prints*, January 2010. arXiv:1001.4538. 88

[99] J. M. Bardeen, J. R. Bond, N. Kaiser, and A. S. Szalay. The statistics of peaks of Gaussian random fields. ApJ, 304:15–61, May 1986. doi:10.1086/164143. 90

[100] F. Menanteau, J. Gonzalez, J.-B. Juin, T. A. Marriage, E. Reese, V. Acquaviva, P. Aguirre, J. W. Appel, A. J. Baker, L. F. Barrientos, E. S. Battistelli, J. R. Bond, S. Das, M. J. Devlin, S. Dicker, A. J. Deshpande, J. Dunkley, R. Dunner, T. Essinger-Hileman, J. W. Fowler, A. Hajian, M. Halpern, M. Hasselfield, C. Hernandez-Monteagudo, M. Hilton, A. D. Hincks, R. Hlozek, J. P.

Hughes, K. M. Huffenberger, L. Infante, K. D. Irwin, J. Klein, A. Kosowsky, Y.-T. Lin, D. Marsden, K. Moodley, M. D. Niemack, M. R. Nolta, L. A. Page, L. Parker, B. Partridge, J. Sievers, N. Sehgal, D. N. Spergel, S. T. Staggs, D. Swetz, E. Switzer, R. Thornton, H. Trac, R. Warne, and E. Wollack. The Atacama Cosmology Telescope: Physical Properties and Purity of a Galaxy Cluster Sample Selected via the Sunyaev-Zel'dovich Effect. *ArXiv e-prints*, June 2010. arXiv:1006.5126. 95

[101] K. Andersson, B. A. Benson, P. A. R. Ade, K. A. Aird, B. Armstrong, M. Bautz, L. E. Bleem, M. Brodwin, J. E. Carlstrom, C. L. Chang, T. M. Crawford, A. T. Crites, T. de Haan, S. Desai, M. A. Dobbs, J. P. Dudley, R. J. Foley, W. R. Forman, G. Garmire, E. M. George, M. D. Gladders, N. W. Halverson, F. W. High, G. P. Holder, W. L. Holzapfel, J. D. Hrubes, C. Jones, M. Joy, R. Keisler, L. Knox, A. T. Lee, E. M. Leitch, M. Lueker, D. P. Marrone, J. J. McMahon, J. Mehl, S. S. Meyer, J. J. Mohr, T. E. Montroy, S. S. Murray, S. Padin, T. Plagge, C. Pryke, C. L. Reichardt, A. Rest, J. Ruel, J. E. Ruhl, K. K. Schaffer, L. Shaw, E. Shirokoff, J. Song, H. G. Spieler, B. Stalder, Z. Staniszewski, A. A. Stark, C. W. Stubbs, K. Vanderlinde, J. D. Vieira, A. Vikhlinin, R. Williamson, Y. Yang, and O. Zahn. X-ray Properties of the First SZE-selected Galaxy Cluster Sample from the South Pole Telescope. *ArXiv e-prints*, June 2010. arXiv:1006.3068. 95

[102] J. Geisbüsch and M. P. Hobson. Cosmology with the Planck cluster sample. MNRAS, 382:158–176, November 2007. arXiv:arXiv:astro-ph/0611567, doi:10.1111/j.1365-2966.2007.12169.x. 95

[103] H. K. C. Yee, M. D. Gladders, D. G. Gilbank, S. Majumdar, H. Hoekstra, E. Ellingson, and the RCS-2 Collaboration. The Red-Sequence Cluster Surveys. *ArXiv Astrophysics e-prints*, January 2007. arXiv:arXiv:astro-ph/0701839. 95